The use of remote sensing data to monitor land use systems and forest variables of the tropical rainforest landscape under transformation in Jambi Province, Sumatra, Indonesia

A dissertation submitted to attain the degree of
Doctor of Philosophy (Ph.D)
at the Faculty of Forest Sciences and Forest Ecology
Georg-August-University of Göttingen

by

Dian Nuraini Melati
Born in Jember, East Java Province, Indonesia

Göttingen, November 2017

First referee	: Prof. Dr. Christoph Kleinn
Second referee	: Prof. Dr. I Nengah Surati Jaya
Examiner	: Prof. Dr. Daniela Sauer
Date of oral examination	: July 27th, 2017

Acknowledgement

It is my great pleasure to acknowledge my supervisor, Prof. Dr. Christoph Kleinn, for the opportunity to conduct this study funded by the DFG, as a part of Collaborative Research Centre (CRC) 990. In particular, I would like to thank for his excellent guidance and support through his valuable comments, advices, and inputs during this research work and the development of my writing skill. I would also like to thank Dr. Lutz Fehrmann, Dr. Hans Fuchs, Dr. Paul Magdon, and Dr. Cesar Pérez-Cruzado who were always there for any questions from me and for the fruitful discussion during my research work.

Moreover, I would also like to acknowledge Prof. Dr. I Nengah Surati Jaya and also other colleagues from the Laboratory of Forest Resources Inventory, Remote Sensing, and GIS– Bogor Agricultural University (IPB). This study would have never been possible without a good collaboration and continuous support from Prof. Nengah and the team. Further, I would also like to thank M.Sc. Mohammad Zuhdi and Dr. Eva Achmad from Jambi University (UNJA) for also giving kindly support during the field work and data collection. Field work was also successfully conducted with a cooperative work from PT. Restorasi Ekosistem Indonesia, I cordially thank colleagues at PT. REKI.

Great thanks also to colleagues at the Chair of Forest Inventory and Remote Sensing: Damayanti Sarodja, Henning Aberle, Dengkui Mo, Xiaolu Tang, Almut Niebuhr, Ramon Trucios-Caciano, Collins Kukunda, Nils Nölke, Philip Beckschäfer, Kira Urban, Wanda Graf, Sabine Schreiner, Haijun Yang, Silvia Wagner, Hendrik Heydcke, and Reinhard Schlote. Thanks a lot also to Jarrett Bleicher for proof reading throughout the text. My thanks also go to my colleagues in The Agency for the Assessment and Application of Technology (BPPT), Indonesia for allowing me temporarily leaving my work activities to continue this study. I would also like to thank for the friendship during my stay in Göttingen: Rahmi Fitriana Herman Djab, Edwine S. Purnama, and Lambok Sagala.

Last but not least, my sincere thanks go to my mother, my husband Jayadi, and all my families for their endless moral support and patience.

Summary

The transformation of land use in the tropics has received major attention in the last decades due to the rapid loss of tropical forests. In particular, large forest areas have been deforested and turned into agricultural lands. In addition to deforestation, unsustainable timber extraction, among others, led to forest degradation. In fact, deforestation and forest degradation have considerably contributed to global CO_2 emissions. Monitoring land use systems and remnant forests in areas of transformation is therefore important, particularly within tropical rainforest landscapes. Such monitoring provides information such as the spatial distribution of land use systems, land use change, and also the quality of the ecosystem over the landscape (e.g. habitat quality, forest carbon stock, etc). This information could be a baseline for respective stakeholders to take action on sustainable landscape management. For this purpose, the use of remote sensing data plays a major role on land use monitoring due to spatially explicit measurements of the ground surface over large areas as well as the ability to measure repetitively. The combination of these data with sample-based field data can reduce the time and cost of field inventory.

This study took place in Jambi province, with a total area of around 4.9 Mha, which is one of the hot spots of land use transformation in Indonesia, primarily in regard to forest conversion. To understand the historical land use change within study area, this study aims to analyze land use transformation in the period of 1990-2013 and the temporal dynamics of land use fragmentation. Some potential factors related to deforestation were also analyzed. As the amount of high spatial resolution images increases, it is expected that such images could provide better information of the ground surface with smaller minimum mapping unit. This will further facilitate efforts to identify the expansion of tree crops and remaining forests at finer scale. In this study, the applicability of high resolution RapidEye images was evaluated to classify land use systems and predict forest variables combined with field inventory data.

The analyses of land use transformation were conducted using time-series of land use maps from 1990, 2000, 2011, and 2013, which were generated by visual interpretation of multi-temporal Landsat images. The results show that, over the period from 1990-2013, the net decrease of primary forests was about 38.2 % (from 1.34 Mha to 0.83 Mha) and of secondary forests was about 30.9 % (from 0.92 Mha to 0.64 Mha). Primary forests were mainly converted into secondary forests and the existing secondary forests in 1990 were

mainly converted into rubber and oil palm plantations. For secondary forest areas, a considerable reduction of the mean patch size (from 4,034 ha to 2,269 ha) was observed, indicating an increase of forest fragmentation.

In regard to deforestation, lowland forests were most affected due to easier accessibility. By analyzing the factors potentially related to deforestation, this study found that rubber and oil palm productivity, among other socio-economic factors, were the most relevant. The rate of forest loss, referring to primary and secondary forest loss, had decreased within the three different periods of 1990-2000, 2000-2011, and 2011-2013. Throughout the study, it was evident that the loss of primary forests in the Jambi province decreased considerably in the last period, from 2011 to 2013, at around 535.4 ha/year. This remarkable decrease indicates a positive impact of the first phase of the forest moratorium policy in the period of 2011-2013. However, the loss of secondary forests was much higher in the same period, at around 11,594.2 ha/year. This could be due to the exclusion of secondary forests from the forest moratorium and, thus, need to pay more attention to protect secondary forests from further loss.

For the study of land use classification in 2013 using RapidEye image, object-based classification approach was implemented. This approach consists of two steps: image segmentation and image classification. Image segmentation is a crucial step because objects that are produced from this step are used as inputs for further classification and, thus, impact the accuracy of the image classification. An operational method to obtain optimum image segmentation was evaluated in this study. In this regard, Hoover metrics was used as the guidance; metrics were calculated from the comparison between segmented objects produced by different parameter settings of segmentation algorithm and the reference objects. The optimum image segmentation was then selected based on the trade-offs between the over-segmentation score and the correct detection score. In this study, the optimum image segmentation was selected from the resulting comparison, as it had high score of over-segmentation while still maintaining correct detection.

The selected optimum image segmentation was then used as the input for image classification. Classification was conducted using random forest classifiers and was validated using ground truthing data. The land use map produced high accuracy in determining the secondary forests and tree crops. The user's accuracies of secondary forest, rubber land, and oil palm plantation were 76.8 %, 84.6 %, and 91.7 %, respectively. The producer's accuracy of secondary forests was 89.2 %, while it was low for rubber land and

oil palm plantations, at 48.9 % and 56.1 %, respectively. Therefore, the spatial distribution of tree crops plantations provided by the map is reliable with high user's accuracy; however, the area can be lesser than existing area due to low producer's accuracy. The confusion that occurred in the classification of rubber land was due to the complex background where rubber trees, depending on the management status, are grown with grasses and other woody vegetation. This confusion was also found for the classification of oil palm plantations, which was due to the presence of grasses among young oil palm plantations.

Another study in this thesis combined sample-based field inventory and high spatial resolution RapidEye images. This study aims to identify the applicability of RapidEye images on the prediction of forest variables in a complex tropical rainforest (i.e. Harapan rainforest). The key variables to be predicted were above-ground biomass, basal area, quadratic mean diameter, and stand density. The model prediction was conducted using multiple linear regressions by linking the values of forest variables with predictor variables generated from RapidEye images. The proposed approach produced predictions of the above-ground biomass, basal area, and quadratic mean diameter with a coefficient of determination (R^2)/relative RMSE ($RMSE_r$) of 0.73/26.8 %, 0.62/25.9 %, and 0.55/18.9 %, respectively. However, the prediction of stand density was low, with an $R^2/RMSE_r$ of 0.29/40 %. Regionalized maps of above-ground biomass, basal area, and quadratic mean diameter were then produced with the derived models. This information can be useful to support the efforts of forest conservation and restoration within the Harapan rainforest, for example by identifying priority areas for action.

Table of contents

List of figures

List of tables

List of abbreviations

AI	Aggregation Index
AGB	Above Ground Biomass
AOT	Aerosol Optical Thickness
BA	Basal Area
BPS	Badan Pusat Statistik (Statistics of Indonesia)
CBD	Convention on Biological Diversity
COP	Conference of the Parties
CO_2	Carbon Dioxide
DEM	Digital Elevation Model
DNs	Digital Numbers
DOD	Diameter Over Deformation
dbh	diameter at breast height
dq	quadratic mean diameter
ETM+	Enhanced Thematic Mapper Plus
GCPs	Ground Control Points
GLCM	Grey Level Co-Occurrence Matrix
GoI	Government of Indonesia
GPS	Global Positioning System
ISPO	Indonesian Sustainable Palm Oil (ISPO)
LOOCV	Leave-One-Out Cross Validation
MDA	Mean Decrease Accuracy
MMU	Minimum Mapping Unit
MPS	Mean Patch Size
NASA	National Aeronautics and Space Administration
NDVI	Normalized Difference Vegetation Index
NES	Nucleus Estates and Smallholders
OBIA	Object-Based Image Analysis
OLI	Operational Land Imager
OA	Overall Accuracy
OOB	Out-of-Bag
PA	Producer's Accuracy
REDD	Reducing Emissions from Deforestation and Forest Degradation
REKI	Restorasi Ekosistem Indonesia
RF	Random Forest
RSPO	Roundtable on Sustainable Palm Oil
SRTM	Shuttle Radar Topography Mission
TOA	Top of Atmospheric
TM	Thematic Mapper
UA	User's Accuracy
UNFCCC	United Nations Framework Convention on Climate Change
USGS	United States Geological Survey
VIF	Variance Inflation Factor

Chapter 1
General Background

1.1. Tropical rain forest and deforestation

Transformations of land use systems are among the most important factors causing the alteration of the global environment (Lambin et al., 2001; Wyman & Stein, 2010). The practices of land use conversion from natural landscapes into other uses to meet human needs, such as agricultural landscapes, have greatly transformed large portions of the earth's surface (Foley et al., 2005). In particular, the clearance of forests in the tropics located across the Amazon, the Congo Basin, and Southeast Asia had reached 227 Mha by 2010, an estimation of annual deforestation rate of 3.8 Mha between 1950 and 2010 (Rosa et al., 2016).

Tropical rain forests act as sources of carbon dioxide (CO_2) due to biomass burning, decomposition, and deforestation or as sinks of CO_2 (Malhi & Grace, 2000; Malhi & Marthews, 2013). Absorption of CO_2 take places during the process of photosynthesis (Marcus, 2009). Thus, a great number of green plants in the tropical rain forest play an important role in the context of the global carbon cycle. These tropical rainforests store extensive carbon stocks in living biomass, dead wood, litter, and soils; in particular, lowland rainforests are able to store an above-ground biomass of 200-600 tons/ha (Ghazoul & Sheil, 2010). Apart from this, tropical rainforests found in Central and South America, Africa, and Southeast Asia also host almost half of the world's biodiversity (Alonso et al., 2001).

The FAO (2015) reported that forest carbon stocks have globally declined in the last 25 years by around 17.4 Gt due to deforestation and forest degradation. However, these carbon stock losses decreased from about 1.2 Gt per year in the 1990s to 0.4 Gt per year between 2000 and 2010, and to 0.2 Gt per year between 2010 and 2015. In 2008, massive deforestation and forest degradation contributed 12 % of the global CO_2 emissions (Van der

Werf et al., 2009). In all of the tropics, more than 55 % of intact forests and 28 % of disturbed forests were converted into agricultural land between 1980 and 2000 (Gibbs et al., 2010). However, the drivers of forest loss were different in the three largest rainforests located across Latin America, Africa, and Southeast Asia. The neotropics rainforests are mostly converted to pasture, as there is a long tradition of cattle ranching in Latin America (Hargrave & Kis-Katos, 2013; Whitmore, 1998). In Africa, the rainforests are predominantly threatened by cattle grazing, fire, agriculture, and a high demand for firewood (Ghazoul & Sheil, 2010; Hosonuma et al., 2012). These threats in Africa mainly originate from poverty and population growth (Corlett & Primack, 2011). In Southeast Asia, the expansion of tree crop plantations and timber industry is apparently the major driver of forest loss (Stibig et al., 2014) .

Timber produced by dipterocarp forests in Southeast Asia is generally straight and light, which results in a high demand of dipterocarps for a low-cost construction and plywood industry (Corlett & Primack, 2011). Timber extraction is typically done by harvesting large, commercial trees and by leaving behind the smaller, non-commercial species; therefore, these forests have become severely degraded (Edwards et al., 2011). These degraded forests are then allowed to be cleared for agricultural land (Koh & Wilcove, 2008). In Malaysia and Indonesia, these clearings have made possible the establishment of economic tree crops like palm oil which have put the surrounding forests under pressure (Casson, 2000; Kartodihardjo & Supriono, 2000; McMorrow & Talip, 2001). Koh & Wilcove (2008) estimated that the expansion of around 56 % of oil palm plantations (about 1.7 Mha) in Indonesia came from lands where primary and secondary forests, as well as forest plantations, were converted.

1.2. Forest loss in Indonesia

From the facts that have been mentioned above, deforestation is a major issue in the tropics. Indonesia was recently reported as the second highest of annual forest loss in the period of 2010-2015 after Brazil's (FAO, 2015). The study on primary forest loss from 2000-2012 across Indonesia, conducted by Margono et al. (2014), revealed that the loss of primary forests, including intact and degraded forests, increased considerably from 2001 to 2012, as depicted in Figure 1.1 In total, they estimated that the primary forest loss from 2000 to 2012 was around 6.02 Mha, which corresponds to about 6.1 % with annual forest loss of about 0.5 Mha (i.e. forest cover decreased from 98.4 Mha in 2000 to 92.4 Mha in 2012).

Large-scale forest loss in Indonesia has occurred since the 1980s when deforestation was around 10 % with annual deforestation of 1.2 Mha (i.e. from 121.7 Mha in 1980 to 109.5 Mha in 1990) (WRI, 1994). This long history of deforestation in Indonesia was mainly due to some government-sponsored programs like transmigration, the development of timber industries, and estate crops (The World Bank, 1994).

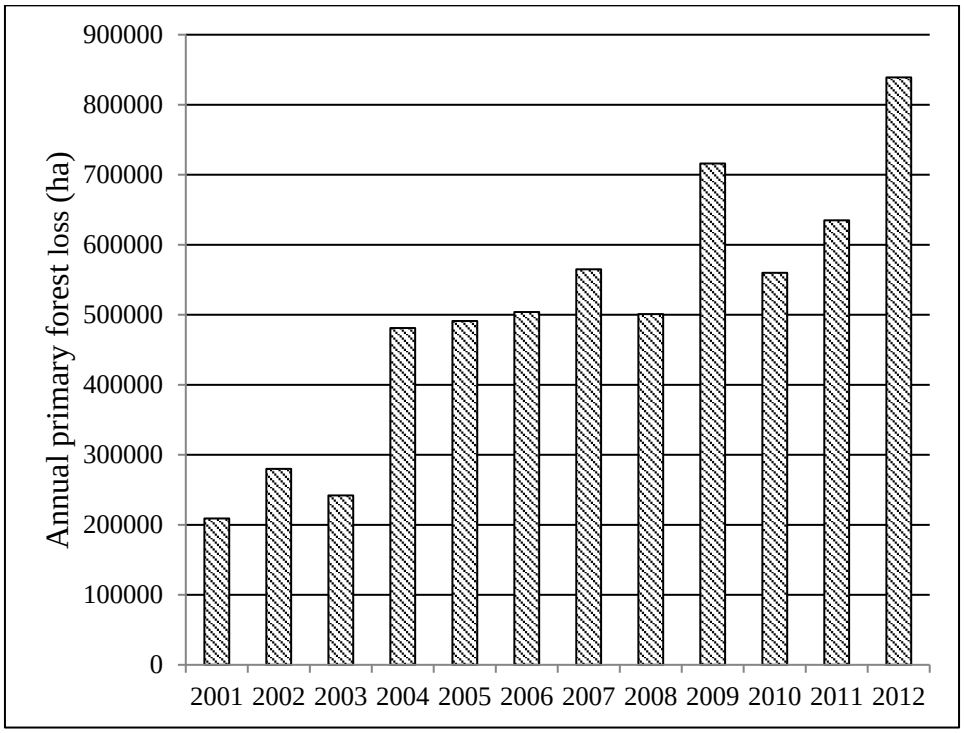

Figure 1.1. Annual loss of primary (intact and degraded) forests in Indonesia between 2001 and 2012 (Margono et al., 2014).

The aim of the transmigration program is to relocate people from the highly-populated islands of Java, Bali, Madura, and Lombok to other islands like Sumatra, Kalimantan, Sulawesi, Mollucas, Nusa Tenggara, and Papua (Hoppe & Faust, 2004). According to Fearnside (1997) and Ghazoul & Sheil (2010), the program offers transmigrants the opportunity to earn money not only through independent smallholder farming, but also through employment in industrial plantation forests. For example, 100 estates of plantation forests were proposed to be established in 1992 and it was necessary for each estate that received the concession to provide houses and other infrastructures for around 300 transmigrant families (Fearnside, 1997). However, it was subsequently found that the industrial plantation forest had caused the loss of forest. For the establishment of plantation forests, the companies were encouraged to plant in grassland areas that were commonly grown with *Imperata cylindrica*. However, these areas were mostly distributed in small

patches and consequently encouraged companies to clear the logged forests around the patches.

Logging concessions contributed to forest loss and degradation due to unsustainable timber extraction. The corresponding logging activities did not actually result in direct deforestation as they were done selectively and considered commercial species and stem sizes. Thus, the logged forests do finally remain forests. Nonetheless, there was a policy in Indonesia in 1990 stating that if the volume of a forest's timber was below 20 m^3ha^{-1}, it was classified as conversion forest and was allowed to be cut down for other plantation activities (Fearnside, 1997). Accordingly, the companies were motivated to log destructively and applied contracts for industrial plantation forest projects in the same land (A. Hadi Pramono, quoted by Fearnside, 1997). In other cases, the degraded logged forests were also converted for agriculture use (e.g. oil palm plantations) (Kartodihardjo & Supriono, 2000). This practice of converting forests into tree-crop plantations, particularly rubber and oil palm, has been of high concern in Indonesia for many years (Feintrenie & Levang, 2009). The expansion of rubber and oil palm has brought Indonesia as one of the largest producer for both crops. Figure 1.2 and Figure 1.3 depict the trend of rubber and palm oil production in Indonesia among the three largest global producers.

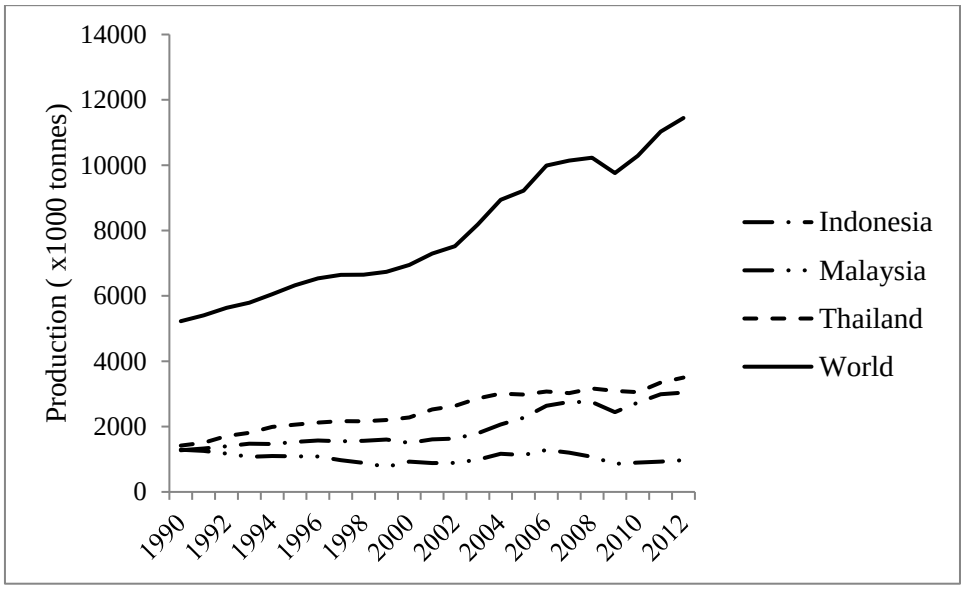

Figure 1.2. Countries with the largest rubber latex production (FAOSTAT, 2016).

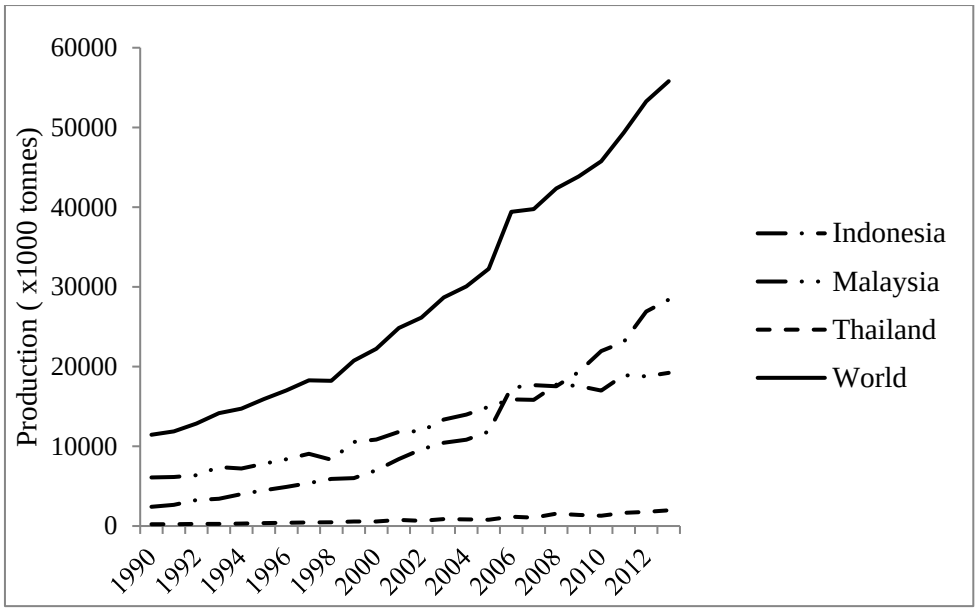

Figure 1.3. Countries with the largest palm oil production (FAOSTAT, 2016).

The land use practices of agricultural expansion through the destruction of tropical forests threatens forest ecosystem functions and services like the conservation of biodiversity, resources of freshwater and forest resources such as large forest carbon stocks (Foley et al., 2005; Whitten et al., 2000). It further spurs habitat loss and fragmentation and, therefore, the loss of biodiversity (Hannah & Lovejoy, 2011; Pimm & Raven, 2000).

Given that Sumatra is a considerable hotspot of biodiversity which includes over 10,000 different species of vegetation, 201 mammal species, and 580 bird species (Whitten et al., 2000), the loss of habitat drives dramatic losses of biodiversity (Drescher et al., 2016). In addition, the land use change and forest loss also produce remarkable emissions of CO_2 and affect global climate change. For instance, the emissions from deforestation and forest fires in Indonesia were found to be five times higher than those from non-forestry sectors (around 2,563 $MtCO_{2e}$ from forestry sectors and around 451 $MtCO_{2e}$ from non-forestry sectors) (PEACE, 2007).

1.3. International and national concern over forested landscape management

The loss of forests, which contributes to GHG emissions and, therefore, global climate change, has become a major concern regarding the management of forested landscapes. In order to tackle global climate change, the United Nations Framework Convention on Climate Change (UNFCCC) was established in 1992. The objective is "…to achieve, in

accordance with the relevant provisions of the Convention, stabilization of greenhouse gas concentrations in the atmosphere at a level that would prevent dangerous anthropogenic interference with the climate system" (UNFCCC, 1992). In 1997, the Parties to the Convention adopted the Kyoto Protocol which is a legal instrument to achieve the objectives of the Convention (Oppenheimer & Petsonk, 2005; UN, 1998).

The Kyoto Protocol required industrialized countries to decrease their greenhouse gas emissions. However, the issue of reducing deforestation was absent from the protocol. Nevertheless, the post-Kyoto negotiations considered a mechanism to reduce deforestation (Hannah & Lovejoy, 2011). It is known as Reducing Emissions from Deforestation and Forest Degradation (REDD), which then developed into REDD-plus (REDD+) at the 13th Conference of the Parties (COP) in Bali in 2007 (Butt et al., 2013). In 2015, the COP 21 in Paris continuously encouraged the parties to take action on REDD+ implementation, as mentioned in the Article 5.2 of the Paris Agreement (UN-REDD, 2015). The main concept is that developed countries compensate developing countries through a carbon market and, thus, developing countries are encouraged to implement the following five activities (Peskett, 2013):

1. Carbon emissions' reduction from deforestation,
2. Carbon emissions' reduction from forest degradation,
3. Forest carbon stocks conservation,
4. Sustainable forest management, and
5. Forest carbon stocks enhancement.

An implementation of forest conservation and management would also enhance biodiversity preservation as an immediate side-effect. According to Thompson et al. (2009), biodiversity is either related to species richness that exists in particular locations or habitat quality provided by certain ecosystems. In order to preserve the global biodiversity, the COP 10 of the Convention on Biological Diversity (CBD) which was held in 2010 in Nagoya, Aichi Prefecture, Japan, adopted the Strategic Plan for Biodiversity for the period of 2011-2020 through its Aichi Biodiversity Targets (CBD, 2010). The fifth of these targets aims to reduce the loss of natural habitats by 2020, including forests, by 50 % and, if possible, by 100 % (CBD, 2013). To deal with deforestation and forest degradation, the 15th target also highlights ecosystem conservation and restoration, by restoring of at least 15 % of degraded land by 2020 as the degradation and fragmentation of habitats leads to global

biodiversity loss. Both targets are also in line with the 15th Sustainable Development Goal, which underlines the implementation of sustainable management of forests, restoration of degraded forest, reduction of deforestation, as well as increasing afforestation and reforestation, by 2020 (UN, 2015).

Considering all these concerns, the perseveration of remaining forests should be of high priority. Indonesia implemented a forest moratorium, initiated by the Presidential Instruction 10 of 2011 to halt deforestation. This initial directive was applied for two years during the period of 2011-2013, followed by the second phase for the period of 2013-2015, and the third phase which was currently extended for the period of 2015-2017. The forest moratorium aims to suspend new concessions in primary forests and peatlands, excluding the following conditions: (1) the new concessions that had already received permission; (2) if the area is needed for national projects including geothermal, oil and gas, electricity, rice, and sugarcane fields; (3) if the current concessions need an extension, as long as their permissions have not expired; and (4) if the area is used for ecosystem restoration. In particular, for the second point (2), a conflict of interest from different sectors could hinder the effectiveness for the forest moratorium.

For the program to succeed, it is necessary to know the spatial extent of the forest moratorium, which is then translated into to the moratorium map. This map is updated every six months. To ensure the effectiveness of the moratorium, high accuracy spatial references of land use maps and forest designation maps including up-to-date permit information of concessions are needed (Murdiyarso et al., 2011). Nonetheless, the boundaries of forest and other land uses are still questioned in Indonesia due to the various and overlapping boundaries created by multiple ministries, such as the Ministry of Forestry, the Ministry of Agriculture, the Ministry of Energy and Mineral Resources, and the National Land Agency (Wibowo & Giessen, 2015). For instance, the existence of settlements within forest area due to overlapping borders among forest estates [1] administered by the Ministry of Forestry and other land uses in which the land ownership is administered by the National Land Agency. According to a report by the Consortium of Agrarian Reform, there were at least 30,000 villages found within forest areas (KPA, 2012).

[1] Forest estate (Kawasan Hutan) refers to the areas that are officially administered by Indonesian Ministry of Forestry. These forest estates do not necessarily have actual forest cover (Enrici & Hubacek, 2016).

In another case, the inconsistent forest areas within the maps produced by Ministry of Forestry and Ministry of Environment were also shown by the Presidential Working Unit for Supervision and Management of Development (UKP4) during the Cabinet Meeting on December 23rd, 2010 (REDD-Monitor, 2012). This issue prompted a directive from President Yudhoyono, i.e. the sixth Indonesian President, to produce one map as a national reference (Samadhi, 2013). In 2011, the Indonesian government initiated the 'One Map Policy' through Law 4 of 2011. The One Map Policy focuses not only on the forestry sector but also on other sectors which include different topics related to agriculture, economics, hazards, cultural heritage, mining, transportation, and others. The scope of the activities within the One Map Policy is a compilation, integration, and synchronization of thematic maps from 19 ministries/agencies and local governments from 34 provinces (BIG, 2016). This compilation involves collecting data from thematic maps of each respective ministry and agency. These maps are then integrated with a standard base map at the scale of 1:50,000 which are produced by the Agency of Geospatial Information (BIG). All of the integrated maps are then synchronized for any issue concerning an overlapping land use designation. These high-accuracy maps produced from the One Map Policy process will provide better information for land-use planning, policy planning and decision-making processes. However, since the Presidential Instruction 10 of 2011 gives higher priority to the energy sector and to food security over the forest moratorium, the disagreement over land use designation may potentially come from the Ministry of Forestry, Ministry of Agriculture, and the Ministry of Energy and Mineral Resources. With these various sectors involved, integrating the aforementioned thematic maps may face many obstacles due to disagreements over land use designation coming from these different agencies/ministries (Wibowo & Giessen, 2015).

In this regard, a serious commitment to accomplishing this program can still be expected from the current government. President Joko Widodo issued Presidential Regulation 9 of 2016 in order to accelerate the implementation of the One Map Policy. Timeline and the goals of respective institutions were structured through this regulation. The integration and synchronization of 85 thematic maps is targeted to be finished in 2019 (BIG, 2016). To achieve the target, each region in Indonesia was given individual precedence (GoI, 2017). In 2016, the priority of finalization stage was delegated to Kalimantan, followed by Sumatra, Sulawesi, Bali, and Nusa Tenggara for the year of 2017. The finalization for

Papua and Maluku is expected in 2018. Lastly, the finalization for Java is expected to finish in 2019. In 2016, 71 out of 79 thematic maps had been integrated for Kalimantan.

1.4. Scope of the study

1.4.1. The EFForTS project

This study is part of the Ecological and Socioeconomic Functions of Tropical Lowland Rainforest Transformation Systems in Sumatra, Indonesia (EFForTS), and, in particular, for Jambi province. It is a Collaborative Research Center 990 (CRC 990) project funded by the Deutsche Forschungsgemeinschaft (DFG), which is a collaboration between Georg-August-University, Göttingen, Germany, and three Indonesian universities (Bogor Agricultural University, Jambi University, and Tadulako University). Detailed information about the project can be found with the following link: https://www.uni-goettingen.de/en/about-us/413417.html. In general, the project aims to provide scientific knowledge about environmental processes, biota, and ecosystem services, as well as human dimensions of forested tropical landscapes where ongoing transformations of land use systems are caused by the expansion of agricultural systems.

1.4.2. Justification of the research

Jambi province, which is located on the Sumatra Island, was found to experience the largest deforestation during the period of 2011-2012, with a rate of 65,734.2 ha/year, compared to the other provinces located in Sumatra, which have deforestation rates between 1,085 and 46,395.9 ha/year (MoF, 2014). How to conserve forest ecosystems and the services they provide, while still improving food or further agricultural production, is sustainability's main challenge (Lambin & Meyfroidt, 2011). Therefore, understanding the transformation of tropical forested landscapes into the current state of mosaic landscapes is necessary to support better planning on sustainable landscape management.

Monitoring land use systems within a landscape is now essential in providing information for historical land use change analyses, and, in particular, information concerning the causes of deforestation over time. Such information would be helpful for supporting land use planning and sustainable management practices in forested landscapes. For instance, an action to protect areas with high deforestation due to agricultural expansion will help to sustain the forested landscape. Satellite images are essential tools for monitoring changes in forest cover and delivering reliable estimates of forest carbon stocks and associated

changes (GOFC-GOLD, 2013). Nowadays, a number of the remote sensing data acquired from different satellite sensors have been considerably developed with much higher spatial and spectral resolution. These remote sensing data can cover huge areas and, thus, reducing much fieldwork effort and time. Additionally, the ability to capture repeated information from the same surface helps to monitor change over landscapes.

There have been several studies conducted in Indonesia that have used remote sensing data to monitor deforestation as a consequence of land use transformation (Broich et al., 2011a; Broich et al., 2011b; Hansen et al., 2009; Margono et al., 2012, Margono et al., 2014). However, these studies have mostly been done either at national level or on some selected islands like Sumatra and Kalimantan. For the Jambi province, there was only one study conducted by Ekadinata & Vincent (2011) who analyzed land use transformation using remote sensing data in a district located in Bungo district. Until now, there has been no study of land use transformation on a provincial level in Jambi, where the expansion of typical tree crop plantations (i.e. rubber and palm oil) occurs intensively and forest lands are under much pressure. In this regard, further scientific knowledge on such a study will support the respective stakeholders (e.g. national and local administration) to take measures towards better landscape management.

Since tree crops are a major cause of deforestation, their mapping within the study area is essential for monitoring because mapping tree crops gives information on their expansion and spatial distribution. In relation to deforestation, this information can be a baseline for land use planning to further reduce deforestation when the expansion of tree crops comes at the expense of forest. On the larger scale of land use/land cover mapping, satellite images with medium spatial resolution, such as Landsat images, were commonly used. The presence of high spatial resolution satellite images such as RapidEye images with a 5 m spatial resolution is expected to classify objects into greater detail compared to Landsat images with a 30 m spatial resolution. Nonetheless, it should be taken into account that high spatial resolution shows objects on the ground as groups of pixels with a relatively-high spectral variability due to complex spectral responses (Blaschke et al., 2014; Rico & Maseda, 2012). Thus, one pixel and nearby pixels may inform different objects, though they represent similar objects. In this regards, an object based image analysis has been seen as an approach to overcome this drawback (Blaschke et al., 2014). Therefore, an object-based classification needs to be further evaluated for the mapping of tree crops and the remaining forests.

The assessment and accurate information of the forest variables is also essential for developing policy decision, so that biodiversity preservation, forest conservation and sustainable management of forests can be achieved. Several studies on assessing forest variables, including above-ground biomass modelling by integrating field inventory and remotely sensed data, have also been done in Indonesia. However, this was conducted specifically in Kalimantan (Englhart et al., 2011; Englhart et al., 2012; Wijaya & Gloaguen, 2009; Wijaya et al., 2010). Such a study in the Harapan rainforest that has been logged intensively and becomes a restoration forest is not yet assessed. Therefore, it is a relevant study to assess the integration of field inventory and high spatial resolution satellite image (i.e. RapidEye image) in order to predict the forest variables.

1.5. Objectives

1.5.1. Overall objective

The overall objective of the study is on the utilization of remote sensing data integrated with field data to serve information on the existing land use, land use dynamics as well as forest variables prediction within Jambi province.

1.5.2. Specific objectives

According to the overall objective, there are three specific objectives:

1. To produce analyses of land use change including the changes of spatial pattern and the identification of driving forces of deforestation.
   The focus was to give information on the land use transformation and the temporal dynamics of the fragmentation over the forested landscape through the utilization of land use maps between 1990 and 2013. Moreover, an investigation into the factors related to deforestation aimed at identifying the drivers of deforestation.

2. To evaluate the use of RapidEye images to differentiate tree crops and the remaining forests within the study area.
   The focus was to evaluate high spatial resolution images for land use classification using an object-based approach. For the image segmentation as the first step before image classification, an investigation into the optimization of segmentation parameters was also part of the goal in this study.

3. To produce an assessment of forest variables in a secondary rainforest by combining the field inventory and remote sensing data derived from RapidEye images.

   Image features derived from remote sensing data were linked to the ground-based measurements. This allows an evaluation of the applicability of high spatial resolution images to predict the forest variables over the secondary rainforest located in Harapan rainforest.

Chapter 2
Materials

2.1. Study Area

This research was conducted within Jambi province through three different studies that were implemented in three different reference areas of different size. The first study involves historical and spatial patterns of land use transformation covering the entire Jambi province (4.9 Mha). The second study regards the evaluation of tree crops mapping using RapidEye images, which was conducted in the Harapan landscape (0.1 Mha)—an area consisting of some villages surrounding the Harapan rainforest concession and the concession itself, which is located in Jambi Province. The last study was the assessment of the forest variables of a secondary rainforest, which was conducted in the Harapan rainforest concession (0.04 Mha). The three study areas are depicted in Figure 2.1.

According to the Statistics Bureau of the Jambi Province (BPS, 2014), the average temperature, average humidity, and precipitation in Jambi in 2013 was 26.8 °C, 86 %, and 2,609.3 mm, respectively. The province's population was around 3.3 million in 2013 (BPS, 2014). Jambi is administratively divided into two municipalities (Jambi city and Sungai Penuh city), which are urban areas, and nine districts that are in rural areas. The population of the rural areas consists of 1) transmigrants, 2) small and large landholders who manage the lands with different types of timber and tree crop plantations, and other types of agriculture such as food crops and fruit trees (Stolle et al., 2003).

Rubber, as the typical tree crop in Jambi, has a long history of cultivation that began in 1904 (Feintrenie & Levang, 2009). Due to the high incomes provided by rubber cultivation, it attracted farmers to cultivate these trees and to grow them with food crops and woody trees from forest regrowth (rubber agroforests), abandoning the transformation of

secondary forest fallow[2] from shifting cultivation of rice and other food crops to rubber agroforestry (Gouyon et al., 1993). However, rubber was replaced by oil palm plantations (Potter & Lee, 1998). This was related to the financial crisis of 1997 in Asia that led to decreasing prices for rubber latex on the global market and the instability of the monetary situation in Indonesia which triggered the farmers for new opportunities to diversification (Feintrenie & Levang, 2009).

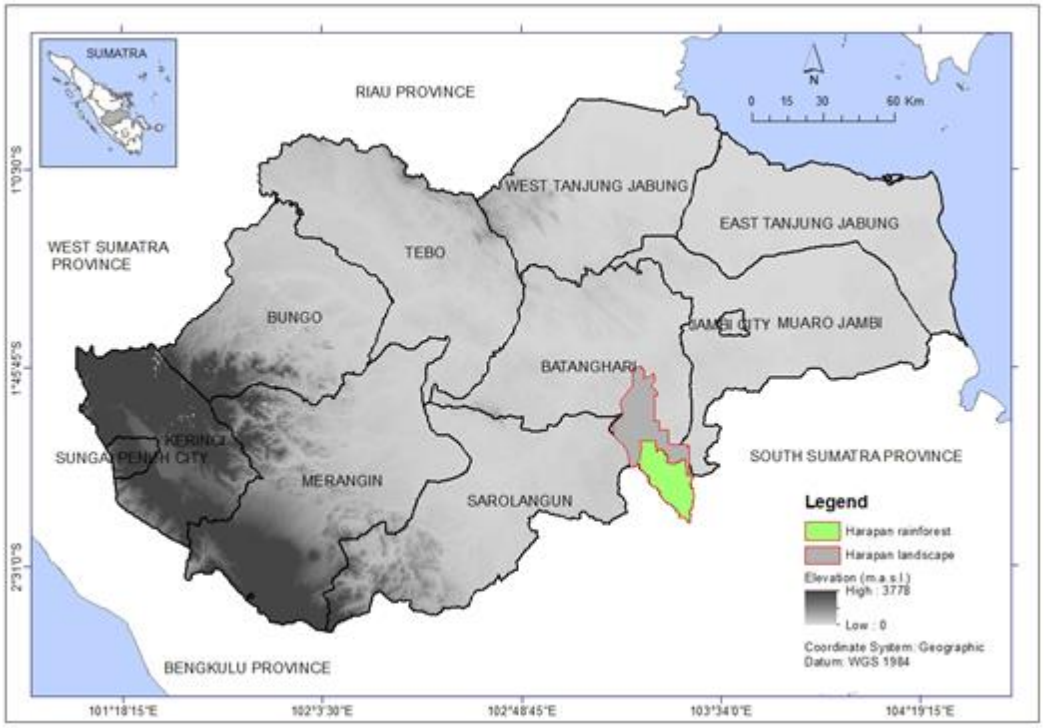

Figure 2.1. The location of the three study areas: 1) Jambi province, Sumatra, Indonesia, 2) Harapan landscape, and 3) Harapan rainforest.

The natural forests of Jambi are mixed dipterocarp rainforests (Beukema & van Noordwijk, 2004; Laumonier, 1997) and they are under heavy pressure (MoF, 2014). The Harapan rainforest, which is part of the study area, is one of the remaining secondary forests in Jambi province and was the first concession in Indonesia to work on ecosystem restoration[3]. In Indonesia, secondary forest is defined as forest cover where any type of human intervention is visible (e.g. agriculture, logging, encroachment, and also forest fires), either took place in the past or presently occurs. A typical of regrowth forest is found in secondary forest

[2] Gouyon et al. (1993) described secondary forest fallow as a result of continued practice of slash-and-burn within natural forest. It was covered by secondary vegetation and had some patches of fallow as an area where rice and food crops were grown.

[3] According to Government Regulation 3 of 2008 (GoI, 2008), an ecosystem restoration concession is granted for 60 years and can only be extended once for another 35 years.

(MoF, 2008; SNI, 2010). Harapan rainforest was established in 2008 and is managed by the PT Restorasi Ekosistem Indonesia (REKI) (Harrison, 2015). PT REKI is a Birdlife consortium which includes Burung Indonesia (i.e. the Indonesian NGO working on bird conservation), The Royal Society for the Protection of Birds (RSPB), and Birdlife International (Hutan Harapan, 2016).

Figure 2.2. Illustration of a) degraded forests along a main road, and b) typical and relatively open secondary forest in a state of recovery within a heavily logged forest.

The Harapan rainforest concession lies between the province of Jambi and South Sumatra provinces. However, this study was only conducted in the Jambi part of Harapan, which has an area of about 40,000 ha (103.25° E – 103.47° E, 2.04° S – 2.36° S). This forest, which is a lowland forests, has experienced both legal and illegal logging over the last 20-30 years (Harrison & Swinfield, 2015). Also, a forest fire took place from 1997-1998 which disturbed the development of the forest, leading to large devastation of remnants woody

vegetation, in particular among the understory (Schmidt et al., 2015). Figure 2.2. depicts the current situation of Harapan rainforest.

The elevation of the Jambi part of the Harapan rainforest ranges between 15-124 m.a.s.l. The topography is mainly flat and about 70 % of the forests having a ≤ 10 % slope. Mean annual rainfall is 2390 mm, and biodiversity is extremely high including 302 bird species, 56 species of mammals excluding bats, as well as about 600 tree species (Harrison & Swinfield, 2015). However, as the Harapan rainforest is a "protected forest island" within an intensively used agricultural landscape with a growing population, illegal logging, and the encroachment of oil palm plantations, there is considerable pressure on almost all sides.

2.2. Historical land use maps

Historical land use maps were available for the years 1990, 2000, 2011, and 2013. These maps were produced from visual interpretation of Landsat images. All of the image processing and visual interpretations involved in classifying the land use systems was carried out by the Forest Resources Inventory – Remote Sensing and GIS Laboratory of the Faculty of Forestry at Bogor Agricultural University (IPB) and was made available for this study. Further details are presented in Appendix A.1. 22 classes of land use systems were distinguished. An accuracy assessment with ground truthing data was conducted by IPB for the 2013 map. The validation points were on a 2 km square grid, considering their accessibility. Accessing the area was not an easy task due to complications in obtaining permissions. 298 ground truthing points were collected and resulted in an overall accuracy assessment of 78.2 %. The confusion matrix is in Appendix A.2. For this study, the 22 classes were aggregated into nine classes as listed in the legend of Figure 2.3 and defined in detail in Table 2.1, Figure 2.4, and Figure 2.5 show the land use for two example sub-regions with distinct dynamics.

Table 2.1. The nine land use systems used in this study. They originate by re-classifying the original 22 classes as used by MoF. Source: SNI, 2010, and MoF, 2008 modified.

Land use systems	Description	Original classes
Primary forest	Forest cover where human interventions cannot be identified.	primary dryland* forest, primary swamp forest, and primary mangrove forest
Secondary forest	Forest cover where any type of human intervention is found, such as agriculture, logging, encroachment, and also forest fires. This class is mostly a regrowth forest.	secondary dryland forest, secondary swamp forest, and secondary mangrove forest
Agriculture	Agricultural areas found either in dry or wetland. These are mostly grown with the following crops: coconut trees, durian (*Durio sp*), cassava, and duku (*Lansium parasiticum*).	dryland agriculture, mixed dryland agricultural, and paddy field
Jungle rubber	Mostly consisting of unmanaged rubber trees where the tree spacing is irregular and the rubber trees' *dbh* is > 10 cm.	jungle rubber
Rubber plantation	Rubber trees with equal spacing and age are found in an intensive managed large plantation, while rubber trees are grown with other non-rubber trees in small holder plantations. Human interventions and tree management are evident.	rubber plantation
Oil palm plantation	Oil palm plantations with equal spacing and age.	oil palm plantation
Plantation forest	Forests which are established by human intervention, e.g. timber estate, pulp and paper plantation. Plantation forests which are planted inside forest area administered by MoEF[4] is part of reforestation. These can refer to IUPHHK-HTI[5] or IUPHHK-HTR[6]. IUPHHK-HTI refers to plantation forests owned by either private or government, while IUPHHK-HTR refers to plantation forests owned by an individual or community. There are also plantation forests resulting from reforestation/afforestation in other areas that are not administered by MoEF.	plantation forest
Shrub/bush	An area that is dominated by regrowth vegetation that experiences succession. This area can be grown with pole-size vegetation having a diameter of < 20 cm, mixed of sparse natural trees having a height of < 5 m, and grasses or alang-alang (i.e. *Imperata cylindrica*).	shrub/bush and swamp bush
Others	The remaining classes.	airport, bare land, fishponds, mining, settlements, transmigration areas, and water bodies

*"Dryland" refers to mineral soil and this term is used to distinguish it from peatland (Marlier et al., 2015).

[4] According to the Presidential Regulation 16 of 2015, Ministry of Forestry (MoF) and the Ministry of Environment (MoE) was integrated in 2015 as the Ministry of Environment and Forestry (MoEF).

[5] According to the MoEF Regulation 42 of 2015, IUPHHK-HTI stands for Izin Usaha Pemanfaatan Hasil Hutan Kayu dalam Hutan Tanaman Industri which is a plantation forest concessionaire for timber production in the Industrial Plantation Forest.

[6] According to the MoEF Regulation 42 of 2015, IUPHHK-HTR stands for Izin Usaha Pemanfaatan Hasil Hutan Kayu dalam Hutan Tanaman Rakyat which is a plantation forest concessionaire for timber production in the Plantation Forest owned by an individual or community.

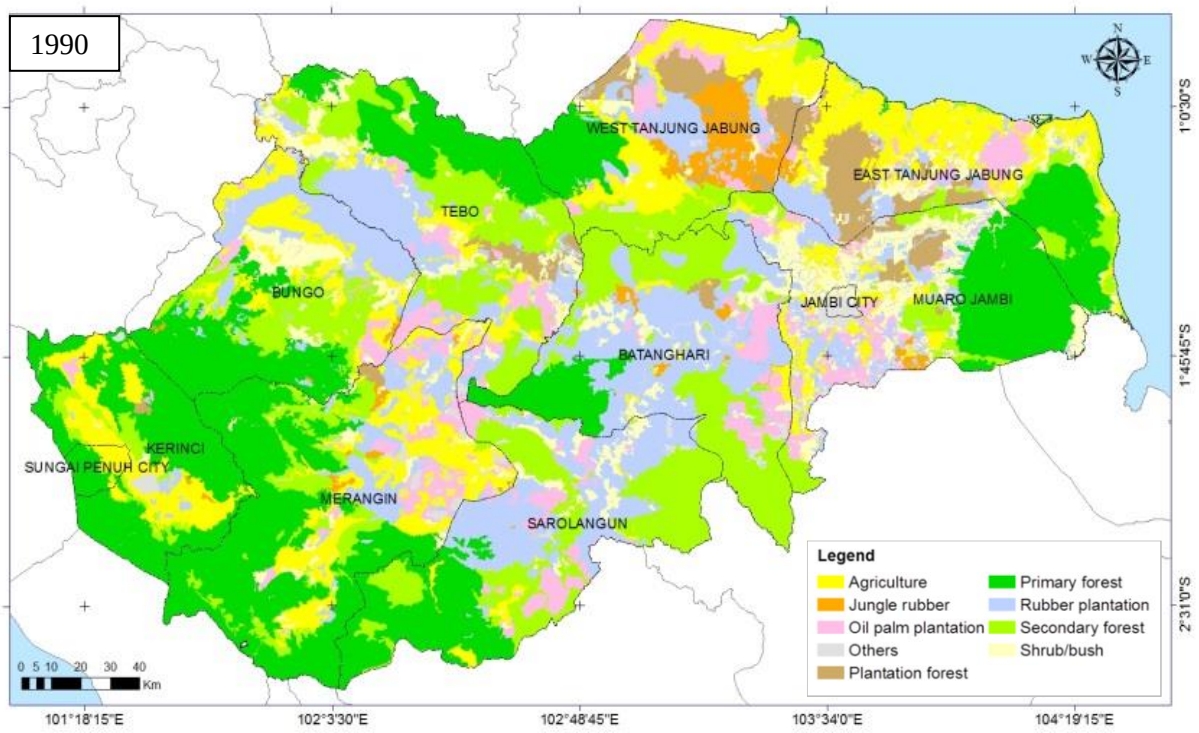
1990
WEST TANJUNG JABUNG
EAST TANJUNG JABUNG
TEBO
BUNGO
JAMBI CITY
MUARO JAMBI
BATANGHARI
KERINCI
SUNGAI PENUH CITY
MERANGIN
SAROLANGUN
Legend
Agriculture
Primary forest
Jungle rubber
Rubber plantation
Oil palm plantation
Secondary forest
Others
Shrub/bush
Plantation forest
0 5 10 20 30 40
Km
101°18'15"E
102°3'30"E
102°48'45"E
103°34'0"E
104°19'15"E
1°0'30"S
1°45'45"S
2°31'0"S

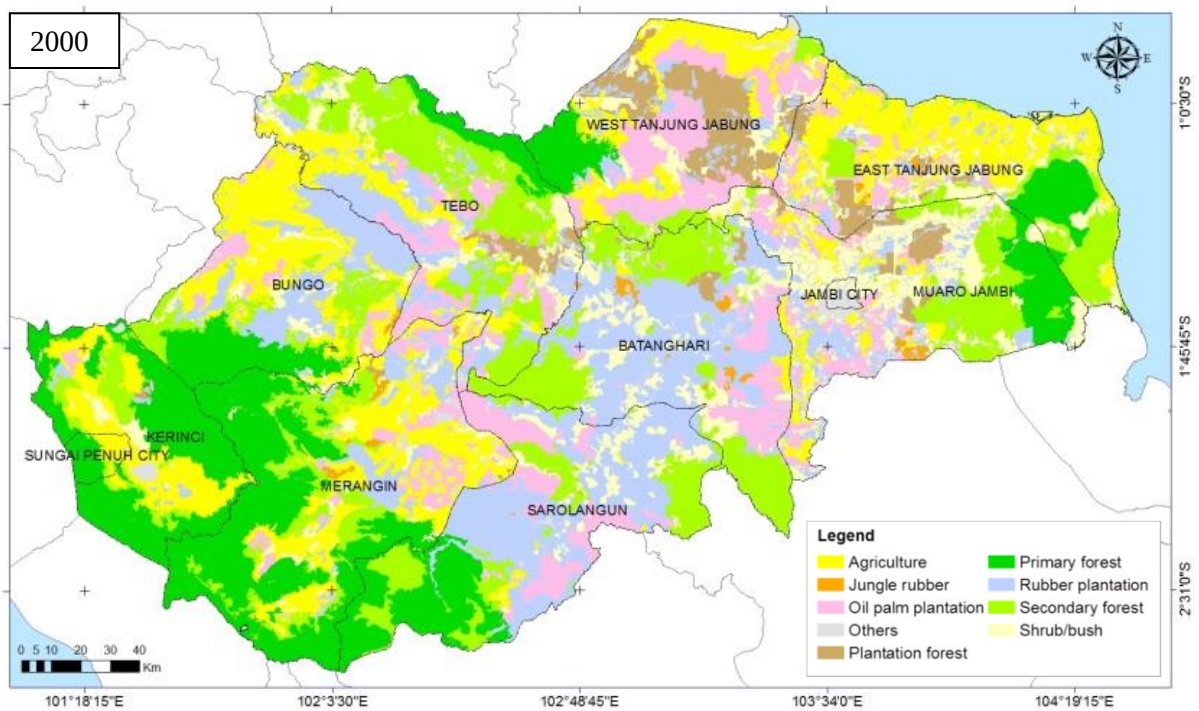
2000
WEST TANJUNG JABUNG
EAST TANJUNG JABUNG
TEBO
BUNGO
JAMBI CITY
MUARO JAMBI
BATANGHARI
KERINCI
SUNGAI PENUH CITY
MERANGIN
SAROLANGUN
Legend
Agriculture
Primary forest
Jungle rubber
Rubber plantation
Oil palm plantation
Secondary forest
Others
Shrub/bush
Plantation forest
0 5 10 20 30 40
Km
101°18'15"E
102°3'30"E
102°48'45"E
103°34'0"E
104°19'15"E
1°0'30"S
1°45'45"S
2°31'0"S

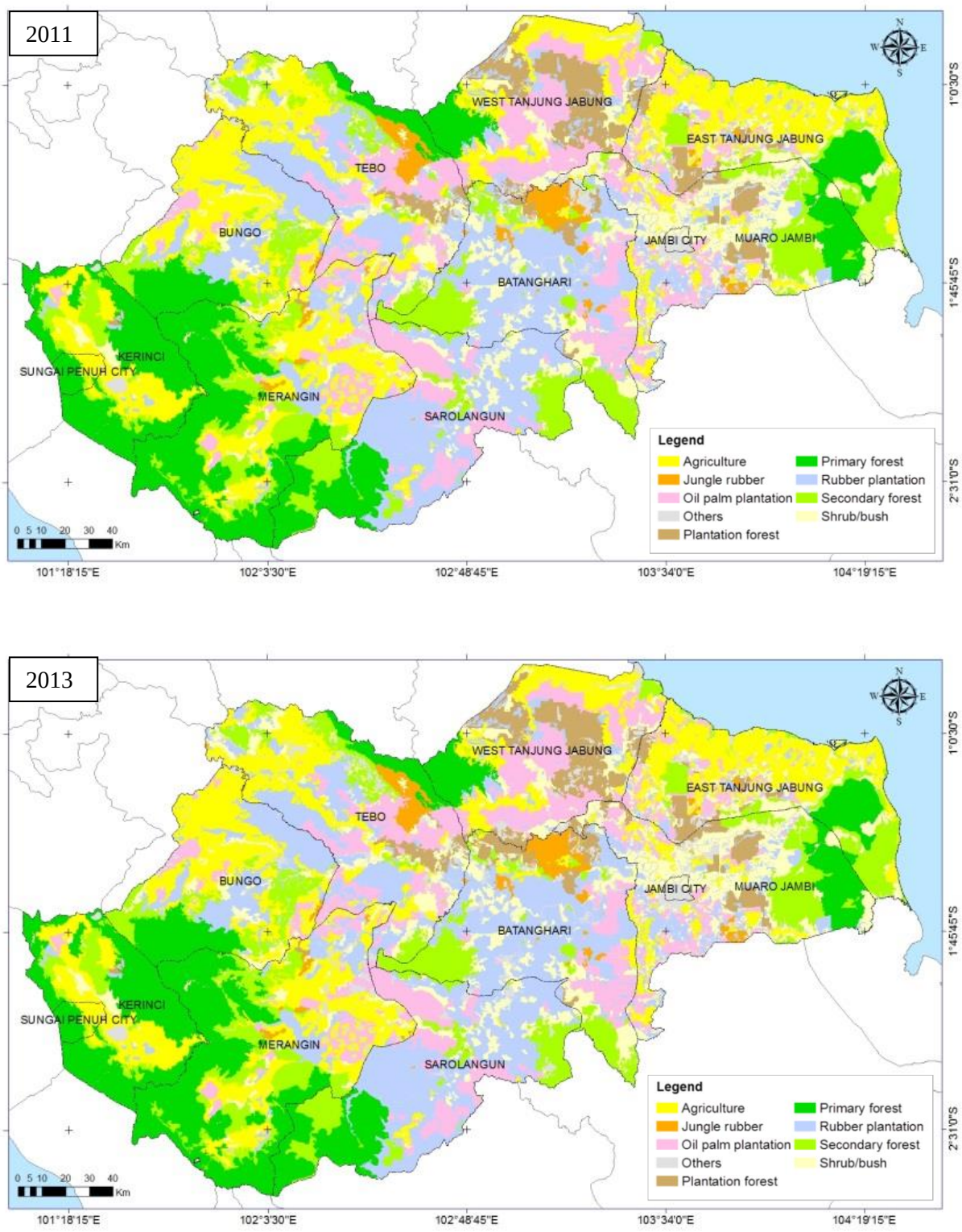

Figure 2.3. The historical land use maps from 1990, 2000, 2011, and 2013 in Jambi province. In these four different points in time, the primary forests that were located in the eastern part of Jambi province decreased in area (Figure 2.4). In the lowland area located in the southern part of Jambi, the high decrease of secondary forest areas is visible (Figure 2.5).

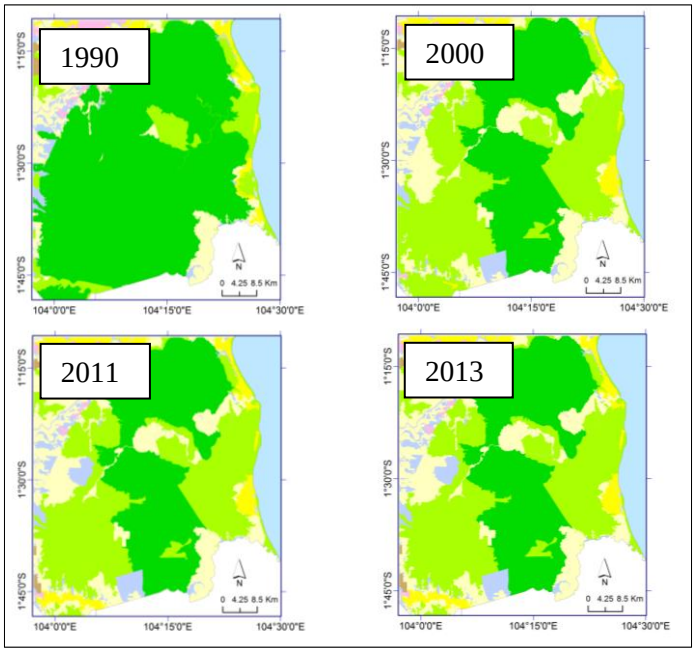

Figure 2.4. The subset of land use maps from 1990, 2000, 2011, and 2013 in the eastern area of Jambi province. The primary forest areas had decreased greatly due to the conversion into secondary forests.

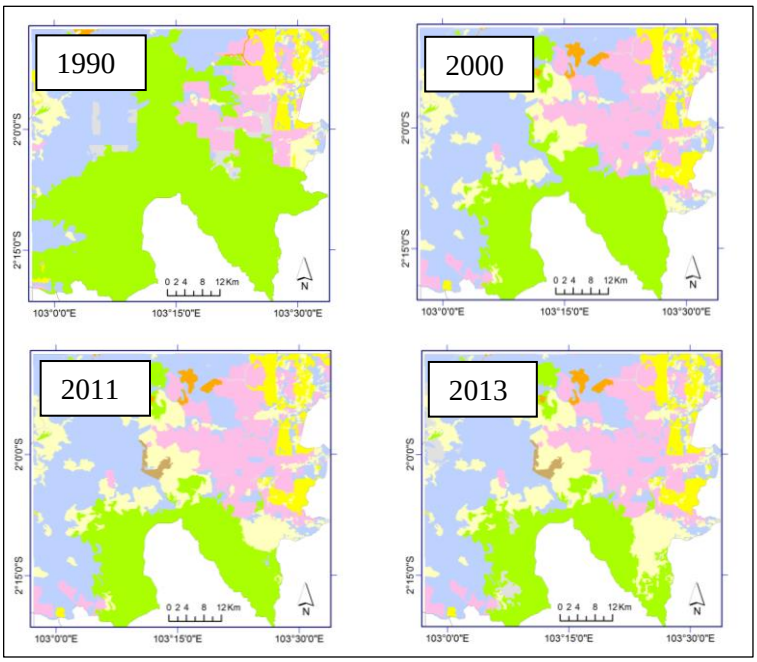

Figure 2.5. The subset of land use maps from 1990, 2000, 2011, and 2013 in the southern area of Jambi province. The secondary forest areas decreased and became fragmented.

2.3. Satellite images used

In this study, RapidEye and Landsat 8 Operational Land Imager (OLI) images were used. RapidEye images were utilized to evaluate the tree crop mapping using an object-based classification and to assess the forest variables of secondary rainforest in the Harapan restoration concession. RapidEye images have a ground spatial resolution of 6.5 m which is then re-sampled into 5 m pixel size, and are composed of five multispectral bands (blue: 440-510 nm, green: 520-590 nm, red: 630-685 nm, red-edge: 690-730 nm, and near-infrared: 760-850 nm) (Blackbridge, 2013). In order to cover the study area, five tiles of RapidEye images from June 19th, 2013, were obtained. These images contain a low cloud cover of around 1-2 %. All the RapidEye images used in this study were made available through the RapidEye Science Archive (RESA) supported by the German Aerospace Center (DLR).

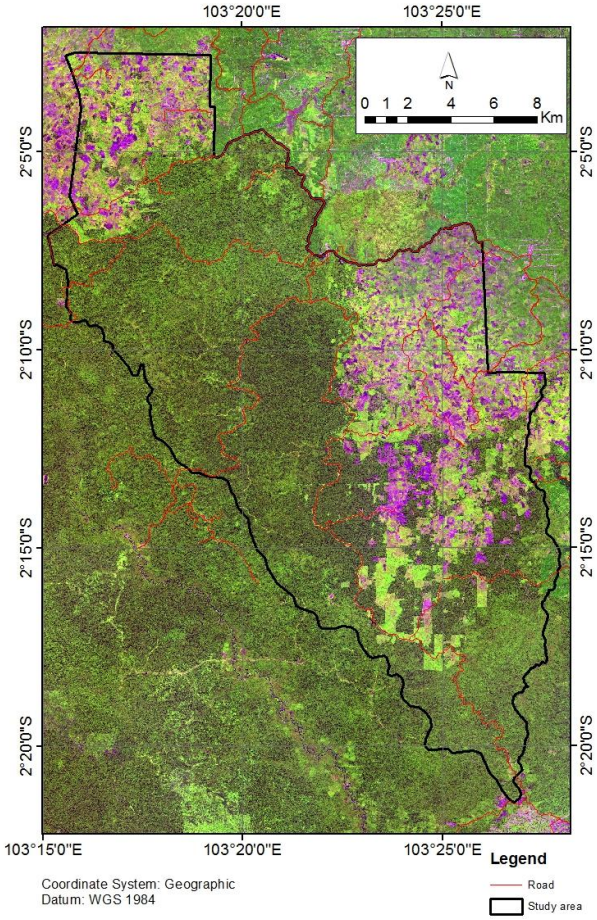

Figure 2.6. Map of RapidEye images around Harapan rainforest concession (black line) with false color composites of red: band 4, green: band 5, and blue: band 3.

Landsat 8 OLI images were used as materials to establish the sampling design for forest inventory. The use of Landsat 8 OLI images required two tiles in this study (path/row

125/61 and 125/62), which were available for free from the USGS website. Both tiles used in this study were acquired on June 27th, 2013. The Landsat 8 OLI image, excluding two thermal infrared bands, is comprised of nine spectral bands, having a 30 m spatial resolution in all except the panchromatic band, with a 15 m spatial resolution (USGS, 2016). These tiles contain a cloud cover of 38.77 % and 12.86 % for path/row 125/61 and 125/62, respectively. However, the cloud cover did not extend into the study area around Harapan rainforest.

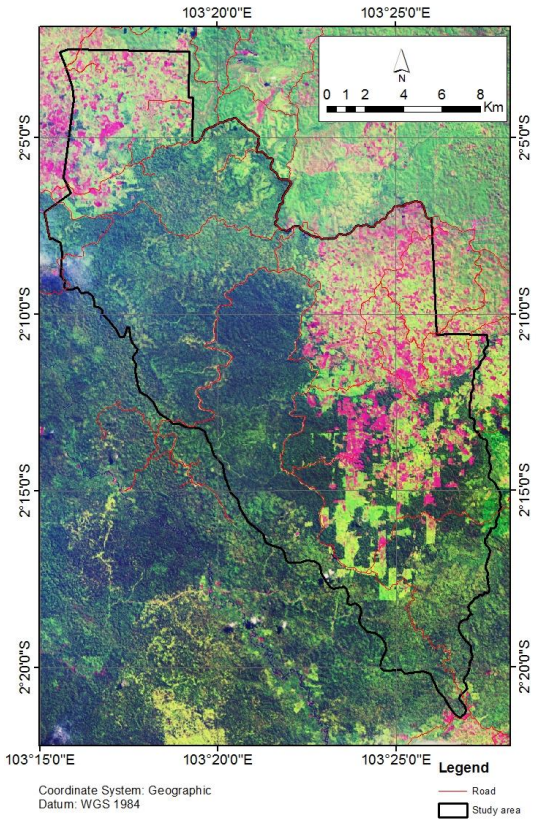

Figure 2.7. Map from Landsat 8 OLI images around Harapan rainforest concession (black line) with a false color composite of red: band 6, green: band 5, and blue: band 4.

RapidEye (Level 3A) and Landsat 8 OLI (Level 1T) images used in this study were delivered as products that were geometrically-corrected and processed with a terrain correction based on available Ground Control Points (GCPs) and Digital Elevation Model (DEM). The source of GCPs for RapidEye products comes from Geocover 2000 and Global Land Surveys (GLS) 2000 datasets, while the DEMs are retrieved from PlanetObserver PlanetDEM 90 (Blackbridge, 2013). For Landsat 8 OLI, the GCPs were obtained from GLS 2000 datasets, while the DEMs were retrieved from GLS DEM datasets (USGS, 2016).

Chapter 3
Methodologies

3.1. Monitoring land use systems

3.1.1. Analyses of land use change and spatial pattern

Analyses of land use change were conducted to evaluate land use transitions in order to give insights into temporal dynamics between classes of transitions. Spatial pattern was also analyzed which did allow an analysis of temporal dynamics of fragmentation. Land use changes and spatial pattern analyses were carried out on land use maps from 1990, 2000, 2011, and 2013 as described in chapter 2. For the purpose of evaluating land use change, the net change of land use systems was quantified. The net change, which can be presented as a net decrease or net increase, quantifies the total changes—including losses and gains (UNEP, 2009). As the changes of primary and secondary forests are of high concern, the quantification of annual gains and losses in three different periods (1990-2000, 2000-2011, and 2011-2013) was also conducted. For the purpose to evaluate land use transitions, transformation matrices were analyzed.

It is, however, insufficient to only understand the change in area from an ecological perspective as the change of land use is also followed by a change of landscape structure (Curatola Fernández et al., 2015). The disturbances that change the landscape would then alter the landscape's pattern and might further impact species diversity (Franklin, 2001). Therefore, the change in the landscape structure was also quantified. The quantification of the landscape structure provides information such as the level of habitat fragmentation, which is of particular interest for understanding the impact of land use transformation on ecological processes (e.g. biodiversity loss) (Fahrig, 2003). Landscape structures consist of landscape composition and configuration (Griffith et al., 2000). Of these, landscape composition measures the presence or extent of each land category with no information regarding spatial connectivity, whereas landscape configuration measures the arrangement or spatial distribution of features within specific landscapes (McGarigal & Marks, 1995). In fact, spatial pattern analyses for quantifying landscape structures have been widely

implemented using landscape metrics (Curatola Fernández et al., 2015; Du et al., 2014; Southworth et al., 2004). The quantification of spatial patterns from the historical land use maps in this study did allow an analysis of temporal dynamics of fragmentation.

While a large amount of landscape metrics are provided by common software, they are mostly correlated (Griffith et al., 2000). In this study, two metrics were selected (i.e. mean patch size and aggregation index) to analyze the spatial pattern of four major land uses where transformation took place, i.e. secondary forest, jungle rubber, rubber, and oil palm plantations. The computation of these metrics was done for all different points in time (i.e. 1990, 2000, 2011, and 2013). It was applied using the 'SDMTools' library in the R package (VanDerWal et al., 2014). Mean Patch Size (MPS) in ha was calculated for each class, representing a ratio of the total area for a given class and number of patches for that class. Small MPS for particular land use types indicates more fragmentation than larger MPS within a landscape (Horning et al., 2010).

The Aggregation Index (AI) provides knowledge on the aggregation level of certain classes, in which a lower index value means a more dispersed and fragmented class (He et al., 2000). The AI is a percentage of the ratio between total shared pixel edges for a given class and maximal shared pixel edges when the class gets clumped as one patch (He et al., 2000; McGarigal, 2015). According to He et al. (2000), the AI is formulated as follows:

$$AI_i = (e_{i,i}/max\_e_{i,i}) \times 100\% \quad (1)$$

where:

AI is aggregation index for class i (%),

as the AI is implemented for raster data, $e_{i.i}$ is the total shared pixel edges among the cells within one class,

$max\_e_{i,i}$ is the maximal shared pixel edges when a particular class clumps in a one patch (this patch does not need to be a square).

$max\_e_{i,i}$ is calculated based on the following formulas,

if $m = 0$, $max\_e_{i,i} = 2n (n - 1)$, or

if $m \leq n$, $max\_e_{i,i} = 2n (n - 1) + 2m - 1$, or

if $m > 0$, $max\_e_{i,i} = 2n (n - 1) + 2m – 2$.

where:

n is the square root of the largest square smaller than A_i (number of pixels of class *i*),

$m = A_i - n^2$

For instance, as class *i* has 11 cells (A_i), the largest square smaller than A_i will be 9 cells, n = 3 and m = 2. Based on these values (i.e. m and n), the maximal shared pixel edges ($max\_e_{i,i}$) are 15.

In order to illustrate the mean patch size and index of aggregation in different levels, the binary landscapes shown in Figure 3.1 are depicted, where 0 is the background (white) and 1 is the class 1 (gray).

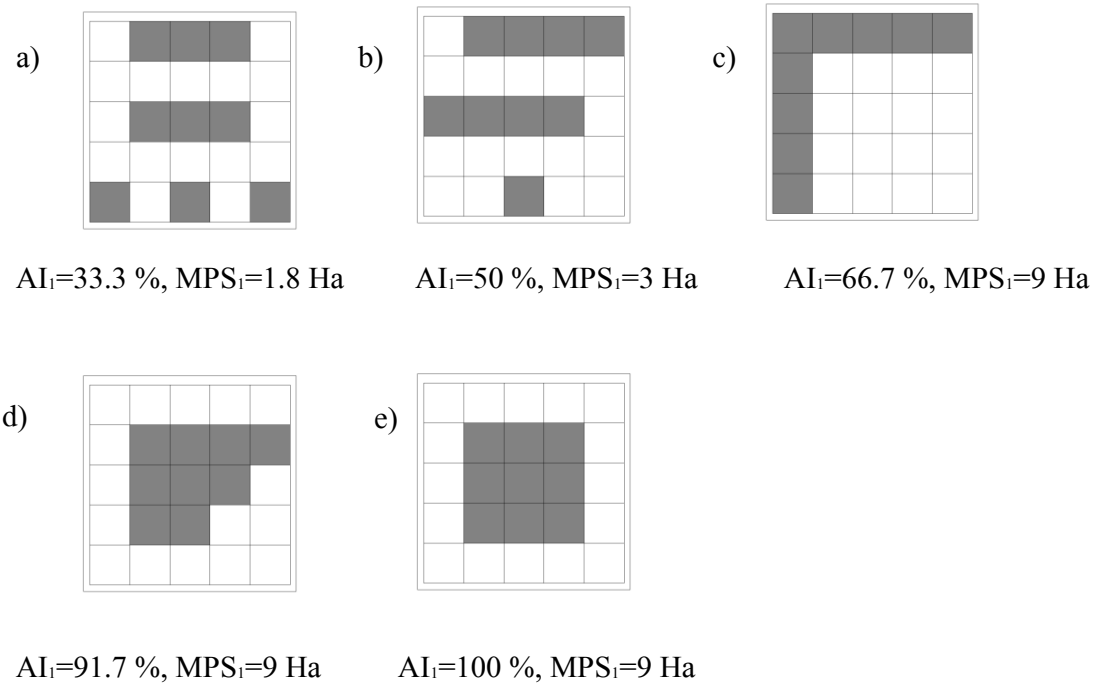

Figure 3.1. Different spatial patterns at class 1 shown in gray (adopted from He et al., 2000).

3.1.2. Factors related to deforestation

In this study, deforestation includes the changes from any forest type to any non-forest type. In order to analyze the factors potentially driving or related to deforestation, the approaches of Geist & Lambin (2002) are followed. Those authors address factors causing tropical deforestation as a combination of underlying driving forces and proximate causes. Proximate causes are "direct causes", such as agricultural expansion, timber extraction, infrastructure development, and other factors. Other factors consist of biophysical factors, slope and elevation. Underlying driving forces imply "indirect causes" like socio-economic factors where the terms are, of course, frequently related to proximate causes.

In this study, two different approaches were applied to analyze factors that are related to deforestation. The first approach incorporated topographic variables, including slope and elevation, taken from NASA's Shuttle Radar Topography Mission (SRTM) with a spatial resolution of 30 m. The slope and elevation maps were masked with the deforestation map for each period (i.e. 1990-2000, 2000-2011, and 2011-2013), and the distribution of deforestation at different levels of slope and elevation was identified.

The second approach analyzed socio-economic variables at district level. Socio-economic variables were computed as the annual change of each variable for each of the nine districts in Jambi province, as was deforestation as the dependent variable (Table 3.1). These socio-economic variables were only completely available for the years 2000/2001, 2010/2011, and 2013; the year 1990 was not completely available.

Table 3.1 Variables used to analyze the relationship of socio-economic factors on district level to deforestation rates.

Variable	Data source	Unit per district
Dependent variable:		
Annual deforestation	Land use maps of 2000, 2011, and 2013	ha/year
Independent variables:		
Population density	Statistics Bureau of the Jambi province	persons/ha
Gross Regional Domestic Product (GRDP) per capita		Rupiah
Rubber productivity	Estate crop Bureau of the Jambi province	kg/ha
Palm oil productivity		kg/ha
Rubber farmers		Number (count)
Palm oil farmers		Number (count)

The relationship of each factor to deforestation was estimated by simple linear regression. In this study, the data set of a province was considered a "population" (= all census of province of Jambi) and not a sample, so that *p*-values, significances, and other sampling statistics were not calculated. The model was implemented using the function lm() in R (R Core Team, 2015).

$$\Delta_i = \beta_0 + \beta_i \cdot x_i + \varepsilon_i \quad (2)$$

where:

Δ_i is the annual deforestation of the i-th observation where $i = 1,\ldots, n$, β_0-β_i are the model coefficients, x_i is the predictive variable (potential driving forces), and ε_i is the random error term.

3.2. Evaluation of the tree crops mapping using high spatial resolution images

3.2.1. Image pre-processing

At the satellite sensor, the reflected electromagnetic radiance of various ground surfaces on the earth is recorded as digital numbers (DNs) for each wavelength or spectral band (Lillesand et al., 2008). The spectral radiances of the ground surface recorded by a satellite sensor are very much dependent on the latitude, weather condition, season, time of image acquisition, and other factors. Therefore, the radiance's intensity of a particular feature on the ground will vary when it is derived from a satellite image with different acquisition times, as different interactions with the atmosphere at different times will be present. In order to bring these radiance to a common standard, so that the same ground feature has the same digital number per spectral channel, radiometric correction needs to be employed.

In this case, the atmospheric effect should be corrected in order to get meaningful measure of ground surface reflectance (Tso & Mather, 2009). However, such atmospheric correction is required depending on the purpose of the study. While this is not necessary to apply when land use mapping is done using a single acquisition date, it is important for change detection where multiple acquisition dates are used (Tso & Mather, 2009). When the atmosphere influence is not considered, the Top of Atmosphere (TOA) reflectance is quantified (Blackbridge, 2013). The value of this reflectance ranges from 0-1 or 0-100 %. For the five tiles of RapidEye images with the same acquisition time used in this study, the TOA reflectance was quantified for each tile following Blackbridge (2013).

3.2.2. Image segmentation

By using high spatial resolution images, the map can be produced with smaller minimum mapping units so that objects are mapped in more detail. It should be taken into account that high spatial resolution shows objects on the ground as groups of pixels with a relatively high spectral variability due to complex spectral responses (Blaschke et al., 2014; Rico & Maseda, 2012). This means that one pixel might inform different objects from nearby

pixels, even though they represent similar objects. Therefore, the pixel-based method for classification might result in low performance and produce salt and pepper effects. This drawback can be overcome using an approach called object-based image analysis (OBIA) (Blaschke et al., 2014).

Object-based image analysis comprises the segmentation and classification of the image (Lillesand et al., 2008). Image segmentation aims at clustering image's pixels into meaningful objects in which neighboring pixels with homogenous features are merged (De Sousa et al., 2012; Marpu et al., 2010). From the objects produced, the target classes (e.g. land use/land cover) are then assigned to a number of objects that are selected as a training area. Based on the training area, classification is then applied to the whole of the image. It is apparent that the segmentation algorithm that creates objects plays an important role in classification accuracy (Neubert et al., 2008).

This study used the mean shift segmentation algorithm that has been commonly implemented in studies of image classification with remote sensing data (Bo et al., 2009; Büschenfeld & Ostermann, 2012; Kun et al., 2010; SushmaLeela et al., 2013; Yang et al., 2013). According to Comaniciu and Meer (2002), Huang and Zhang (2008), the OTB Development Team (2015), and Xiao-gu et al. (2009), the mean shift segmentation approach is described (Figure 3.2):

1. Firstly, the two radii of the search window, the spatial radius h_s and the range (= spectral radius) h_r, are defined in order to collect a number of pixels to further define a segment in the n-dimensional feature space. The n-dimensional is $2 + p$, where two represents the spatial domain and p represents the spectral domain. The spatial radius (h_s) represents the maximum spatial distance (in pixels) to adjacent pixels that are incorporated in the analysis and the range radius (h_r) represents the maximum spectral distance included within an object representing the distance of grey level (see Table 3.2). A larger radius produces fewer objects, as such approach is more inclusive,
2. The mean or mass center is computed from these pixels,
3. After the mean is determined, the central point of those pixels is shifted to the determined mean,
4. This mean becomes a central point of a new window, and the mean among a set of pixels is iteratively calculated. This leads to continuously shifting the central point towards the dense pixels until it converges to the mean.

5. When convergence is achieved, the pixels that are associated to the last central point are clustered to an object. For clustering, a minimum region size (M_r) is defined to reduce small objects and, thus, cluster which has region size less than M_r is merged.

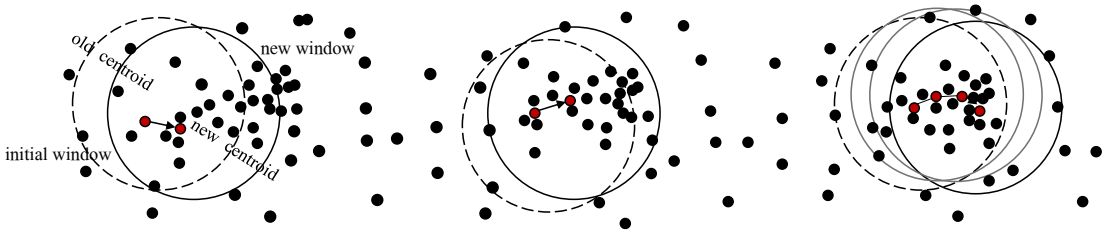

Figure 3.2. An illustration of mean shift algorithm approach (adopted from Xiao-gu et al., 2009). According to the defined h_s and h_r, a set of pixels were selected at the initial window. The central point of the initial window is then shifted to the mean value of this group of pixels becoming new central point of new window. This new central point is continuously shifted until it converges.

Table 3.2 Selected parameter settings for image segmentation.

Parameter	Levels	Unit
Spatial radius (h_s)	5, 10, 15	Pixel
Range radius (h_r)	0.005, 0.01, 0.015, 0.02	TOA reflectance
Minimum region size (M_r)	10, 30, 50	Pixel

Different compositions of segmentation parameters were determined in this study, as can be seen in Table 3.2. By combining these parameters, the mean shift segmentation was carried out using the Orfeo Toolbox (OTB Development Team, 2015).

3.2.3. Identification of suitable segmentation parameters

The mean shift segmentation using different parameter settings produced a number of segmented images. As the objects produced by segmentation parameter settings play a key role in the classification accuracy, criteria need to be defined to find the best segmented image for a given purpose and given image resolution. The selection of optimal segmentation parameters is a challenge (Smith, 2010). Until now, there are no standard approaches to quantitatively evaluate "segmentation accuracy". Smith (2010) used SPOT 4/5 imageries to classify six land cover classes including perennial, crop, trees, open water, wetland vegetation, and urban area. For image segmentation, he selected the optimum parameter settings by comparing different results of segmented images based on the classification accuracy produced by a classifier. He applied the Random Forests algorithm to derive the classification models for each segmented image. From these different classification models, the one having the lowest error rate was selected as the best

parameter settings. Other approaches conducted by Carleer et al. (2005) and Marpu et al. (2010) have evaluated the selection of optimum parameter settings by comparing segmented images and pre-defined reference objects which were visually digitized.

The study of Carleer et al. (2005) aimed to evaluate and compare different kinds of segmentation algorithms. IKONOS Panchromatic image was used in their study. Pre-defined reference objects used as a comparison to the segmented image were derived from five reference images with different land use types. The extent of each reference image is 256 x 256 m. Each reference image represents a particular land use type; one of a rural area, a residential area, an urban administrative area, an urban dwelling area, and a forest area. Each feature at each reference image was then visually delineated as reference objects, with a minimum object of four pixels chosen. The different segmented images produced by different segmentation parameter settings were then evaluated based on the percentage of the mis-segmented pixels of the total pixels in the segmented image and also the average percentage of mis-segmented pixels for every reference region. They also evaluated over-segmentation and under-segmentation by calculating the ratio between the number of objects in segmented images and the number of objects in the reference, where a ratio > 1 means over-segmentation and a ratio < 1 means under-segmentation. In their study, the optimum segmentation was chosen when low percentage of mis-segmented pixels was achieved and under-segmentation did not occur.

The study of Marpu et al. (2010) aimed to analyze segmentation results by defining under- and over-segmentation. They used two scenes of IKONOS images from two different regions for evaluating the segmentation results. Of these, ten reference objects were visually delineated for each scene. The criteria to define the reference objects were that they must be a distinctly separable feature and varied in land cover class, texture, form, contrast, and area. The reference objects covered six classes including built areas, roads, gardens, open areas, forest cover, and water bodies. In their study, the collection of reference objects was purposively selected. Comparisons between segmentation results and reference objects were then conducted to find optimum parameter settings through an evaluation of the under- and over-segmentation. When the reference object is segmented into different sub-objects, the percentage of the biggest sub-object, after eliminating the "extra pixels", is defined as over-segmentation. "Extra pixels" are defined as the pixels of the sub-objects that are not overlapped with the reference object. Besides extra pixels, they also defined "lost pixels". "Lost pixels" are the pixels that are found in reference objects but not as part of the segmented image. The percentage of extra pixels and lost pixels are

defined as under-segmentation in their study. In the study by Marpu et al., the best parameter setting was selected according to the high percentage of over-segmentation.

However, no approaches that have been mentioned above consider the correct percentage of overlapping segments between the segmented image and reference objects. This metric is relevant to be an indicator to evaluate the segmentation. An approach that considers the correctly identified percentage was developed by Hoover et al. (1996) and provides a number of performance metrics. These metrics are then called Hoover metrics and consist of over-segmentation, under-segmentation, correct detection, missed detection, and noise detection.

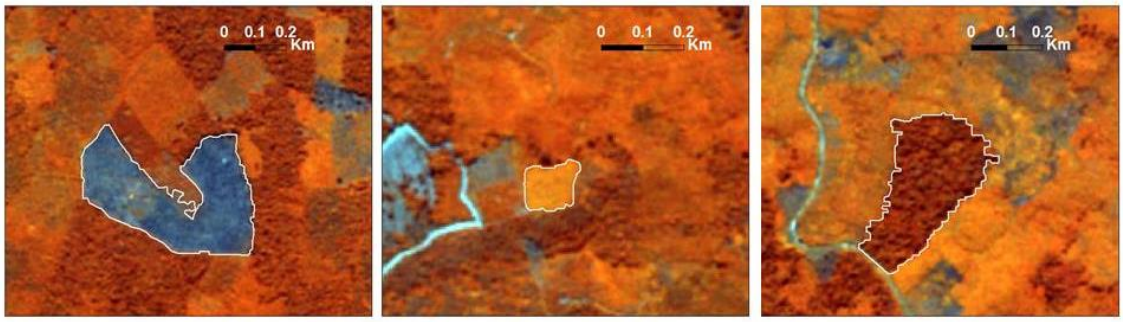

Figure 3.3. Representation of the digitized reference objects (shown in the white polygon). The objects (from left to the right) are bare land, shrub/bush, and forest, accordingly.

In order to select the best segmentation parameter settings, comparisons between the reference objects and the segmented images based on the Hoover metrics were done in this study. Reference objects were created from one single RapidEye tile in order to reduce the time required for comparing segmentations. This tile was selected because it has all specified land cover classes, including a large river within the study area. In regard to the similarity of spectral reflectance of the ground surface, this tile is comparable to the other four tiles used in this study due to the same time of acquisition. These reference objects were selected following the criteria as mentioned in Marpu et al. (2010). The selection of reference objects was purposively made, where all the features that were selected as reference objects must be distinctly separable objects. Moreover, they were distributed across the image as can be seen in Figure 3.4 and covered different land cover types including vegetated and non-vegetated area. Altogether, thirty objects were visually digitized (see examples in Figure 3.3).

The calculation of Hoover metrics was conducted using the Orfeo Toolbox (OTB Development Team, 2015). Referring to Hoover et al. (1996), these metrics are explained

in the following descriptions: M is the number of objects from the segmentation algorithm and N is the number of reference objects. P_m is the number of pixels for each object or region, R_m ($m = 1 \ldots M$), and P_n is the number of pixels for each reference region, R_n ($n = 1 \ldots N$). Then, $O_{mn} = R_m \cap R_n$ denotes the number of pixels that overlap within the regions R_m and R_n. In case of no overlap, $O_{mn} = 0$, and a perfect overlap, $O_{mn} = P_m = P_n$. Thus, a M x N table for $m = 1 \ldots M$ and $n = 1 \ldots N$ is constructed, where the percentage of O_{mn} is implicitly calculated for each entry. The calculation of overlapping percentages is done for each object in respect to the size of the object from the segmentation algorithm as O_{mn}/P_m and of the reference object as O_{mn}/P_n. The percentage is further used to define whether the region is classified as correct detection, over-segmentation, under-segmentation, missed detection, or noise. The procedures to define the metrics are strictly based on a defined threshold T, which shows the percentage of overlapping pixels. It means that the threshold T defines how strict the overlapping area which will be counted. It has been defined that the range is between $0.5 < T \leq 1$. The highest threshold which is 1 means that overlap area between the segmented image and reference object must be 100 %. In this study, a medium strictness where the threshold $T = 0.75$ was defined. To calculate each metric, the following definitions are used (Hoover et al., 1996):

1. Correct detection

   Both objects of R_m in the segmented image and R_n in the reference are classified as correct detection if

   a. $O_{mn} \geq T$ x P_m (at least T% of the pixels in R_m overlap in R_n), and

   b. $O_{mn} \geq T$ x P_n (at least T% of the pixels in R_n overlap in R_m).

2. Over-segmentation

   An object R_n in the reference set and a number of objects $R_{m_1}, \ldots, R_{m_x}$, ($2 \leq x \leq M$), in the segmented image are classified as over-segmentation if

   a. $\forall i \in x$, $O_{m_i n} \geq T$ x P_{m_i} (for all i of object 1,…, x, at least T% of the pixels for all objects in R_{m_i} overlap in R_n), and

   b. $\sum_{i=1}^{x} O_{m_i n} \geq T$ x P_n (at least T% of the pixels in R_n overlap in the union of regions $R_{m_1}, \ldots, R_{m_x}$).

3. Under-segmentation

A number of reference objects in $R_{n_1},\ldots, R_{n_x}$, ($2 \leq x \leq N$), and an object R_m in a segmented image are classified as under-segmentation if

a. $\sum_{i=1}^{x} O_{mn_i} \geq T$ x P_m (at least T% of the pixels in R_m overlap in the union of regions $R_{n_1},\ldots, R_{n_x}$), and

b. $\forall i \in x$, $O_{mn_i} \geq T$ x P_{n_i} (for all i of object 1,…, x, at least T% of the pixels for every objects in R_{n_i} overlap in R_m).

4. Missed detection

   An object R_n in the reference set that is not classified as correct detection, over-segmentation, or under-segmentation is defined as missed.

5. Noise

   An object R_m in a segmented image that is not classified as correct detection, over-segmentation, or under-segmentation is defined as noise. It is also part of missed classification.

For each metric, the score is computed as described in Appendix A.6.

Compared to under-segmentation, over-segmentation is preferable because objects can still be grouped in the post-processing when over-segmentation occurs, while one might lose objects when under-segmentation happens (Marpu et al., 2010). However, the advantage in carrying out the segmentation before classification can be lost if over-segmentation is too high (Carleer et al., 2005). Having a high amount of over segmentation is not the only main purpose of image segmentation as the correctness of segmented images also plays an important role for further steps of image classification. Moreover, the higher the over-segmentation, the more time is needed for further steps towards image classification. Therefore, in this study, the best segmentation parameter settings were selected when the respective settings produced a high over-segmentation score but still performed a correct segmentation. A trade-off between over-segmentation and correct detection score was identified to select the best parameter settings of image segmentation.

3.2.4. Training data collection

Training data were collected on a 2.5 km square grid from a systematic sample (Figure 3.4). A number of regular grids with a distance of 2.5 km were established. For each grid point ($n = 155$), a square 200 m by 200 m plot was visually interpreted for land use systems for all segments that either fully or partially overlapped with the plots.

Table 3.3 Classification key for segmentation. Source: SNI, 2010, and MoF, 2008 modified.

Land use systems	Description
Secondary forest	Forest cover where any activity due to human intervention is found either earlier or current event, such as agriculture, logging with visible logging tracks, encroachment, and also natural events such as forest fires. This class is mostly a regrowth forest.
Jungle rubber	An area that is similar to secondary forest where human intervention takes place and is mostly grown with unmanaged rubber trees where the tree spacing is irregular and the rubber trees' *dbh* is > 10 cm.
Rubber plantation	Rubber trees with equal tree spacing and age. In small holder plantations, rubber trees are grown with non-rubber trees. Human interventions and tree management are evident.
Oil palm plantation	Homogenous plantations with equal tree spacing and age of oil palm.
Shrub/bush	An area that is dominated by regrowth vegetation. This area can be grown with pole-size vegetation having a *dbh* of < 20 cm, mixed of sparse natural trees having a height of < 5 m, and grasses or alang-alang (i.e. *Imperata cylindrica*). Home gardens and swidden agriculture are categorized in this class.
Bare land	Open areas such as burnt areas, roads, and cleared areas. Roads were classified in this class as most of the roads were only an open land without asphalt.
Settlement	An area where people reside with certain infrastructure.
Water body	Ponds, lakes, and rivers.

In addition to the segments that overlapped into the plots, additional training data were added as the systematic sampling design yielded only few training data for more rare land use types like settlement and water body. To get better results from the classification model, training data for those classes were manually added by defining some areas that were easily recognized. As a result, the selection of training data was a mix of statistical sampling and non-statistical sampling. Some land use types that were recognized within the study area are described in Table 3.3. These land use types came from the same references as Table 2.1 with a slight difference because of some aggregation classes in Table 2.1. The land use classes for entire Jambi province are more varied than in this study area and, thus, the classes here are lesser.

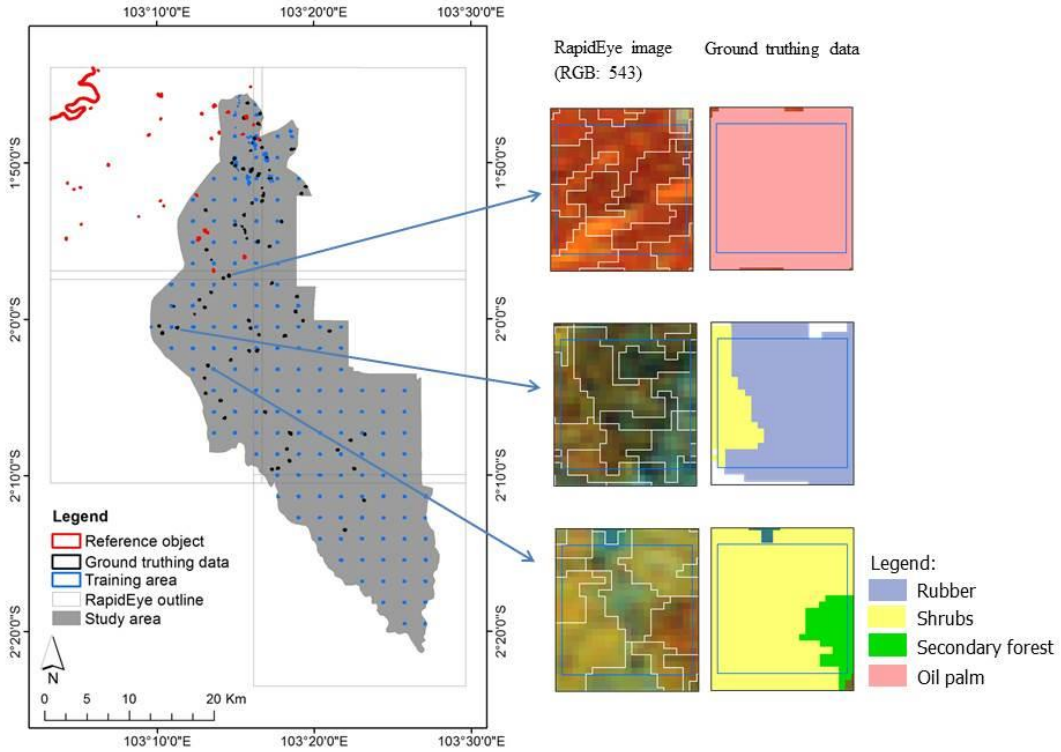

Figure 3.4. Location of reference objects, ground truthing data, and training area within Harapan landscape. Some examples of ground truthing data at three different plots are depicted.

Local knowledge based on field observations within the study area and Google Earth images with higher spatial resolution in some parts of study area were used to assist during the interpretation of training data. As the images from Google Earth were not up-to-date, an adjustment was applied. For instance, if a secondary forest was identified in Google Earth images but was obviously shrub/bush when interpreted in RapidEye. That is the RapidEye image was used as reference for interpretation. In this case, it would then be interpreted as shrub/bush because the RapidEye images were more recent.

3.2.5. Image classification

The predefined training data, as previously described, were used as the input for image classification. In order to apply object-based classification, the Random Forests (RF) classifier developed by Breiman (2001) was implemented using the 'randomForest' R package (Liaw et al., 2014). This classifier is widely applied in remote sensing for vegetation and land use mapping (Chan et al., 2010; Chapman et al., 2010; Duro et al., 2012; Immitzer et al., 2012; Magdon et al., 2014; Puissant et al., 2014; Rodriguez-Galiano et al., 2012).

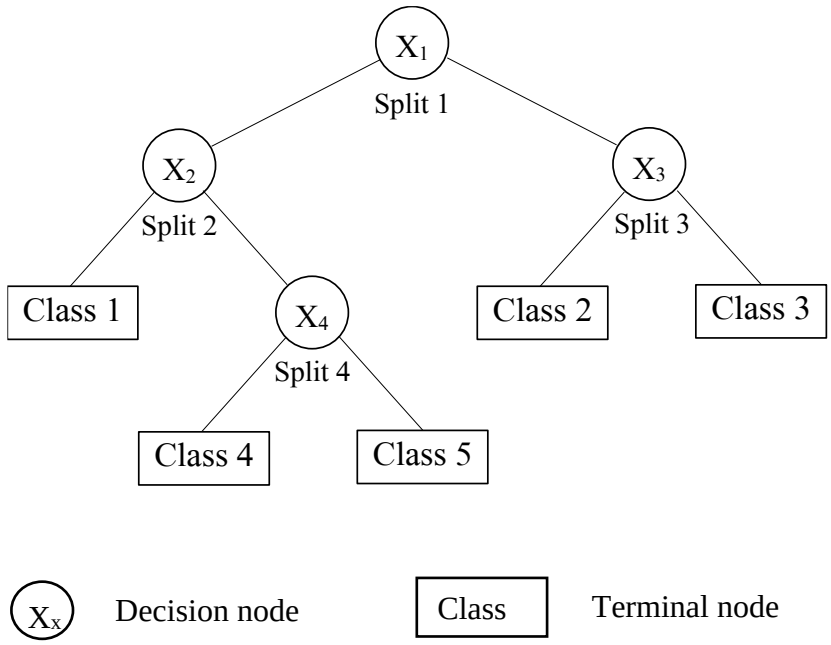

Figure 3.5. Structure of a decision tree (adopted from Breiman et al. 1984).

The RF classifier generates a number of decision trees and assigns the final class based on a majority vote within all the trees (Breiman, 2001; Liaw & Wiener, 2002). Basically, each decision tree consists of binary decisions that are constructed by several nodes connected by branches and continues to grow to reach terminal nodes where a class assignment is eventually achieved (Breiman et al., 1984; Horning, 2010). The structure of such an individual decision tree is depicted in Figure 3.5. A decision tree is grown by a process that randomly selects a subset of training data with replacements (so that there is no data exclusion for the next subset), the so-called bootstrapping (Breiman & Cutler, 2004; Liaw & Wiener, 2002). RF uses two-thirds of the original training data in the bootstrapping process and the remaining samples of training data (one-third), the so called Out-Of-Bag (OOB) samples, are used to estimate the error of the predicted model (Liaw & Wiener, 2002). When growing the tree, the root node or initial node will be split into other nodes based on the best-splitting variable among a subset of randomly-selected predictor variables. The best split is defined by using the Gini Index which measures the degree of impurity (or purity). Through this measure, the best split of each node is defined with the decrease in impurity. This means that the descendant node is "purer" than the parent node (Breiman et al., 1984). The smallest impurity (or highest purity) occurs when only one class is found at a node.

A default of two predictive variables for each split and 500 decision trees was implemented in this study. The number of decision trees was chosen as the gain in accuracy of the model

from more than 500 decision trees has been found to be generally low (Breiman and Cutler, 2004). Overall, eight predictor variables were used here, consisting of five RapidEye's bands with a TOA reflectance value of band 1 (B1), band 2 (B2), band 3 (B3), band 4 (B4), and band 5 (B5), the Normalized Difference Vegetation Index (NDVI) (Gamon et al., 1995), NDVI Red-edge (NDVI_RE) (Schuster et al., 2012), and the ratio between the perimeter and area of each segment (PARA). For each predictor variable, the mean value was generated for each segment.

In order to minimize the overfitting due to correlated predictive variables used in the RF model for further classification, fewer predictive variables were selected (Magdon et al., 2014). The classification was further implemented by choosing the variables according to the mean decrease in accuracy derived from the RF algorithm, where the variable importance is measured (Liaw & Wiener, 2002). Essentially, the variable importance is measured from the error produced by the permutation of the OOB data for particular predictor variables, while other predictor variables are not altered. When the permutation of certain variables produces a high decrease in accuracy, it means that these variables are highly important.

3.2.6. Map validation and accuracy assessment

With the RF classifier, there is the possibility to quantify the model-based error from the OOB samples when predicting the model from the training data. Nonetheless, the quality of the produced map needs to be validated as well. A set of independent data is required for this map validation and such data was collected from the field.

A stratified random sampling that also considered accessibility was implemented to collect the independent land use data. A buffer extending 500 m from the road was generated to locate the ground truthing data. Such distance was chosen due to the challenging terrain and land cover in some areas. For instance, there was considerable understory found in secondary forests, jungle rubber, unmanaged rubber plantation, and shrubs so that much effort is needed to reach the point. Therefore, a buffer of 500 m was expected as a relevant distance for reducing time spent walking to reach the validation points.

For each land use system in the classified map, 100 sample points were randomly selected within the buffered area. A generation of 100 sample random points gave a chance to select the most accessible validation points. The validation points that were located in a challenging area with high risk of security due to illegal encroachment as well as limited

access to concessionaire properties were not taken. Among these points, a selection of validation points was then taken proportionally according to the extent of each land use system. The amount of validation points for each land use system was 50 % from the percentage area of land use systems. For example, if the area of forest in the study area is 40 %, then the validation points are 20 points. To get appropriate validation points for smaller land use systems areas, a minimum number of 10 validation points was set up.

As land use mapping was based on object-based classification, map validation was evaluated for each segment (= object) (Myint et al., 2011; Pu et al., 2011). Thus, a square plot of 100 x 100 m was centered at each validation point. Within this square plot, segments produced by the best parameter settings were superimposed. For each segment that was accessible, land use was observed in the field according to the classes in Table 3.3. However, selected plots for the secondary forest class at around twelve plots were not visited because those plots were located inside a forest concession with limited accessibility. Thus, the land use systems were defined from the visual interpretation of RapidEye images. The unselected points from the 100 random points that were excluded from validation points were taken when accessibility allowed as additional validation points. Field work was done from October to November 2014. The distribution of ground truthing data are shown in Figure 3.4. Validation points for water bodies were not taken, as water bodies can be clearly differentiated with high spatial resolution RapidEye images.

A confusion matrix was then produced, and the computation of Overall Accuracy (OA), User's Accuracy (UA), Producer's Accuracy (PA) were conducted to assess accuracy (Foody, 2002). The confusion matrix depicts the confusion between classes of each classified land use system relative to the reference data. OA accuracy shows the overall percentage of correctly-classified objects. Accuracy can also be assessed for each class, as UA and PA. UA quantifies the quality of the map by quantifying the correct classification for each class (e.g. fifty objects of settlements are correctly classified among sixty objects in the map), while PA depicts the quality of classification process by quantifying how many objects for each class in the ground are correctly classified (e.g. forty objects of oil palm plantations in the ground are correctly classified among a total of sixty objects).

3.3. Assessment of key variables of secondary rainforest

3.3.1. Image pre-processing

For quantitative analyses combining field inventory and remote sensing data, such as biomass estimations, an atmospheric correction is necessary (Lu et al., 2002). In this study, atmospheric correction was done for the RapidEye images which were used to assess the key variables of the secondary rainforest by combining field inventory and remote sensing data. Atmospheric correction was carried out using the Second Simulation of the Sensor Signal in the Solar Spectrum (6S) model (Vermote et al., 2006). This 6S model was applied in the ForestEye Processor, and the parameter settings to use for correction are either provided by standard method or derived from MODIS (Magdon et al., 2011). In this study, standard method was used. To implement the 6S model, the aerosol's model and the atmospheric profile must be determined. The aerosol's model of maritime among other aerosol's models such as continental, urban, background deserts, biomass burning, and stratospheric was used since the study area is located between Indian Ocean and South China Sea. An atmospheric profile of the tropics was used as the study area is located in the tropical area. For this model, the visibility value was required. According to Bojanowski (2007), it was computed using equation (3).

$$v = \exp(-\log(AOT/2.7628) / 0.79902) \quad (3)$$

where:

v = visibility

AOT = aerosol optical thickness

For this calculation, the AOT value is available at NASA's Aerosol Robotic Network (AERONET) and determined for the acquisition time of the images. For the images used in this study $AOT = 0.199147$ and, thus, $v = 26.88$ km.

3.3.2. Field inventory

Field data collection was implemented with stratified sampling. NDVI strata generated from a TOA-preprocessed Landsat 8 OLI were used as a proxy for forest variables. This is because of the lack of information about forest variables prior to field inventory. Landsat images needed to be used because RapidEye images became available only after the field surveys. RapidEye images were then used for further analyses on the prediction and regionalization of forest variables. The NDVI values of Landsat OLI were classified into six classes. Such unsupervised classification was implemented in ArcMap 10.3 by using

Jenks natural breaks clustering, which minimizes the differences within classes but maximizes it between classes (ESRI, 2011).

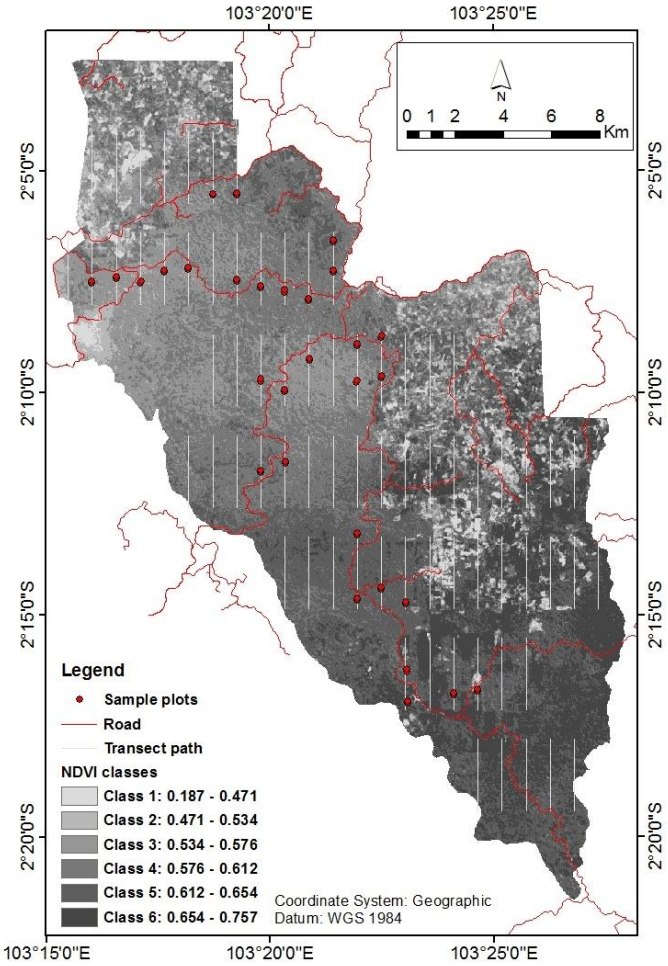

Figure 3.6. The distribution of sample plots within Harapan rainforest.

To locate the sample plots, only the NDVI classes for forest area were used. To distinguish forest and non-forest areas among NDVI classes, a comparison between NDVI classes and RapidEye image by visual interpretation was done. The classification results from the RapidEye images conducted in this study were basically used to guide during interpretation. Each class of NDVI was visually observed through the RapidEye images, and then defined it whether this class represent forest cover. As the result, NDVI classes 3 (NDVI: 0.534-0.576), 4 (NDVI: 0.576-0.612), and 5 (0.612-0.654) were defined as representatives of the forest area.

Due to the challenges of accessibility, the sample plots were restricted to no more than one km distance from the road and located within the transect of a rectangular plot from the previous systematic inventory conducted by PT REKI. Each transect of this rectangular plot was a 3 km-long survey strip with a 20 m width as depicted in Figure 3.6. The

implementation of the plot design was modified from the MoF Decree 33 of 2009 on the guideline of periodical forest inventory in production forests and has a plot design of 20 x 125 m. By locating the sample plots within this transect, it was expected to be more accessible and save walking time. Moreover, the areas where illegal encroachment activities occurred were avoided in locating sample plots for the sake of security during field work. Altogether, thirty sample plots were proportionally located in regard to the percentage area of each NDVI class that represents the three forest classes as mentioned above. Based on the NDVI values generated from selected sample plots, it can be seen in Figure 3.7 that the NDVI ranges of the entire forest were covered by the NDVI ranges of the sample plots. In this way, the sample plots represent the population of forest area.

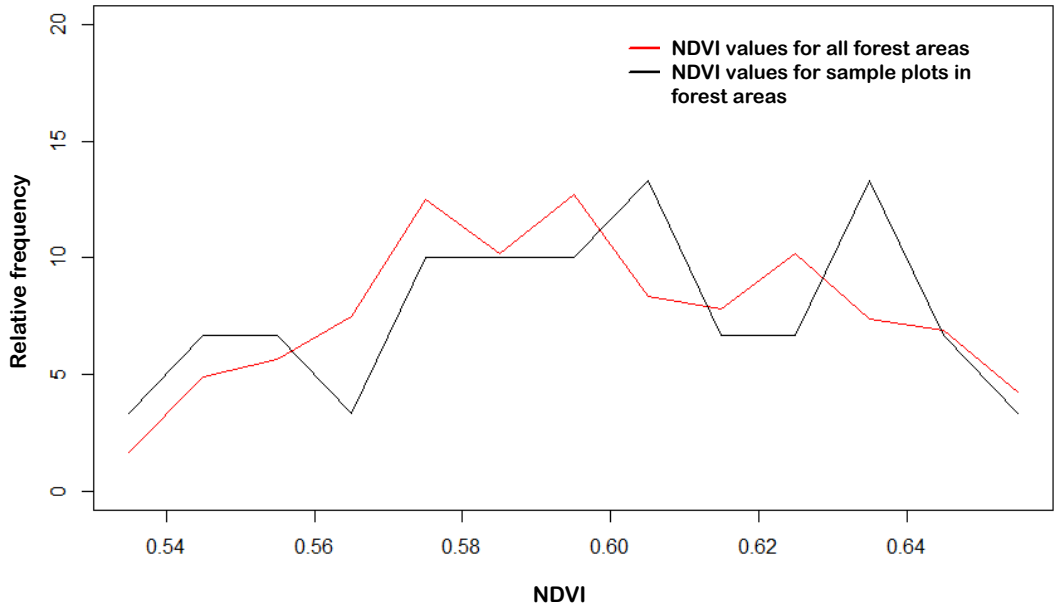

Figure 3.7. Relative frequency of NDVI for all forest areas and sample plots in forest areas.

In this study, a cluster of two nested rectangular subplots was established where a single nested subplot is 20 x 50 m. This plot design was made in order to reduce time. With this plot design, two sample plots were able to be tallied in one day. The size of the nested subplots is depicted in Figure 3.8, including the threshold of the selected trees. A Global Positioning System (GPS) of eTrex 30 by GARMIN was used to store the geographical coordinates of the sample plots and to find the locations in the field. These recorded coordinates were the bottom center of the first subplot which is located in the south. Once the location of a plot was identified, the subplots of 5 x 5 m and 10 x 10 m were established. For all nested subplots, the diameter at breast height (*dbh*) was measured for trees of defined diameter classes (Figure 3.8).

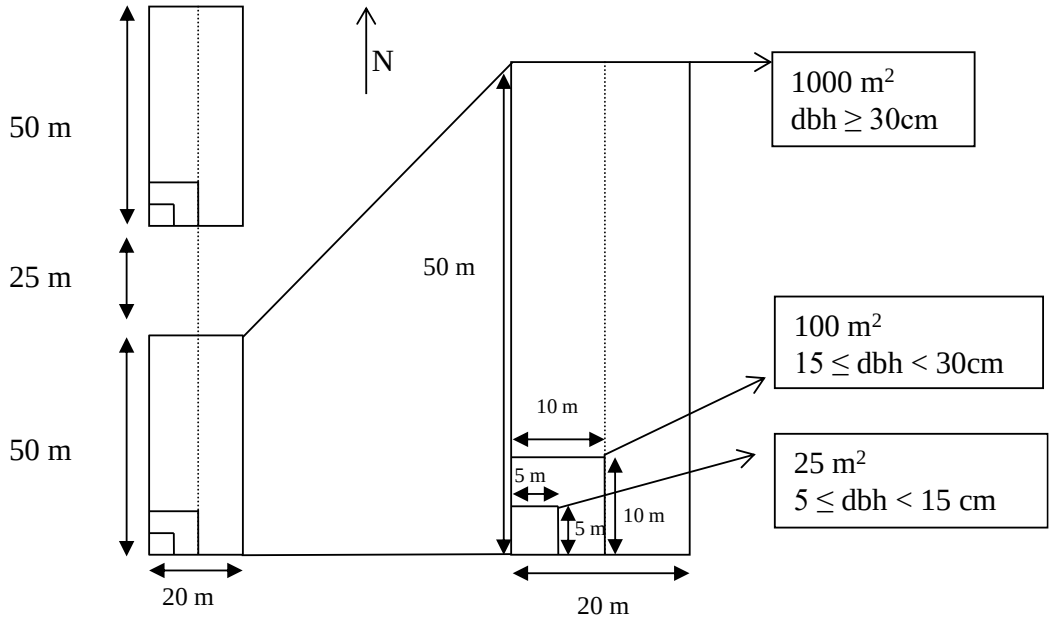

Figure 3.8. A cluster of two nested subplots each with three different sizes of rectangular and square sub-plots.

3.3.3. Dependent variables

Target variables were above-ground biomass (AGB, ton/ha), basal area (BA, m^2/ha), stand density (N, trees/ha), and quadratic mean diameter (dq, cm). The generic model provided by Brown (1997) and updated by Pearson et al. (2005) and Chave et al. (2005) has frequently been used to quantify the AGB in tropical forests (Rutishauser et al., 2013). A recent study on the quantification of the AGB around the study area by Kotowska et al. (2015), which had a different sampling design, used allometric equation developed by Chave et al. (2005). In the present study, the AGB was quantified using the allometric equation for moist tropical forests developed by Brown (1997) and updated by Pearson et al. (2005) (equation (4)) because of the absence of wood density information. This allometric equation was also used by Laumonier et al. (2010) in a study that included Jambi province as part of their study area. For their study, the average of AGB was 361±7 $Mgha^{-1}$.

$$AGB = \exp\{-2.289 + 2.649 \text{ x } \ln dbh - 0.021 \text{ x } \ln dbh^2\} \quad (4)$$

where: AGB is in kg per tree and dbh is in cm.

The quadratic mean diameter provides larger weight to larger trees. In forest areas where the tree diameters are small and the ranges are narrow, the difference between arithmetic mean diameter and quadratic mean diameter is small. However, if the tree diameters are

large and the ranges are wide, the difference is considerable. dq represents the average diameter with the mean basal area, and, thus, has strong relationship with basal area. The calculation of dq can be advantageously used to measure the stand volume (Curtis & Marshall, 2000).

An example of the calculations for all target variables from the field measurement is described in Appendix A.3. The value of each target variable which is the value per ha of AGB, BA, N, and dq for each plot is calculated from the mean of two subplots. After having all the values for each plot, the population mean of each target variable was estimated. Even though the selection of sample plots in this study did not follow the probability sampling design, the estimators of probability sampling design for stratified random sampling were implemented. This was done to compromise the statistical sampling design implemented in a challenged area. In this study, the sample design followed a stratified sampling but the sample plots were not located randomly due to accessibility challenges, as mentioned in the previous section. Equation (5) was used to estimate the population mean and, accordingly, the standard error of the estimated population mean (SE) was also estimated using equation (7) following Van Laar & Akça (2007).

The estimated population mean is calculated as follows:

$$\bar{y} = \sum_{h=1}^{L} \frac{N_h}{N} \bar{y}_h \tag{5}$$

where:

$$\bar{y}_h = \frac{\sum_{i=1}^{n} y_{ih}}{n_h} \tag{6}$$

The estimated standard error of the estimated population mean is calculated as follows:

$$\mathrm{SE} = \sqrt{\hat{\mathrm{var}}(\bar{y})} \tag{7}$$

where:

$$\hat{\mathrm{var}}(\bar{y}) = \sum_{h=1}^{L} \left(\frac{N_h}{N}\right)^2 \frac{s_h^2}{n_h} \tag{8}$$

$$s_h^2 = \frac{\sum_{i=1}^{n} (y_i - \bar{y}_h)^2}{n_h - 1} \tag{9}$$

For the above equations, each of the notations is described as follows:

L : number of strata, h = 1,…, L,

N : population size,

N_h : stratum size, where $N = \sum_{h=1}^{L} N_h$,

y_{ih} : measured value of the *i*-th sampling unit in the *h*-th stratum,

$\bar{y}$: estimated population mean

$\bar{y}_h$: estimated mean of the *h*-th stratum

n : total sample size

n_h : sample size in stratum h

s_h^2 : estimated variance in stratum h

$\hat{var}(\bar{y})$: estimated error variance of the estimated population mean

SE : estimated standard error of the estimated population mean

For the 95 % confidence interval (CI), it is calculated as follows:

$$CI = \bar{y} \pm t_{\alpha,(n-1)} * SE \quad (10)$$

3.3.4. Predictor variables

RapidEye images served to provide area-wide predictor variables, where surface reflectance of the five bands was used and, vegetation and texture indices were computed by the ForestEye Processor (Magdon et al., 2011).

Vegetation indices can be derived by rationing the pixel values from one spectral band to the pixel values from a second spectral band for the same area, where the selection of the bands takes into account the purpose of study. This has an impact on minimizing the illumination variation due to the topographic effect (Mather & Koch, 2011). For example, similar objects with different illumination have different spectral reflectance due to the shadowing effect as an impact of topographic variation. The rationing between one spectral band and another spectral band (e.g. near-infrared and red band) results in similar values, which then allows for easier classification of similar objects.

Table 3.4 Vegetation indices used as remote sensing based predictor variables in this study.

Vegetation indices	Equation	Reference
Normalized Difference Vegetation Index (NDVI)	$\mathrm{NDVI} = \frac{\mathrm{NIR} - \mathrm{Red}}{\mathrm{NIR} + \mathrm{Red}}$	Gamon et al. (1995)
NDVI Red-edge (NDVI_RE)	$\mathrm{NDVI\_RE} = \frac{\mathrm{NIR} - \mathrm{RE}}{\mathrm{NIR} + \mathrm{RE}}$	Gitelson & Merzlyak, (1997)
Green NDVI (NDVI_Green)	$\mathrm{NDVI\_Green} = \frac{\mathrm{NIR} - \mathrm{Green}}{\mathrm{NIR} + \mathrm{Green}}$	Buschmann & Nagel (1993)
Ratio	$\mathrm{Ratio} = \frac{\mathrm{NDVI\_RE}}{\mathrm{NDVI\_Green}}$	Marx (2010)
Chlorophyll Green Model (CGM)	$\mathrm{CGM} = \frac{\mathrm{NIR}}{\mathrm{Green}} - 1$	Gitelson et al. (2005)
Chlorophyll Red-edge Model (CRM)	$\mathrm{CRM} = \frac{\mathrm{NIR}}{\mathrm{RE}} - 1$	Gitelson et al. (2005)

There are more vegetation indices that incorporate subtraction and summation of different spectral bands, as listed in Table 3.4. For instance, the subtraction values of the red band from near-infrared band. In the case of healthy vegetation, a maximum reflectance is found at the near-infrared wavelength due to high reflectance, while a low reflectance is found at the red wavelength due to high absorption. However, unhealthy vegetation will result in an increase of red reflectance (Lillesand et al., 2008). The subtraction between near-infrared and red band will result higher difference for healthy vegetation than the unhealthy vegetation with lesser chlorophyll (Richardson & Everitt, 1992). Therefore, healthy vegetation will be easily identified.

NDVI measures the greenness of the canopy, while the chlorophyll index measures the vegetation stresses (Gitelson & Merzlyak, 1997). Other vegetation indices that incorporate the Red-edge wavelength, such as CRM and Red-edge NDVI, are also an advantage. This is a unique wavelength that differentiates RapidEye images from most of other satellite images allowing for the detection of green vegetation health (Jung-Rothenhäusler et al., 2007).

Texture is defined as the tonal variations or a structural arrangement of pixel values in relation to neighboring pixels (Haralick et al., 1973; Mather & Koch, 2011). In order to

measure texture indices, first- and second-order statistics were used in this study as listed in Table 3.5.

In the first-order texture index, the respective index is counted from all the neighboring pixel values. The difference between first- and second-order statistics is that the first-order statistics do not consider the relationship between two neighboring pixel values in calculating the texture indices as the second-order statistics do (Hall-Beyer, 2007). The second-order texture index represents the co-occurrence of two neighboring pixel values (i,j), one pixel value i and another pixel value j, separated at a certain distance (d) and direction (θ) (Haralick et al., 1973). It is known as Grey Level Co-Occurrence Matrix (GLCM). There are four directions that define the spatial relation of direct pixel neighbors: 0°, 45°, 90°, and 135°. For both approaches, a moving window for defining the neighboring pixels to be evaluated was determined as the first step by defining the number of columns and rows of the window. The corresponding texture index is calculated from the windows pixel values and the result is assigned as a new value at the center pixel. Subsequently, the window is shifted by one pixel and the corresponding texture index is continuously calculated for all the pixels in the image.

In this study, texture indices were generated from RapidEye's near-infrared band. This wavelength has high reflectance of vegetation (Basuki et al., 2013) which is expected to be more sensitive to identify vegetation characteristics. As the target variables are forest variables, the use of NIR is beneficial for calculating the texture index aimed at characterizing the target variables. Three different sizes of moving windows were used (i.e., 3 x 3, 9 x 9, and 15 x 15).

Table 3.5 Texture indices used as predictor variables (k = number of spectral values, x_i = spectral value in pixel i, i = the pixel within the defined window, μ = mean of spectral values, N = number of gray levels, $p(i,j)$ = probability occurrence of two neighboring pixels, i.e. pixel i and pixel (i,j), σ = standard deviation).

Texture Indices	Equation	Reference
First-order texture indices (TXO)		
Mean (ME)	$\mathrm{TXO\_ME} = \frac{1}{k}\sum_{i=1}^{k} x_i$	Castillo-Santiago, et al. (2010)
Standard Deviation (SD)	$\mathrm{TXO\_SD} = sqrt\,(\frac{1}{k}\sum_{i=1}^{k}(x_i - \mu)^2)$	Castillo-Santiago, et al. (2010)
Second-order texture indices (TX)		
Angular Second Moment	$\mathrm{TX\_ASM} = \sum_{i,j=0}^{N-1} p(i,j)^2$	Haralick et al. (1973)
Contrast	$\mathrm{TX\_CON} = \sum_{i,j=0}^{N-1} p(i,j)(i-j)^2$	Haralick et al. (1973)
Entropy	$\mathrm{TX\_ENT} = -\sum_{i,j=0}^{N-1} p(i,j)\log(p(i,j))$	Haralick et al. (1973)
Inverse Difference Moment	$\mathrm{TX\_IDM} = \sum_{i,j=0}^{N-1} \frac{1}{1+(i-j)^2} p(i,j)$	Haralick et al. (1973)
Correlation	$\mathrm{TX\_CORR} = \frac{\sum_{i,j=0}^{N-1} \mathrm{p(i,j)} - \mu_i\mu_j}{\sigma_i\sigma_j}$	Haralick et al. (1973)
Dissimilarity	$\mathrm{TX\_DISS} = \sum_{i,j=0}^{N-1} p(i,j)\lvert i-j\rvert$	Haralick et al. (1973)
Mean	$\mathrm{TX\_ME} = \sum_{i,j=0}^{N-1} p(i,j)(i)$	Haralick et al. (1973)
Variance	$\mathrm{TX\_VAR} = \sum_{i,j=0}^{N-1} p(i,j)(i-\mu)^2$	Haralick et al. (1973)

3.3.5. Model prediction and validation

For the model prediction, 29 of 30 plots were used, as one plot was only covered by shrub/bush and dead trees. Another subplot, containing a tree with a *dbh* > 2m, was also excluded since the allometric equation used in this study for biomass modelling (Brown,

1997) does not cover a *dbh* range greater than 2 m. Prior to the implementation of statistical modeling, the mean values of the dependent variables and the predictor variables were generated for the 29 plots. For the dependent variables, these values characterize the average value of forest variables from two subplots at each plot. For the predictor variables, the mean values characterize the average value of all pixel values for corresponding image features from two subplots at each plot. By extracting the mean pixel value, it minimizes the mismatching of geolocations between the image and the sample plots (Beckschäfer et al., 2014; Fuchs et al., 2009).

The calculated mean values of 41 independent variables (i.e. the surface reflectance of five bands, six vegetation indices, and ten texture indices with three different moving windows) were transformed using the Box-Cox transformation (Box & Cox, 1964) for normality and linearity of the variables. The Box-Cox transformation was applied using the 'MASS' library of the R package (R Core Team, 2015). Among these predictor variables, a subset of variables was selected through a stepwise exhaustive search approach that takes into account all possible combinations of predictor variables. This approach was applied using the 'leaps' library of the R package (Lumley & Miller, 2009; R Core Team, 2015). Through different subsets of predictor variables, a multiple linear regression that relates each dependent variable with each subset of predictor variables by using equation (11) was then implemented to find the best model.

$$y_i = b_0 + b_1.x_1 + \cdots + b_i.x_i + \varepsilon_i \quad (11)$$

where:

y_i are the dependent variables (i.e. *AGB, BA, dq, N*) of the i-th observation where $i = 1, 2,\ldots, n$; x_1-x_i are the predictor variables including spectral reflectance of five bands, vegetation, and texture indices; b_0-b_i are the model coefficients, and ε_i is the random error term.

The best model was selected by evaluating the adjusted R^2 and p-values for the estimated coefficients, where a p-value of < 0.1 was used as threshold. The variance inflation factor (VIF) was also taken into account to identify multicollinearity among the independent variables. VIF was calculated using the 'car' library of the R package following the equation (12) (R Core Team, 2015). The VIF identifies the degree of multicollinearity. VIF measures the coefficient of determination R^2 within the predictor variables (Fahrmeir et al., 2013) where each predictor variable acts as a dependent variable. The larger the correlation

within predictor variables, the larger the R^2 is, and therefore the VIF will be larger (Fahrmeir et al., 2013). If the R^2 = 0, the VIF will be one, which means there is no multicollinearity. In this study, a common threshold of VIF > 10 was used to define multicollinearity (Eckert, 2012; Fahrmeir et al., 2013; Hair et al., 2010; Sarker & Nichol, 2011). With the chosen models, forest variables were then predicted.

$$VIF = \frac{1}{1-R^2} \tag{12}$$

In order to validate the model, a Leave-One-Out Cross Validation (LOOCV) was done because of the low sample size of the plots (n = 29). The 'boot' library of the R package (R Core Team, 2015) was used, estimating the Root Mean Square Error ($RMSE$) and the relative RMSE ($RMSE_r$). For all observations, this method leaves out one observation and fits the model to the rest of the observations. The generated model is then used to estimate the value of one observation left out y_i resulting $\hat{y}_i$. $RMSE$ and $RMSE_r$ are then calculated using equation (13) and (14) (James et al., 2013).

$$RMSE = \sqrt{\frac{\sum_{i=1}^{n}(y_i-\hat{y}_i)^2}{n}} = \sqrt{MSE} \tag{13}$$

$$RMSE_r = \frac{RMSE}{\bar{y}}\ x\ 100\% \tag{14}$$

where:

n = observation number

y_i = observed value of i

$\hat{y}_i$ = estimated value of i

$\bar{y}$ = estimated population mean

With the identified models, maps of the target variables were then produced for the area classified as forest which was masked out following the approaches described in subsection 3.2. A value of zero was set for each negative value within the modeled maps (Fuchs et al., 2009).

Chapter 4
Results

4.1. Monitoring land use systems

4.1.1. Analyses of land use change

The quantification of land use change produced information to analyze the transition between classes and, thus, temporal dynamics among the classes are able to be evaluated. As depicted in Table 4.1, the decrease of primary forests and secondary forests between 1990 and 2013 took place at a considerable rate in Jambi province. The area of primary forest decreased from 1.34 Mha in 1990 to 0.83 Mha in 2013, which corresponds to a loss of 38.2 % with annual forest loss of about 1.7 %. Secondary forest area decreased from 0.92 Mha in 1990 to 0.64 Mha in 2013, corresponding to a loss of 30.9 % with annual loss of 1.3 %. Comparing the 2000 land use maps produced by Hansen et al. (2013) and the one produced in present study demonstrates that the forest areas (i.e. tree cover ≥ 30 %) by Hansen et al. (2013) covered 91.7 % of the Jambi province, while forest areas (i.e. primary, secondary, and plantation forests) in this study covered 39.8 %. Overall, around 42.5 % of the forest areas produced by Hansen et al. (2013) overlapped with those in this study. The remaining forest areas were mismatched with other land use systems, as can be seen in Appendix A.4. This mismatching can be interpreted due to their definition of forests as "all vegetation taller than 5 m in height", which might overestimate the forest cover areas.

The area of rubber and oil palm plantations, however, has increased between 1990 and 2013. The net increase of oil palm plantations was around 77.2 %, from 0.34 Mha in 1990 to 0.60 Mha in 2013 which corresponds to an annual net increase of 3.4 %. The net increase of rubber plantations was relatively small, at around 6.8 %, from 0.86 Mha in 1990 to 0.92 Mha in 2013 with an annual net increase of 0.3 %. Among the agricultural systems, the annual net increase of oil palm plantations was highest in the period of 1990-2000, at around 6.4 %. However, the area of jungle rubber had declined with an annual net decrease of around 0.8 %, from a total area of 0.1 Mha in 1990 to 0.08 Mha in 2013. This figure is, however, less certain due to the confusion of land use classification between jungle rubber and rubber plantation with a low producer's accuracy of 48.1% (Appendix A.2.). Compared

to oil palm plantations and jungle rubber, the areas of rubber plantation were the largest during the period of 1990-2013.

Table 4.1. Land use in Jambi province between 1990 and 2013.

Land use systems	1990		2000		2011		2013	
	Area (Ha)	%	Area (Ha)	%	Area (Ha)	%	Area (Ha)	%
Primary forest	1,335,299.7	27.1	887,494.2	18.0	826,531.4	16.8	825,460.6	16.8
Secondary forest	919,817.5	18.7	882,625.0	17.9	657,911.8	13.4	635,449.6	12.9
Agriculture	717,745.2	14.6	868,130.6	17.7	926,888.9	18.8	926,238.5	18.8
Jungle rubber	97,185.0	2.0	26,070.1	0.5	79,068.2	1.6	79,068.2	1.6
Rubber plantation	856,667.2	17.4	890,389.9	18.1	966,039.9	19.6	915,033.1	18.6
Oil palm plantation	338,266.4	6.9	555,507.3	11.3	602,594.8	12.3	599,391.3	12.2
Plantation forest	182,819.1	3.7	189,026.8	3.8	207,857.8	4.2	232,593.6	4.7
Shrub/bush	360,082.7	7.3	493,557.5	10.0	519,920.4	10.6	519,239.4	10.6
Others	110,432.6	2.2	125,514.1	2.6	131,502.2	2.7	185,841.1	3.8

Table 4.2. Transformation of land use systems (%*) in Jambi province. The status in 1990 is compared here with the status in 2013.

	Land use systems in 1990	Land use systems in 2013									Total 1990	Loss
		1	2	3	4	5	6	7	8	9		
1	Primary forest	16.8	5.6	1.6	0.3	1.2	0.3	0.0	1.1	0.2	27.1	10.4
2	Secondary forest	0.0	6.8	1.4	0.7	3.4	2.9	1.0	2.1	0.5	18.7	11.9
3	Agriculture	0.0	0.0	12.4	0.0	0.3	1.1	0.0	0.4	0.2	14.6	2.2
4	Jungle rubber	0.0	0.0	0.1	0.4	0.0	0.0	1.2	0.2	0.0	2.0	1.6
5	Rubber plantation	0.0	0.0	1.5	0.1	13.1	1.5	0.4	0.4	0.5	17.4	4.3
6	Oil palm plantation	0.0	0.0	0.5	0.0	0.2	5.6	0.2	0.2	0.2	6.9	1.3
7	Plantation forest	0.0	0.3	0.3	0.0	0.2	0.4	2.0	0.4	0.2	3.7	1.7
8	Shrub/bush	0.0	0.1	0.9	0.0	0.1	0.2	0.0	5.8	0.1	7.3	1.5
9	Others	0.0	0.0	0.1	0.0	0.1	0.2	0.0	0.0	1.8	2.2	0.4
Total 2013		16.8	12.9	18.8	1.6	18.6	12.2	4.7	10.6	3.8	100.0	
Gain		0.0	6.1	6.4	1.2	5.5	6.6	2.7	4.8	1.9		

*Percentages depict the proportion of each land use transformation of the total study area.

The transformation matrix showing the changes of land use systems during the 1990-2013 period can be seen in more detail in Table 4.2. This table compares the status of 1990 with the status of 2013. All other intermediate dynamics and transitions within this period are not visible here. Primary forests in 1990 were largely converted to secondary forests in 2013, while secondary forests in 1990 were largely converted into oil palm and rubber plantations in 2013, as well as shrub/bush. The conversion into these tree crop plantations means that economic tree crops were the main cause of secondary forest losses. The land conversion also took place from rubber plantation into oil palm plantations.

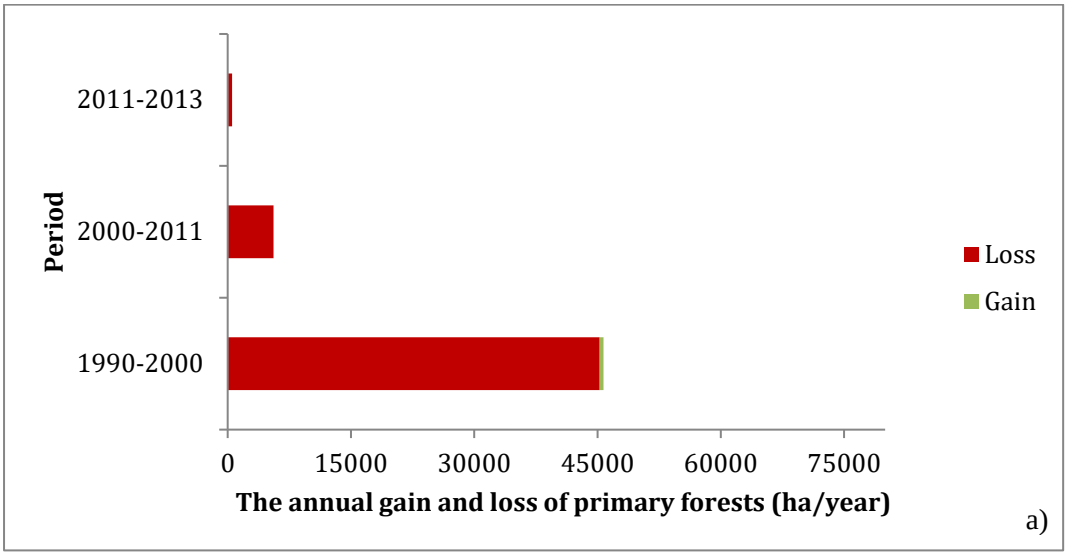

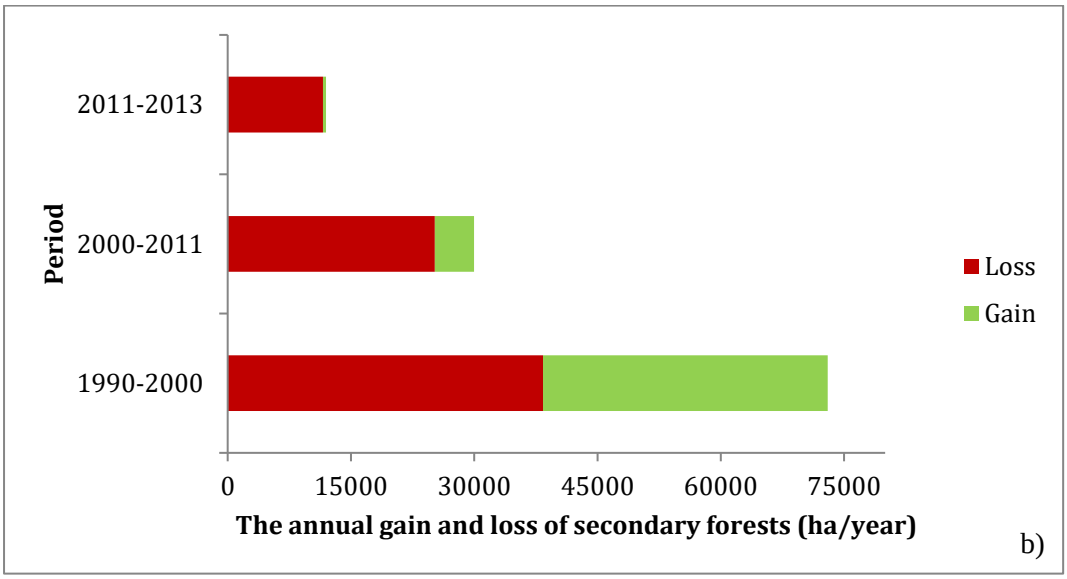

Figure 4.1. The annual gain and loss (ha/year) of a) primary forests and b) secondary forests in different periods.

Among the three periods from 1990-2013, as seen in Figure 4.1, the highest annual loss of primary and secondary forests took place in the period of 1990-2000. The primary forest loss was mainly due to the high transformation into secondary forest from 1990 to 2000 (Table 4.3), an indication of high forest degradation in this period. This had created a high increase of secondary forest area as seen in Figure 4.1. This transformation of primary forest into secondary forest also took place from 2000 to 2011 to a smaller extent (Table 4.4). A low gain value of primary forest area from 1990-2000 was due to the conversion of secondary forest into primary forest (Table 4.3). In this case, a misinterpretation between both classes may occur where the old growth secondary forest might be interpreted as primary forest.

Table 4.3. Transformation of land use systems (%*) in Jambi province. The status in 1990 is compared here with the status in 2000.

	Land use systems in 1990	Land use systems in 2000									Total 1990	Loss
		1	2	3	4	5	6	7	8	9		
1	Primary forest	17.9	5.9	1.0	0.0	0.8	0.3	0.0	1.1	0.1	27.1	9.2
2	Secondary forest	0.1	10.9	0.9	0.0	3.0	2.0	0.2	1.5	0.2	18.7	7.8
3	Agriculture	0.0	0.2	12.3	0.0	0.3	1.1	0.0	0.4	0.2	14.6	2.3
4	Jungle rubber	0.0	0.0	0.1	0.4	0.0	0.0	1.2	0.2	0.0	2.0	1.6
5	Rubber plantation	0.0	0.3	1.5	0.0	13.4	1.5	0.3	0.4	0.1	17.4	4.0
6	Oil palm plantation	0.0	0.1	0.5	0.0	0.2	5.6	0.2	0.2	0.1	6.9	1.3
7	Plantation forest	0.0	0.3	0.3	0.0	0.4	0.4	2.0	0.4	0.0	3.7	1.7
8	Shrub/bush	0.0	0.2	0.9	0.0	0.1	0.2	0.0	5.8	0.0	7.3	1.5
9	Others	0.0	0.0	0.1	0.0	0.1	0.2	0.0	0.0	1.9	2.2	0.4
Total 2000		18.0	17.9	17.7	0.5	18.1	11.3	3.8	10.0	2.6	100.0	
Gain		0.1	7.0	5.4	0.1	4.7	5.7	1.8	4.2	0.7		

*Percentages depict the proportion of each land use transformation of the total study area.

From the Figure 4.1, a high annual loss of secondary forest in the period of 1990-2000 indicated high expansion of tree crop plantations (i.e. oil palm and rubber plantations) as also seen in Table 4.3. Nonetheless, the area of secondary forest in 2000 was similar to the area in 1990 (Table 4.3) due to the aforementioned high degradation from primary forest into secondary forest.

Table 4.4. Transformation of land use systems (%*) in Jambi province. The status in 2000 is compared here with the status in 2011.

	Land use systems in 2000	Land use systems in 2011									Total 2000	Loss
		1	2	3	4	5	6	7	8	9		
1	Primary forest	16.8	1.0	0.1	0.0	0.1	0.0	0.0	0.0	0.0	18.0	1.2
2	Secondary forest	0.0	12.3	1.0	1.1	1.4	0.8	0.4	0.8	0.2	17.9	5.6
3	Agriculture	0.0	0.0	17.7	0.0	0.0	0.0	0.0	0.0	0.0	17.7	0.0
4	Jungle rubber	0.0	0.0	0.0	0.5	0.0	0.0	0.0	0.0	0.0	0.5	0.0
5	Rubber plantation	0.0	0.0	0.0	0.0	18.1	0.0	0.0	0.0	0.0	18.1	0.0
6	Oil palm plantation	0.0	0.0	0.0	0.0	0.0	11.3	0.0	0.0	0.0	11.3	0.0
7	Plantation forest	0.0	0.0	0.0	0.0	0.0	0.0	3.8	0.0	0.0	3.8	0.0
8	Shrub/bush	0.0	0.1	0.1	0.0	0.0	0.1	0.0	9.7	0.0	10.0	0.3
9	Others	0.0	0.0	0.0	0.0	0.0	0.0	0.0	0.0	2.5	2.6	0.1
Total 2011		16.8	13.4	18.8	1.6	19.6	12.3	4.2	10.6	2.7	100.0	
Gain		0.0	1.1	1.2	1.1	1.5	1.0	0.4	0.8	0.2		

*Percentages depict the proportion of each land use transformation of the total study area.

Table 4.5. Transformation of land use systems (%*) in Jambi province. The status in 2011 is compared here with the status in 2013.

	Land use systems in 2011	Land use systems in 2013									Total 2011	Loss
		1	2	3	4	5	6	7	8	9		
1	Primary forest	16.8	0.0	0.0	0.0	0.0	0.0	0.0	0.0	0.0	16.8	0.0
2	Secondary forest	0.0	12.9	0.0	0.0	0.0	0.0	0.2	0.1	0.1	13.4	0.5
3	Agriculture	0.0	0.0	18.8	0.0	0.0	0.0	0.0	0.0	0.0	18.8	0.0
4	Jungle rubber	0.0	0.0	0.0	1.6	0.0	0.0	0.0	0.0	0.0	1.6	0.0
5	Rubber plantation	0.0	0.0	0.0	0.0	18.6	0.0	0.1	0.0	1.0	19.6	1.0
6	Oil palm plantation	0.0	0.0	0.0	0.0	0.0	12.2	0.0	0.0	0.1	12.3	0.1
7	Plantation forest	0.0	0.0	0.0	0.0	0.0	0.0	4.2	0.0	0.1	4.2	0.1
8	Shrub/bush	0.0	0.0	0.0	0.0	0.0	0.0	0.0	10.4	0.1	10.6	0.2
9	Others	0.0	0.0	0.0	0.0	0.0	0.0	0.2	0.0	2.4	2.7	0.2
Total 2013		16.8	12.9	18.8	1.6	18.6	12.2	4.7	10.6	3.8	100.0	
Gain		0.0	0.0	0.0	0.0	0.0	0.0	0.6	0.2	1.3		

*Percentages depict the proportion of each land use transformation of the total study area.

The annual loss in secondary forests was consistently larger than in primary forests for the later periods where the transformation into tree crop plantations continuously took place during the 2000-2011 period (Table 4.4). However, the transformation of secondary forest into tree crop plantations was not found in the last period of 2011-2013 (Table 4.5). Among the three periods of land use transformation as seen in Table 4.3, Table 4.4, and Table 4.5, transformation dynamics was mostly found between 1990 and 2000 indicating a remarkable land use change in this period.

4.1.2. Spatial pattern analysis

In order to identify alterations of landscape patterns due to land use transformation, a spatial pattern analysis was conducted by landscape metrics. Two landscape metrics, mean patch size and aggregation index, were computed from the land use maps for the major land use classes. Figure 4.2 depicts the results of this analysis.

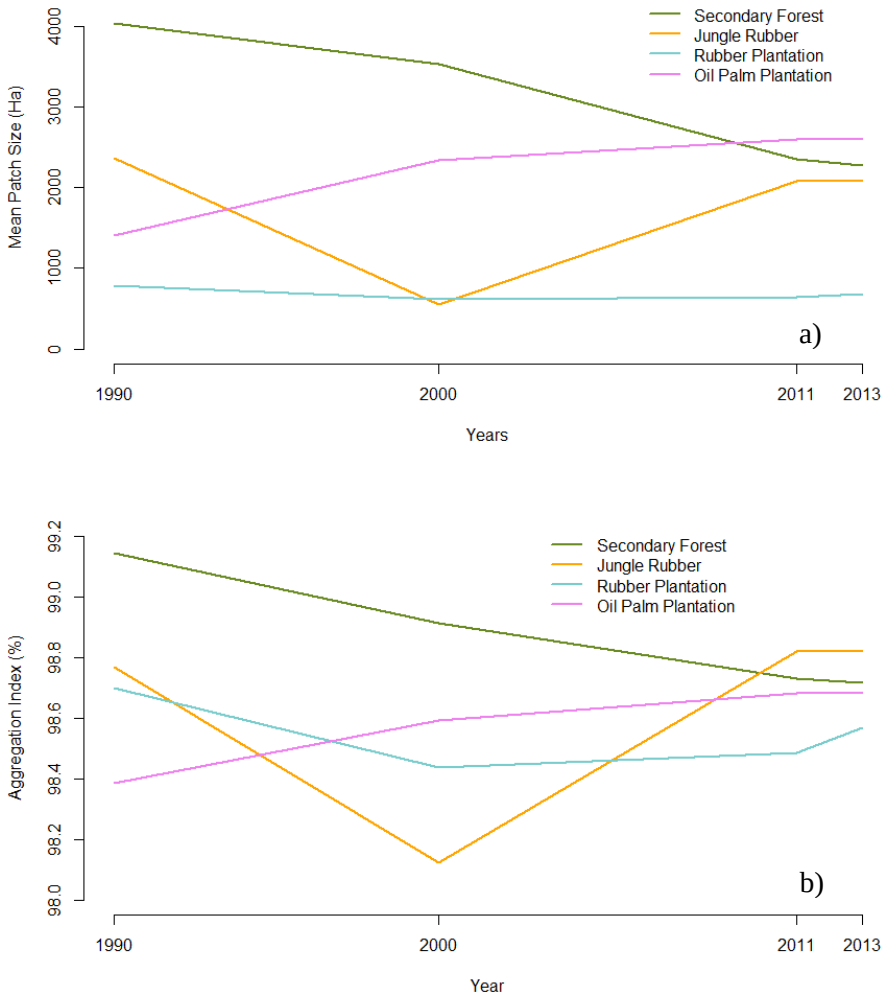

Figure 4.2. a) Mean patch size and b) Aggregation index in the period of 1990-2013.

Secondary forests and oil palm plantations show the most dynamic transformation processes: mean patch size continually decreased for secondary forests and increased for oil palm plantations. For the aggregation index, a similar trend can be observed: while secondary forests became more and more disaggregated with a decreasing aggregation index over the period 1990-2013, the opposite can be seen for oil palm plantations. In this case, the decrease of secondary forest area over the period studied had an impact of decreasing both the MPS and the AI. This can also be seen for oil palm plantations where the increase of its area was followed by the increase of its MPS and AI.

For the MPS and AI of rubber plantations, there was no trend within the observed time frame. A similar trend was seen in the area extent of rubber plantations as there was no considerable change in the total area for rubber plantation (Table 4.1). For jungle rubber that has an overall very small area extent only and is difficult to distinguish from rubber plantations, an uneven trend was observed. The decline of both metrics in 2000 can be interpreted due to high loss of jungle rubber area (Table 4.1). However, the fragmentation had about the same value in 1990 and 2013.

4.1.3. Factors related to deforestation

The relation of socio-economic and topographic factors to deforestation was analyzed. These factors were then used to interpret the potential drivers of deforestation. Figure 4.3 shows the area of deforestation depicted as a function of elevation and slope. In 1990, forests were mostly located in an elevation of around 0 to 200 m.a.s.l and at a slope gradient from 0 to 20 %. In the analyses of three different study periods, deforestation mostly took place in low elevations, around < 100 m.a.s.l., as well as at low slope gradients, around < 10%. This demonstrates that lowland areas were mostly deforested, as they are less challenging to access and to establish agriculture in.

The relationships between the annual change of socio-economic variables and the annual deforestation at the district level have also been analyzed. Jambi city has no forests and the forests in Sungai Penuh city remained stable within the study period. Socio-economic variables were available for the periods of 2000-2011 and 2011-2013. As forest cover was found to be close to stable in the period of 2011-2013 for the nine districts in Jambi province, analyses were only performed for the period of 2000-2011.

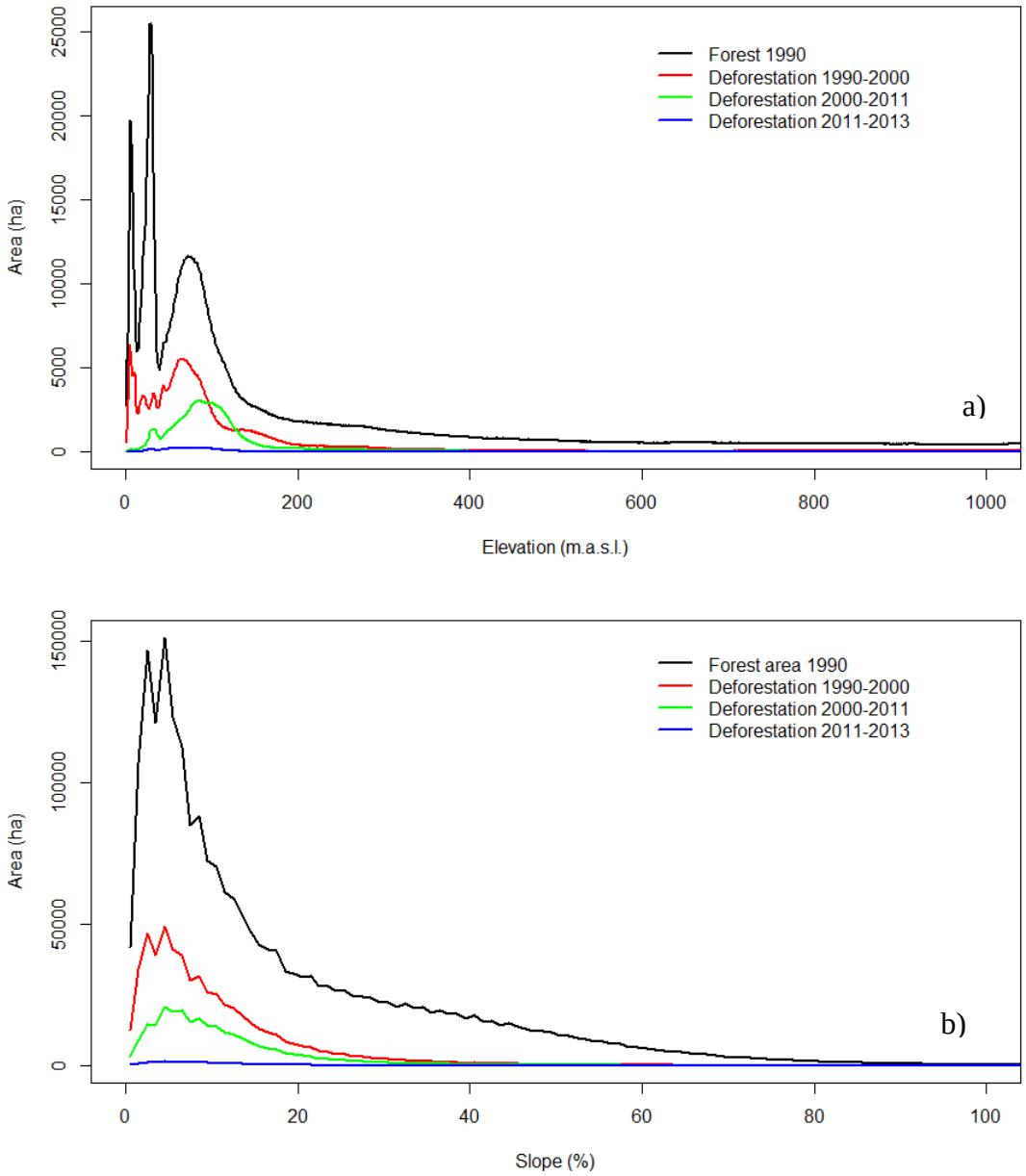

Figure 4.3. Distribution of forest areas in 1990 and deforestation in the Jambi province at different periods (1990-2000, 2000-2011, and 2011-2013) according to different a) elevation and b) slope. These figures show the total area.

Table 4.6 shows the relationships between deforestation and some socio-economic variables, of which district data were available. In this study, the 9 districts were considered as the population of interest so that statements about statistical significance are not made here, but interpretation is restricted to the value of the calculated coefficient. Therefore, our interpretation focuses on the relevance of the subject-matter and not on statistical significance. The value of the calculated coefficient is taken as a measure of relevance. Following this interpretation, the GRDP per capita and the number of oil palm farmers were not found to be relevant in relation to deforestation because the coefficients have low

values. Equally, the number of rubber farmers and the population density have coefficients that are relatively small. These were indications of lesser relevance. However, rubber and oil palm productivity were the two factors that are highly and relevantly related to deforestation with high coefficients. This result, of course, was to be expected, and underlines the identification of tree crops as major drivers of forest conversions.

Table 4.6. Results of a simple linear regression between the annual change of socio-economic variables and annual deforestation for the period of 2000-2011. Statistics of significance are not given here, because these calculations refer to the population of all 9 districts.

Variable	Regression coefficient
Population density	-2.5
GRDP per capita	0.0
Rubber productivity	6.8
Oil palm productivity	14.6
Number of rubber farmers	2.3
Number of oil palm farmers	-1.2

4.2. Evaluation of the tree crops mapping using high spatial resolution images

4.2.1. Selection of segmentation parameters

The different parameter settings of spatial radius, range radius, and minimum region size generated thirty-six segmented images. In order to select the best parameter settings, comparisons between reference objects and segmented images were made and they produced correct detection, over-segmentation, and missed detection scores. Under-segmentation scores were not found at any segment comparison. The results of the different comparisons for each parameter setting were ordered from highest to the lowest scores of the correct detection as shown in Table 4.7.

From Table 4.7, one sees that the higher the correct detection score, the lesser the over-segmentation score. The lowest over-segmentation score is the result of image segmentation with largest h_s, h_r and M_r (i.e. $h_s/h_r/M_r$ of 15/0.02/50), while the highest over-segmentation score is oppositely found for the smallest radius of h_s, h_r and M_r (i.e. $h_s/h_r/M_r$ of 5/0.005/10). For the missed detection score, one cannot see any distinctive pattern.

Table 4.7. The scores generated from comparisons between reference objects and segmented images with different parameter settings using Hoover metrics (sorted by the

level of correct detection). The smallest the radius of parameter settings, the highest the over-segmentation score. However, the correct detection score is the smallest. There is no distinctive pattern for missed detection score.

ID	Parameters			Correct detection	Over-segmentation	Missed detection
	h_s	h_r	M_r			
1	15	0.02	50	0.75492	0.23193	0.03412
2	15	0.02	30	0.75153	0.2404	0.03412
3	15	0.02	10	0.74047	0.26461	0.03412
4	5	0.015	50	0.73835	0.27436	0.00867
5	10	0.015	30	0.72426	0.28769	0.01479
6	5	0.015	30	0.72211	0.29672	0.0079
7	10	0.015	50	0.72206	0.27073	0.02615
8	15	0.01	50	0.71432	0.30313	0.00972
9	15	0.015	50	0.71382	0.26493	0.04824
10	10	0.015	10	0.71326	0.3253	0.00561
11	15	0.015	30	0.71025	0.2882	0.03627
12	10	0.02	50	0.7058	0.24695	0.05173
13	10	0.01	50	0.70415	0.3239	0.00352
14	15	0.01	30	0.70357	0.32499	0.00666
15	10	0.02	30	0.70196	0.26205	0.05173
16	5	0.01	50	0.70042	0.31618	0.02139
17	15	0.015	10	0.69994	0.31402	0.02504
18	5	0.015	10	0.69966	0.33525	0.0079
19	5	0.02	50	0.69825	0.26093	0.05291
20	5	0.02	30	0.69375	0.27681	0.05167
21	10	0.01	30	0.69112	0.33952	0.00919
22	5	0.01	30	0.68916	0.34662	0.01104
23	15	0.01	10	0.68735	0.37315	0.00124
24	10	0.02	10	0.6866	0.28565	0.04631
25	5	0.02	10	0.68404	0.30292	0.05167
26	10	0.01	10	0.6734	0.38641	0.00352
27	5	0.01	10	0.6708	0.39876	0.00124
28	15	0.005	50	0.66001	0.37823	0.00666
29	10	0.005	50	0.65421	0.38211	0.01697
30	15	0.005	30	0.64625	0.41322	0.00666
31	10	0.005	30	0.63834	0.42222	0.01332
32	5	0.005	50	0.62243	0.44329	0.01104
33	15	0.005	10	0.62114	0.4688	0.00352
34	10	0.005	10	0.60567	0.49449	0.00376
35	5	0.005	30	0.59634	0.49818	0.00666
36	5	0.005	10	0	0.58886	0.00124

To observe the effect on the number of polygons and the size of the objects (i.e. the maximum and average object sizes), the resulting segmented images with different parameter settings (h_s and h_r) but the same M_r were further evaluated. As can be seen in Table 4.8, the use of the same M_r and h_s settings yielded a smaller number of polygons with a higher h_r. Higher mean and maximum object sizes were derived with higher h_r. Other settings with the same M_r and h_r produced smaller numbers of polygons for higher values of h_s. However, the higher values of h_s lead to an increase of mean object size, except for the lowest h_r (i.e. $h_r = 0.005$), which resulted in similar mean sizes. For the maximum size, the higher the h_s, the higher the maximum object size was also; however, this trend was not found for h_s/h_r 5/0.015 and 10/0.015 and for 10/0.005 and 15/0.005. As expected, it was obvious that the higher of both spatial and range radius produced smaller number of polygons, but higher maximum and average object sizes.

Table 4.8. Number of polygons and object sizes produced by each parameter setting for segmentation with different h_s and h_r but same M_r (= 30).

M_r	h_s	h_r	Number of polygons	Max. (Ha)	Mean (Ha)
30	5	0.005	543354	1.27	0.18
30	5	0.01	459219	134.10	0.21
30	5	0.015	281949	1741.49	0.35
30	5	0.02	137382	3786.89	0.72
30	10	0.005	539701	5.78	0.18
30	10	0.01	415919	187.55	0.24
30	10	0.015	235553	1444.57	0.42
30	10	0.02	110358	6387.17	0.89
30	15	0.005	535681	3.91	0.18
30	15	0.01	385601	236.63	0.26
30	15	0.015	198818	2304.18	0.50
30	15	0.02	87032	6493.71	1.13

The median of the object sizes was similar for the different parameter settings (see Figure 4.4). However, the ranges of the polygon sizes varied considerably. Among the parameter settings, the highest h_s at 15 and h_r at 0.02 produced the largest range of object sizes. The comparison of object sizes with different parameter settings, including the smallest ($h_s/h_r/M_r$ of 5/0.005/30) and the highest parameter settings ($h_s/h_r/M_r$ of 15/0.02/30) are depicted in Figure 4.5. The figures show that the objects are partitioned into larger pieces with the

highest parameter settings of h_s = 15 and h_r = 0.02 than the smallest parameter settings of of h_s = 5 and h_r = 0.005.

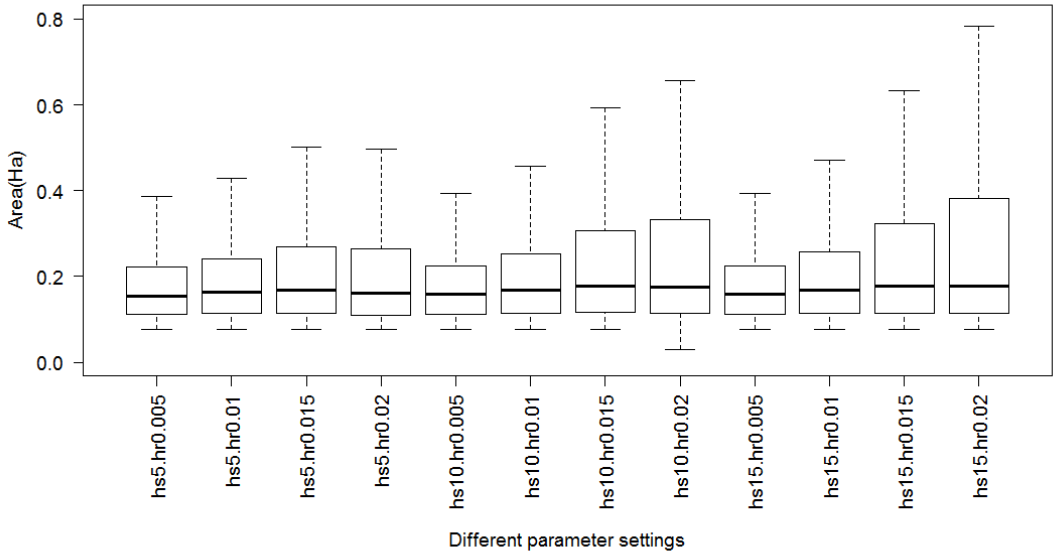

Figure 4.4. Boxplot of object sizes for each parameter setting with different h_s and h_r but constant M_r (=30) for the whole study area (outliers are not depicted). For each parameter setting, there were a number of outliers found across the entire objects (i.e. from h_s 5, h_r 0.005 to h_s 15, h_r 0.02: 4 %, 6.1 %, 9.6 %, 10.3 %, 3.9 %, 7.2 %, 10.6 %, 12 %, 4.1 %, 8 %, 12.2 %, and 13.6 % out of the total objects, respectively).

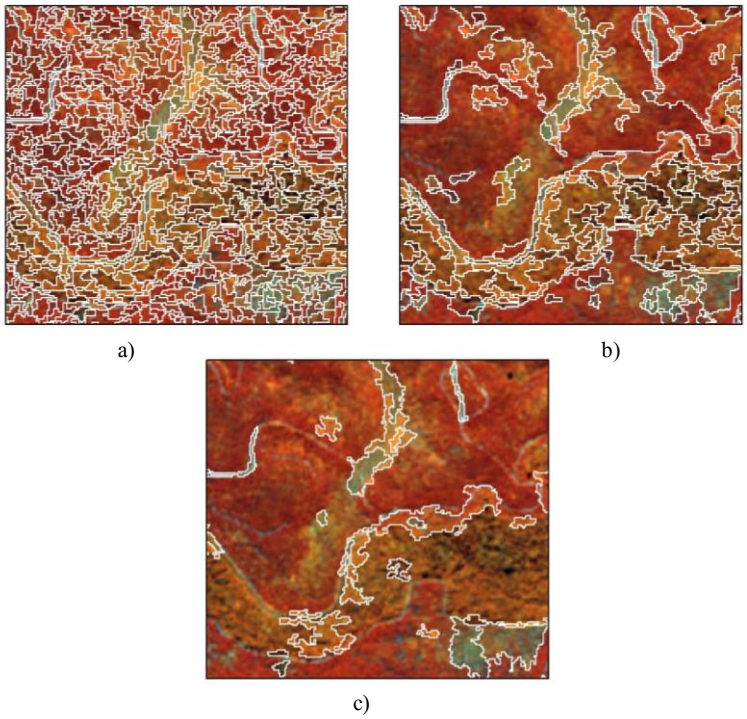

Figure 4.5. Different results of image segmentation with parameter settings $h_s/h_r/M_r$ of a) 5/0.005/30, b) 5/0.015/30, and c) 15/0.02/30 for the same image (RapidEye image with false color composite of RGB 543). The number of objects and average size of each example is 598 objects and 0.16 Ha, 198 objects and 0.48 Ha, and 37 objects and 2.59 Ha, respectively.

From these outputs of image segmentation, the best parameter settings were selected using the Hoover metrics by following these steps:

1. Compiling each score of the Hoover metrics for each parameter setting,
2. Sorting the parameter settings according to the score of correct detection (Table 4.7),
3. Creating scatter plots (Figure 4.6) depicting the scores of correct detection, over-segmentation, and missed detection that were ordered based on the second step,
4. Choosing the best parameter settings for the highest score of over-segmentation; however, the score of correct detection is not zero which means that overlapped objects between reference objects and objects from the segmented image are still present.

By following the above-mentioned criteria, we see in Figure 4.6, the highest over-segmentation score was found for ID = 36, however the score of correct detection was zero. In this study, the best parameter setting was therefore selected for ID = 35 with the combination of $h_s = 5$, $h_r = 0.005$, and $M_r = 30$, as shown by the red line.

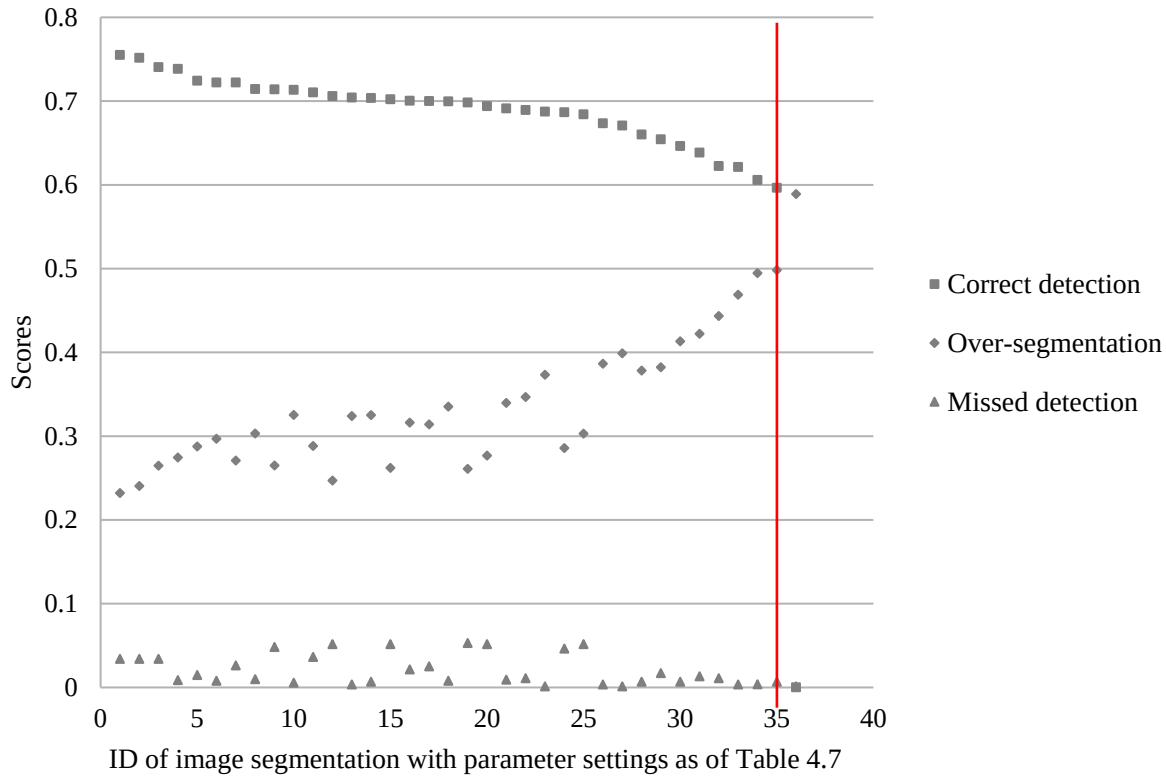

Figure 4.6. The scatterplot of correct detection, over-segmentation, and missed detection scores with different parameterized segments (ordered according to the highest correct detection score). The best parameter setting is shown by the red line with the high score of over-segmentation and correct detection is present.

4.2.2. Image classification

With the best selected parameter setting, further steps in object-based image classification were done. By using the Random Forest classifier, the five most important variables among the eight predictor variables were selected based on the largest value of mean decrease of accuracy produced by RF as explained in subsection 3.2.5. From Figure 4.7, NDVI_RE, B5, B4, NDVI, and B1 with the high value of mean decrease of accuracy were selected as the predictor variables.

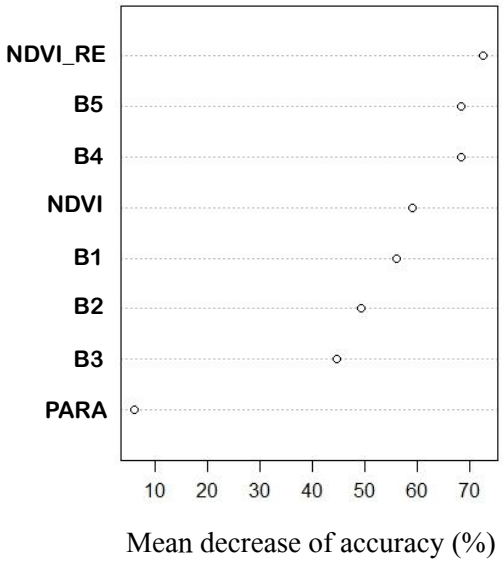

Figure 4.7. The importance of predictor variables based on OOB data. Predictor variables consist of spectral reflectance values of RapidEye for Band 1 (B1), Band 2 (B2), Band 3 (B3), Band 4 (B4), Band 5 (B5), and the values of NDVI Red-edge (NDVI_RE), NDVI, as well as the ratio of perimeter and area of each segment (PARA).

The evaluation of the land use classification was done in two different ways, through the accuracy assessment of the classification model using OOB data that were randomly generated by RF classifier, and through ground truthing data collected in the field. The classification model generated an OA of 81.8 % (Table 4.9). Regarding the tree crops mapping, the model performed better for the classification of oil palm plantations than for jungle rubber and rubber plantations. The classification of oil palm plantations had a PA/UA of 78.2 %/86.5 %. On the other hand, less accuracy was found for jungle rubber, with a PA/UA of 50.2 %/52.3 %, and for rubber plantations of just 19.4 %/40.6 %. The most successful classification was found for secondary forest, with a PA/UA of 85.4 %/83.7 %.

By using an independent data set from ground truthing data, the map validation produced an OA of 64.1 % (Table 4.10). The most successful land use classification was found for the class of secondary forest with a PA/UA of 89.2 %/76.8 %. The classification of jungle rubber and rubber plantation was less successful, with the PA being less than 50 %. In this case, jungle rubber was frequently classified as shrub/bush and was also classified as rubber plantation and secondary forest, to a lesser extent. Rubber plantations were mostly confused with jungle rubber and shrub/bush. The UA of jungle rubber was very low at around 25.5 %, due to confusion with rubber plantation. The confusion between jungle rubber and rubber plantation was found due to mixtures of rubber plantations with other vegetation on the ground. The field survey revealed that rubber plantations were not only always grown with rubber tress but with other woody vegetation, as well as grasses that depend on their management status (examples are in Figure 4.8). As also found in Table 4.9 where OOB data were used for accuracy assessment, the confusion also occurred between jungle rubber and rubber plantation as well as shrub/bush.

Table 4.9. Confusion matrix from OOB data.

		Classification									
		Secondary forest	Jungle rubber	Rubber plantation	Oil palm plantation	Shrub/ bush	Bare land	Settlement	Water body	Total	PA (%)
Reference	Secondary forest	1325	26	2	78	118	1	0	2	1552	85.4
	Jungle rubber	27	101	10	2	61	0	0	0	201	50.2
	Rubber plantation	3	21	13	0	24	6	0	0	67	19.4
	Oil palm plantation	107	4	0	737	85	9	0	0	942	78.2
	Shrub/ bush	118	40	6	31	1778	66	0	2	2041	87.1
	Bare land	1	1	1	4	89	462	12	4	574	80.5
	Settlement	0	0	0	0	1	22	13	0	36	36.1
	Water body	2	0	0	0	1	3	0	17	23	73.9
	Total	1583	193	32	852	2157	569	25	25	5436	
	UA (%)	83.7	52.3	40.6	86.5	82.4	81.2	52.0	68.0		
	OAA (%)	81.8									

Table 4.10. Confusion matrix from independent ground truthing data.

		Classification								
		Bare land	Jungle rubber	Oil palm plantation	Rubber plantation	Secondary forest	Settlement	Shrub/ bush	Total	PA (%)
Reference	Bare land	54	0	1	1	0	5	5	66	81.8
	Jungle rubber	0	12	0	2	1	0	13	28	42.9
	Oil palm plantation	6	2	111	0	18	0	61	198	56.1
	Rubber plantation	10	28	5	24	10	2	28	107	22.4
	Secondary forest	1	2	1	0	116	0	10	130	89.2
	Settlement	17	0	0	3	0	27	3	50	54.0
	Shrub/bush	4	3	3	1	6	0	106	123	86.2
	Total	92	47	121	31	151	34	226	702	
	UA (%)	58.7	25.5	91.7	77.4	76.8	79.4	46.9		
	OAA (%)	64.1								

Due to insufficient accuracy in distinguishing between jungle rubber and rubber plantations, both classes were then aggregated into one class, the so-called rubber land. With this aggregation, the classification accuracy of rubber land increased with a UA at about 84.6 % and PA at about 48.9 %. This led to the increase of the OA to 68.4 %.

The classification accuracy of oil palm plantation was low in terms of the PA, at about 56.1 %. This class was frequently confused with shrub/bush, especially for young oil palm plantations. A reason for that maybe that young oil palm plantations are typically surrounded by shrub/bush (examples are in Figure 4.9). This finding was also in line with the low UA of shrub/bush, a class that was frequently confused with oil palm plantations.

According to the land use classification (Table 4.11), oil palm was the largest tree crops around the Harapan landscape compared to rubber. These oil palm plantations were mainly in the eastern part of the study area (see Figure 4.10), consisting of mostly mature oil palm (approximately 25-year-old). The largest area in this landscape was covered by shrub/bush, and then followed by secondary forests

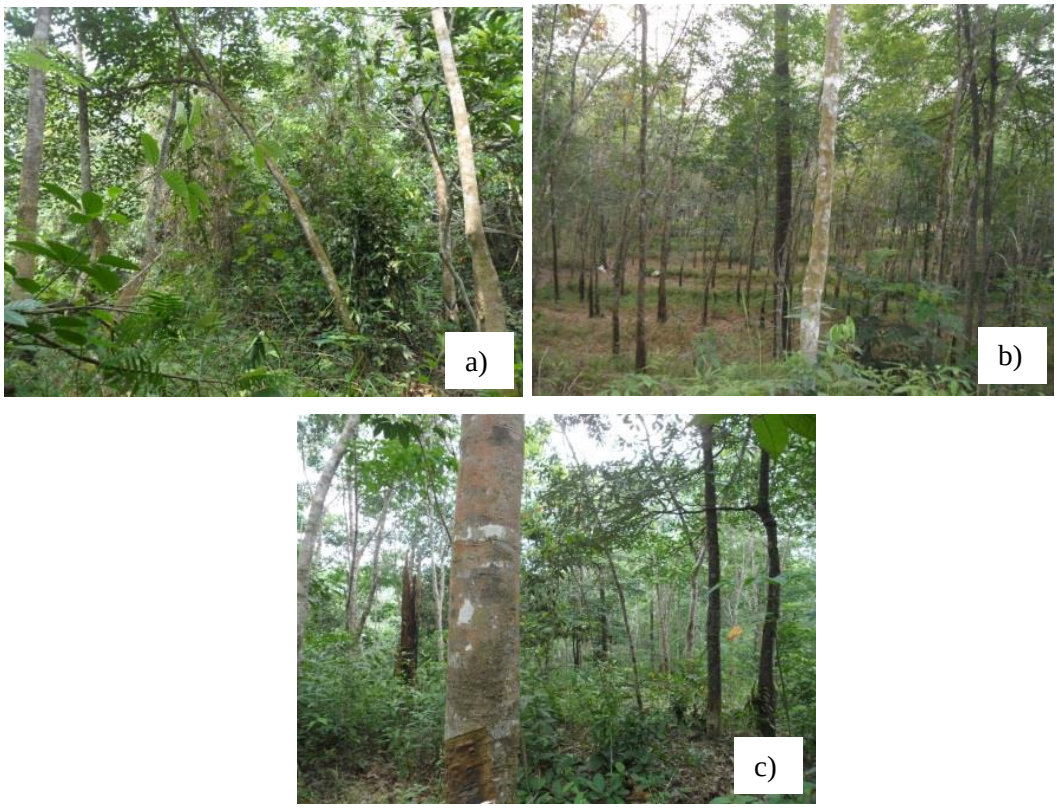

Figure 4.8. a) jungle rubber, b) managed rubber plantation, c) less-managed rubber plantation.

Figure 4.9. a) young oil palm plantation, b) mature oil palm plantation.

Table 4.11. The extent of land use systems in Harapan landscape.

Land use systems	Area (ha)	%
Secondary forest	30604.99	31.1
Rubber land	3687.78	3.7
Oil palm plantation	17116.88	17.4
Shrubs/bush	37667.85	38.3
Bare land	9053.30	9.2
Settlement	81.77	0.1
Water body	169.25	0.2

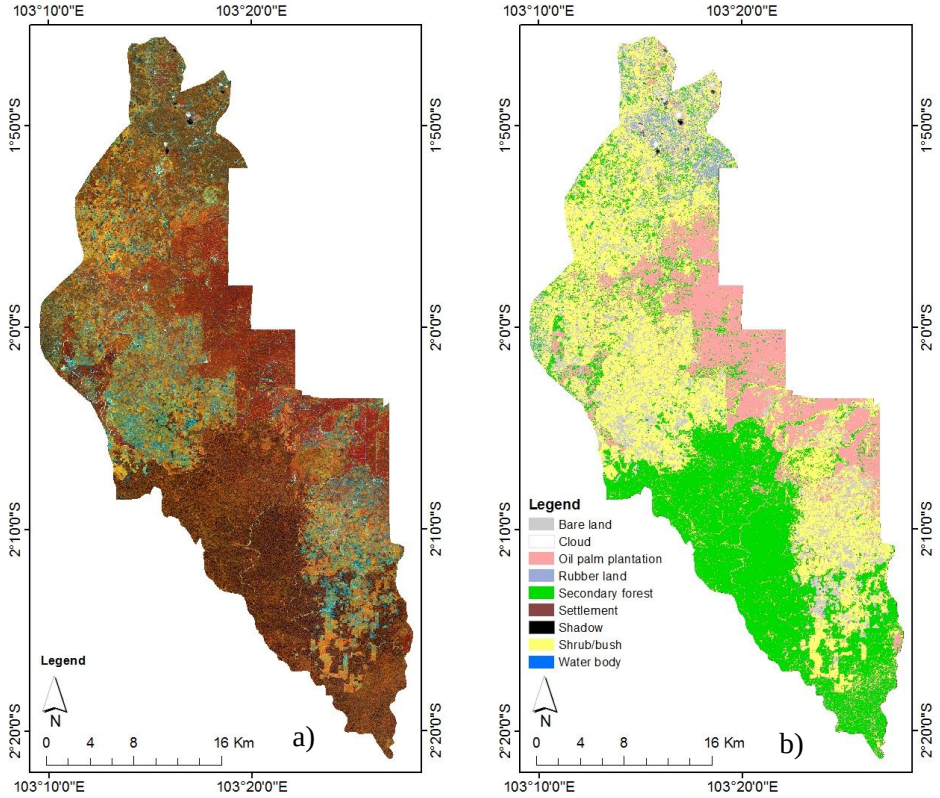

Figure 4.10. Maps of Harapan landscape of a) RapidEye image with false color composite of RGB: 543, and b) land use systems. To highlight this, a large area of oil palm plantations can be seen in the map showing a large industrialization. In the southern part, secondary forest is preserved under the concession of Harapan rainforest where fragmented forests are seen in the southern area of the concession.

4.3. Assessment of key variables of secondary rainforest

4.3.1. Forest variables

A forest inventory was conducted to further relate with remote sensing data to produce an assessment of forest variables across large areas in Harapan rainforest. Field work took place in August and September, 2013 ($n = 29$). The summary statistics for forest variables in the Harapan rainforest are in Table 4.12 and the typical *d*-distribution as well as above ground biomass distribution are depicted in Figure 4.11. From this figure, one sees that trees with *dbh* values between 10 and 40 cm contributed a large amount of above ground biomass.

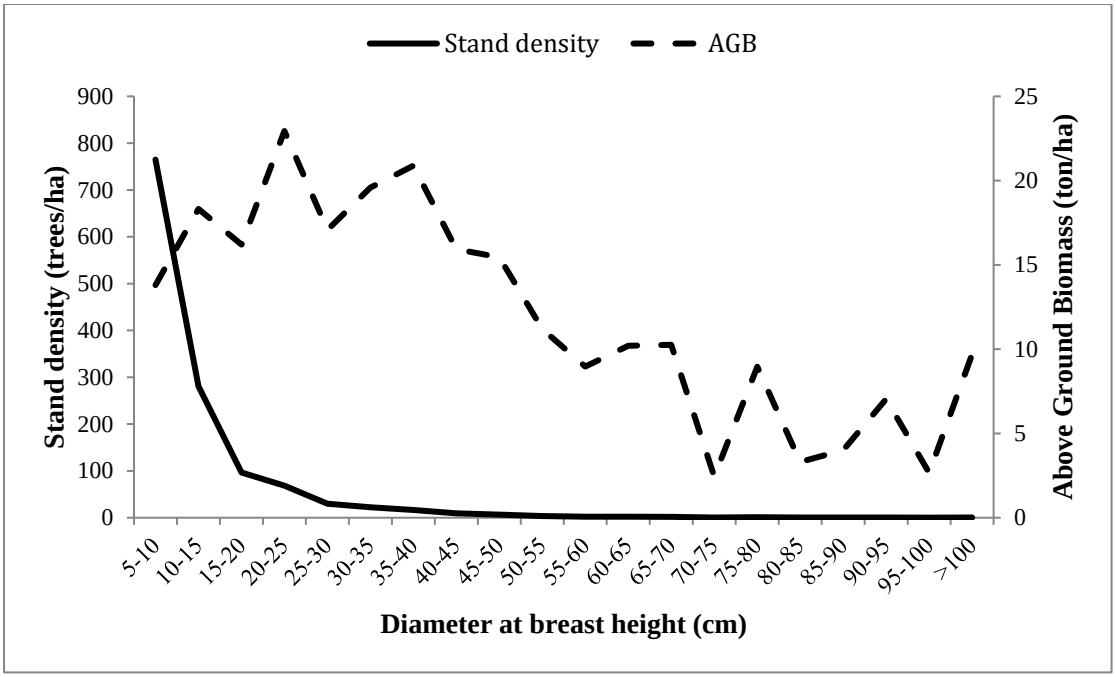

Figure 4.11. Diameter and above ground biomass distribution in the Harapan rainforest from $n = 29$, where one sample plot is a cluster of two subplots of 1000 m^2.

Table 4.12. Major mensurational characteristics of the study area in Harapan rainforest from $n = 29$.

Forest structures	Range	Mean	SE	SE (%)	CI
AGB (ton/ha)	35.26 – 446.89	238.82	19.32	8.1	238.82 ± 39.56
BA (m^2/ha)	6.80 – 42.56	23.55	0.53	2.2	23.55 ± 1.08
dq (cm)	7.21 – 27.26	17.06	0.86	5.1	17.06 ± 1.76
N (trees/ha)	510 - 3145	1321	110	8.3	1321 ± 225.28

4.3.2. Prediction of forest variables from remote sensing data per plot and validation

According to the feature selection as a result of a stepwise exhaustive search and model fitting through multiple linear regressions, the final models were chosen to predict the forest variables as shown in Table 4.13. For each prediction, models for AGB, BA, and dq were obtained with Adj. R^2 of 0.68, 0.56, and 0.50, respectively. The lowest prediction quality was found for the N with Adj. R^2 of 0.24. All the predictor variables were significant in predicting AGB, G, dq, and N, with p-value < 0.1. Among these selected predictor variables, texture indices were mostly chosen for the model prediction of AGB, BA, and dq. All predictor variables were different for each model prediction except TX9_ASM which built the model prediction for AGB and BA. It indicated that texture variable of angular second moment (ASM) using moving window size of 9 has a remarkable role that needs to be further investigated.

Table 4.13. Linear regression analyses for each forest variable.

Dependent variables	Independent variables	Estimate	Std. Error	Pr(>|t|)	Adj. R^2	VIF
AGB					0.68	
	(Intercept)	10361.75	2180.23	8.62E-05		
	CRM	-435.20	77.85	1.09E-05		1.2
	TX9_ASM	61.64	14.38	0.000275		2.31
	TX9_VAR	-1491.30	288.06	3.01E-05		8.06
	TX15_ENT	-382.36	89.90	0.000300		6.02
	TX15O_SD	-8915.72	2542.25	0.001895		4.58
BA					0.56	
	(Intercept)	203.709	37.4395	1.37E-05		
	NDVI	-189.82	37.9334	4.11E-05		1.58
	TX9_ASM	7.0001	1.3429	2.43E-05		2.36
	TX15_ASM	-2.041	0.4465	0.000123		5.73
	TX15_CORR	-206.58	56.3389	0.001217		4.34
dq					0.50	
	(Intercept)	-76.796	20.518	0.000956		
	NDVI_RE	37.169	7.336	3.14E-05		1.23
	TX3_VAR	24.074	8.14	0.006684		9.46
	TX9O_SD	-375.3	161.874	0.028893		9.20
N					0.24	
	(Intercept)	6178	1582	0.000597		
	CGM	-19259	5902	0.003077		1.30
	B3	874873	483042	0.081684		1.30

As can be seen in Figure 4.12 (a-d), the model predictions of AGB, BA, and dq were superior compared to that of N. They have R^2 values of > 0.5, i.e. 0.73, 0.62, and 0.55 for AGB, BA, and dq, respectively. In fact, a high deviation of the regression line from 1:1 line for N was observed. From the results of the model prediction, the mean value of AGB was predicted to be smaller than the observed AGB at 237.77 ton/ha. For BA, the mean value was predicted with a similar value to the observed BA at 23.49 m^2/ha. This was also found for the dq prediction with a similar mean value to the observed dq at 17.02 cm. The predicted mean value of stand density was, however, predicted to be smaller than the observed stand density at 1316 trees/ha. Given the plots of residual versus predicted dependent variables as shown in Figure 4.12 (e-h), it can be seen that the residuals increase with increasing values of the dependent variables.

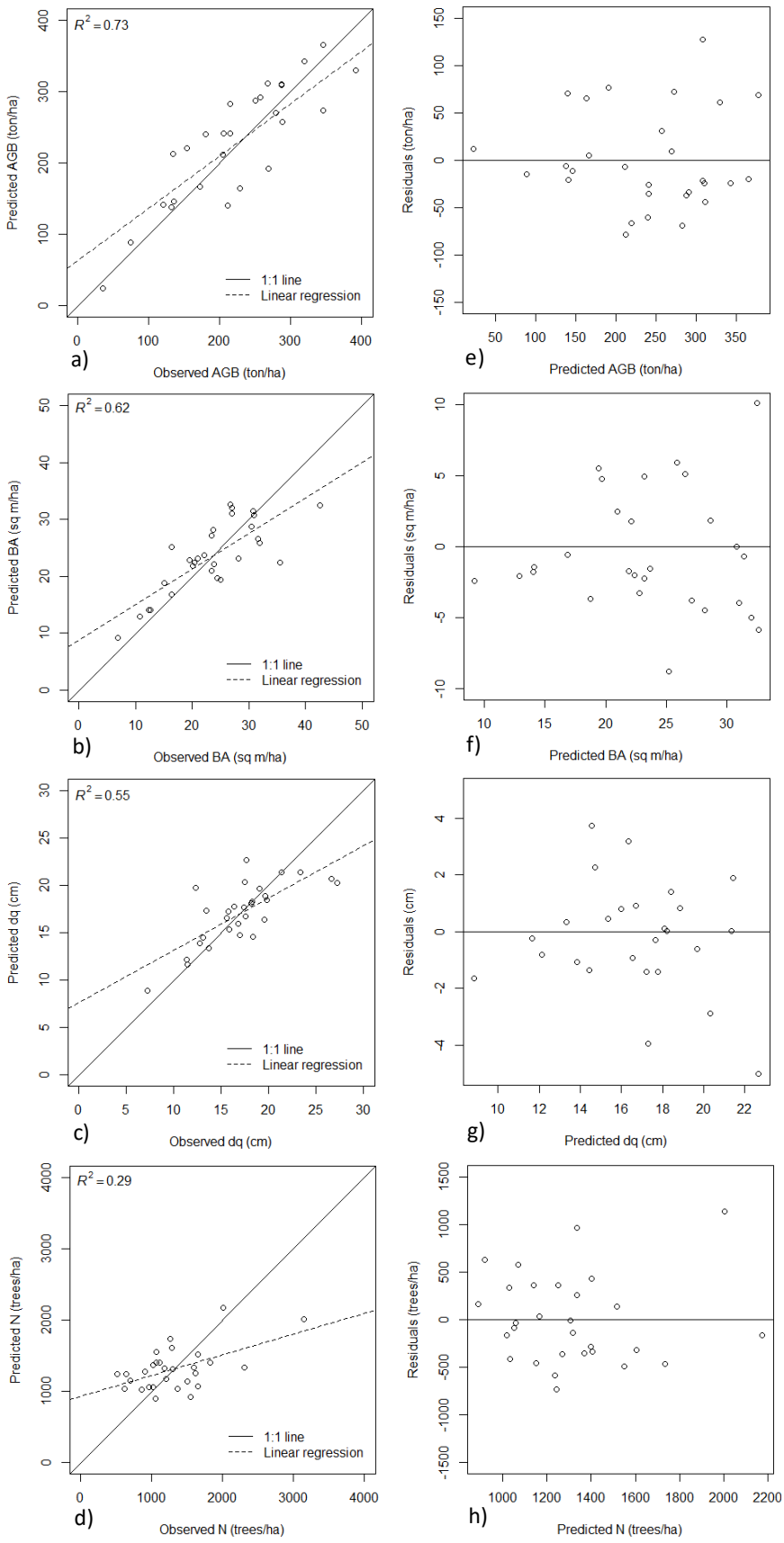

Figure 4.12. Predicted versus observed values and residual versus predicted values of AGB, BA, dq, and N for the $n = 29$ measured field sample plots.

Additionally, cross validation was done. The $RMSE_r$ of AGB, BA, and dq was lower, at < 30 %, than those of N as shown in Table 4.14. The $RMSE_r$ of N was the highest, at 40 %. The potential reason for the lowest prediction quality of N is discussed in the next chapter.

Table 4.14. The cross-validation of each forest variable based on LOOCV.

Dependent variables	$RMSE$	$RMSE_r$ (%)
AGB	64.02 ton/ha	26.8
BA	6.09 m^2/ha	25.9
dq	3.23 cm	18.9
N	528 trees/ha	40

Regionalization was only done for AGB, BA, and dq, as can be seen in Figure 4.14. A map of N was not produced due to the low model prediction with $R^2 < 0.5$ and high $RMSE_r$. Negative values occurred and were then replaced with 0. From the enlarged frame, one might expect to find similar pattern between AGB and BA. However, it is not seen from this figure. The reason could be explained by the imperfect model prediction for both variables which does not adequately represent the observed data. Therefore, the similar pattern of AGB and BA distribution on the regionalization map cannot be expected.

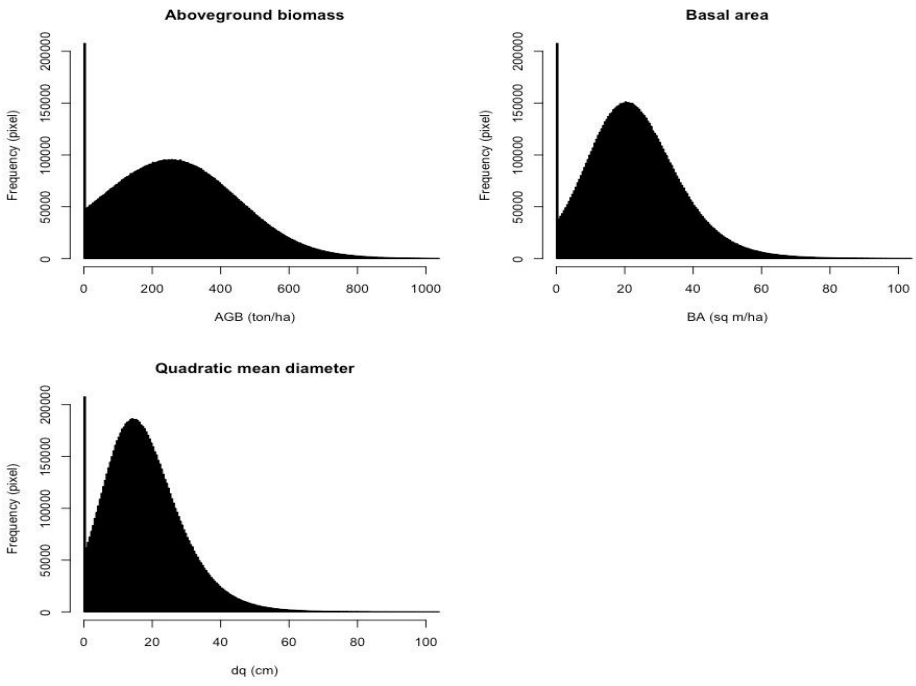

Figure 4.13. The histograms of a) AGB, b) BA, and c) dq. Frequency shows the number of pixels.

As the result of regionalization, the histograms that show the frequencies (in pixel) of the respective variable values are depicted in Figure 4.13: the AGB values were mostly found

in the range of 0 - < 600 ton/ha. The BA values were mostly found in the range between 0 - < 50 m^2/ha, while the dq values were mostly found in the range between 0 – < 40 cm. These figures allow us to compare with other forest areas to give insight about the forest resources.

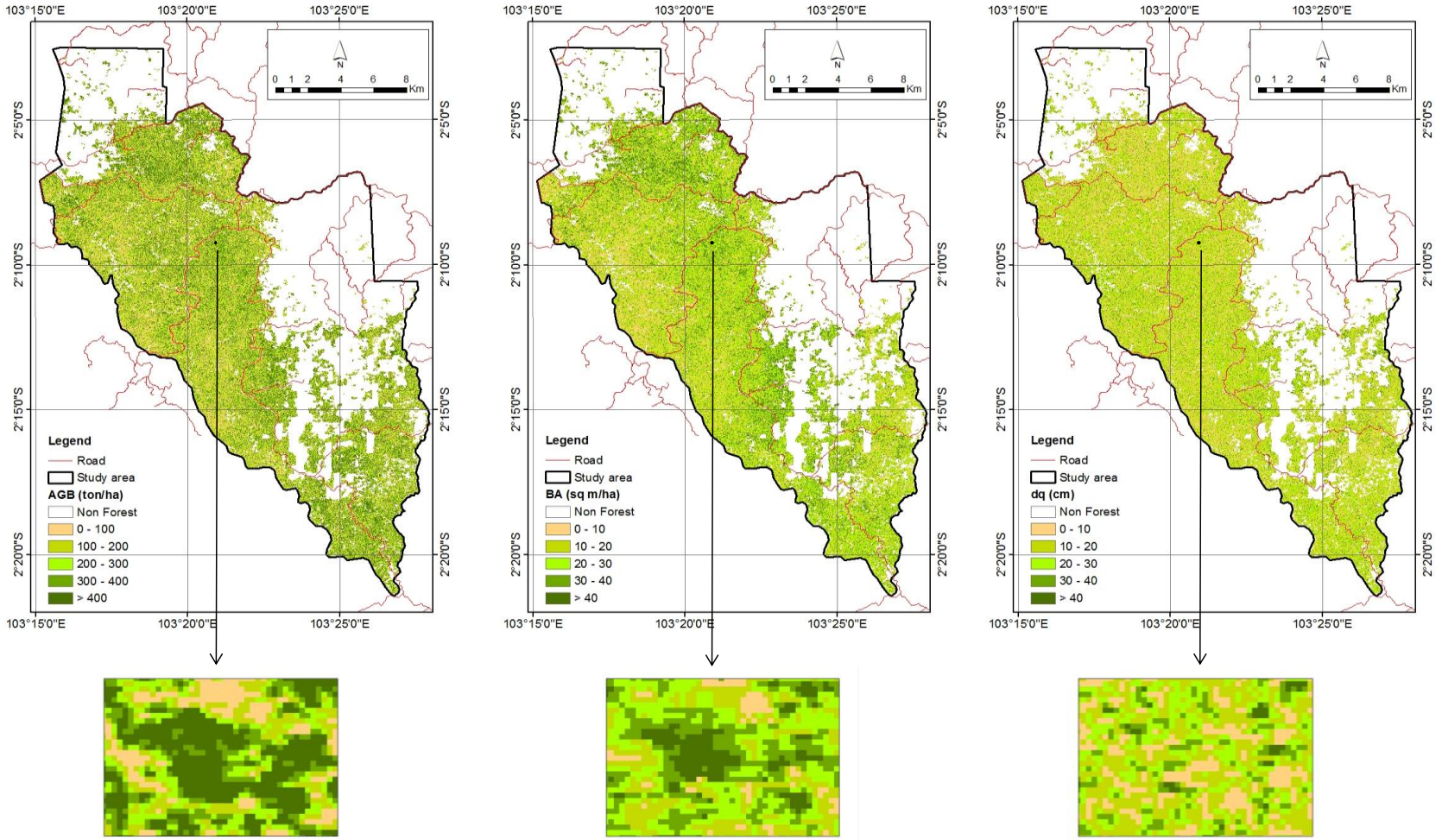

Figure 4.14. The forest variables maps of a) AGB, b) G, and c) dq. The enlarged frame shows an area of interest depicting the spatial distribution of AGB, BA, and dq. From the respective class categories, a priority area can be identified to take further action related to forest conservation and restoration.

Chapter 5
Discussion

5.1. Monitoring land use systems

Monitoring land use systems is necessary because it provides important baseline information for historical land use change analyses. In this study, time series of land use maps were analyzed for the 1990-2013 period, which provided information regarding the transformation of land use systems and temporal dynamics of fragmentation as well as the causes of deforestation. Temporal dynamics of fragmentation was only analyzed for the whole Jambi Province in this study. It is recommended for the future study to analyze the fragmentation at each district. In this way, the spatial pattern of land use transformation can provide information on which district the dynamics is prominent.

The time series of land use maps were the major source, in which they were used to analyze the change in land use systems and spatial patterns within Jambi province at four different points in time: 1990, 2000, 2011, and 2013. The accuracy assessment of the map based on ground truthing data was only available for the 2013 map, where the OA reached 78.2 %. In this study, map validation based on ground truthing data was not possible for the earlier maps from 1990, 2000, and 2011. The earlier maps were all produced in the later years and ground truthing data were only able to be collected in 2014 to validate for the 2013 map. Therefore, the accuracy of earlier maps was assumed to be similar to the 2013 map, as the applied methodology was also similar (Caldas et al., 2015; Villamor et al., 2013).

There are many studies have been done to analyze the land use change that are based on time series of remote sensing data. However, few studies had analyzed the land use change in the Jambi province. In regard to the comparison of the extent of land use change, only the area loss of forests from 2000 to 2011 in this study can be compared with other studies by Margono et al. (2012) and Hansen et al. (2013). Both studies observed the loss of forest covers based on Landsat images as well. In the study of Margono et al. (2012), the loss of forest cover in Jambi province, including primary intact and primary degraded (secondary) forests within a slightly different period, between 2000 and 2010, was found to be around

0.30 Mha. The terms of primary intact and primary degraded forests used by Margono et al. share a similar definition with the terms of primary and secondary forests used in present study. In the present study, the loss of forest cover for the period of 2000 to 2011, including primary and secondary forests, was slightly different, at around 0.34 Mha (Appendix A.5.). Nonetheless, it was greatly different when compared to the results presented by Hansen et al. (2013), where the decrease of forests for the period of 2000-2011 was at around 0.87 Mha. The forest cover map produced by Hansen et al. (2013) was actually criticized by Tropek et al. (2014), arguing that the forest cover areas are overestimated. Tropek et al. (2014) found that typical plantations (e.g. rubber, coconut, oil palm, etc) were interpreted as forests. In this case, the forest dynamics by Hansen et al. (2013) were based on the definition of forest as tree cover including "commercial forestry dynamics" (Margono et al., 2014). The calculation of forest loss included the clearing of oil palm and forest plantations and, thus, it might produce high forest loss.

The present study documented a remarkable decrease in forest areas in the Jambi province between 1990 and 2013, which is also pointed out by Drescher et al. (2016). Primary forests were mainly transformed into secondary forests, while secondary forests were mainly transformed into rubber and oil palm plantations. This means that the expansion of tree crops came at the expense of secondary forests, particularly between 1990 and 2000. Furthermore, oil palm plantation expansion also took over rubber plantation areas, indicating high profitability of oil palm plantation (see Table 4.2), which corresponds to the results of the study by Gatto et al. (2015). They studied the land use dynamics and oil palm expansion in Jambi province based on village surveys in 90 villages with data from 1992 to 2012. Apart from rubber land, they found that oil palm plantations were mainly grown in formerly-fallow land. According to their definition, fallow land represents "over-logged forests or unproductive plantation land", also associated with swidden agriculture. Based on historical land use maps from 1990 to 2013, the present study also found that oil palm plantations came at the expense of agricultural land (Table 4.2).

However, Gatto et al. (2015) found that oil palm expansion did not mainly come at the expense of secondary forests, even though they found the correlation that deforestation occurred considerably when oil palm plantations expanded. This contradicting finding can be interpreted as resulting from some limitations that were also mentioned in their study. Principally, the drawbacks of their survey data come when they asked interviewees to recall land use systems from ten to twenty years back. Inconsistencies in the "perceptions, definitions, and memories" are likely to be present (Gatto et al., 2015). Therefore, they

stated that the accuracy of land use information based on surveys is lower than that from remote sensing data. Moreover, it should be considered that the approach of 'wall-to-wall' mapping provides information on the extent of the change covering the whole study area, which cannot be covered by a survey that is based on a sampling approach.

As can be seen in Table 4.2, the gain of area of oil palm plantations in 2013 was higher than that of rubber plantations. This is driven by greater profits from oil palm cultivation due to lesser labor costs and faster returns, considering that the harvesting of palm oil takes four years from the first planting while it takes around seven to ten years to harvest rubber from the first planting (Schwarze et al., 2015). The expansion of oil palm plantations showed a continuous increase of mean patch size, which indicates massive industrialization from 1990 to 2013. The transmigration program in the late 1980s maybe one reason for that, as the government provided patches of land of about 2.5 ha to transmigrants for their settlement which included areas on which to grow profitable oil palm (Gatto et al., 2015; GoI, 1986). Thus, the farmers grew oil palm plantations next to oil palm companies that were either publicly- or privately-owned following the Nucleus Estates and Smallholders (NES) scheme. Through this scheme, the smallholders who grew their palm oil could get the benefit of processing their fruits soon after the harvest in the palm oil mill established by the companies (Feintrenie et al., 2010). In addition to the contracted farmers, the independent smallholders who were not involved in the NES scheme or other kind of contracts with companies tended to increasingly also grow palm oil. Starting in the mid-1990s, they grew palm oil surrounding the established oil palm plantations because of better access to palm oil mills (Euler et al., 2015). This fact explains the increase of mean patch sizes and the aggregation index of oil palm expansion. The above-mentioned government programs such as transmigration followed by NES scheme had brought a notable impact on the land use dynamics. It is seen that the expansion of profitable plantations at the cost of nature took place to improve wealth and income.

The spatial pattern of rubber plantations did not change much during the period of 1990-2013 as evidenced by the metrics of mean patch size and the aggregation index. This can be understood with the evidence that rubber trees were mostly grown by smallholders (83 %) while oil palm plantations were mostly owned by large-scale companies (66 %) (Susila 1998, *in* Kartodihardjo and Supriono 2000). These large enterprises have more options to expand their plantations because of larger capitals. However, rubber plantations were still the dominant crop with the largest area covering Jambi province, with around 17.4 % of the total area in 1990 and 18.6 % in 2013 (see Table 4.1). The reason for this could be that

growing rubber is common for smallholder farmers and was cultivated much earlier. Furthermore, rubber farmers are not dependent on the mills, which belong to companies, for the processing of their harvest as are the palm oil farmers (Ketterings et al., 1999). That is, rubber farmers are more independent. When changing the land into oil palm, they would be highly linked to and dependent on the large companies.

Regarding deforestation, the lowland forests were most affected because of easy access. According to the empirical model, variables that were most associated with deforestation were rubber and oil palm productivity. This finding corresponds to the expansion of both plantation types. In our model that related district-wise socio-economic variables to deforestation, the population density was negatively correlated to deforestation which came as a surprise. In fact, DeFries et al. (2010), who also looked at the variables related to deforestation from 2000 to 2005 across 41 countries in the tropics, found the same trend of population growth with a negative coefficient. In contrast to overall population growth, they found that urban population growth was associated with deforestation. They argued that this was an impact resulting from urbanization, where the demand related to biofuel as an agricultural product from rural areas had increased and thus threatened the surrounding tropical forests.

Overall, it is a result of these analyses that the expansion of rubber and oil palm plantations came at the expense of secondary forests in the Jambi province in the period of 1990-2013. This transformation came with a decline of biomass, as well as plant and animal diversity (Drescher et al., 2016) which brings a negative impact to the environment. However, it also increased household welfare. In particular, the adoption of oil palm plantations as the source of livelihood across the Jambi province had a positive impact on consumption expenditure, including food and non-food expenditure, along with calorie consumption, both of which indicate a better welfare (Euler et al., 2015). In fact, the transformation of rubber plantations into oil palm plantations described in this study indicates that oil palm provides more economic value than rubber plantations. From the period of 2004-2012, the price of the palm oil fruit increased from 64 USD/ton to 133 USD/ton (108 %). This increase was higher than the price of natural rubber that was about 467 USD/ton in 2004 and 877 USD/ton in 2012 (88 %) (FAOSTAT, 2016). Additionally, in that same period from 2004 to 2012, the demand for oil palm from the three biggest importers had increased from about 11 to 20 Mt (by about 75 %), while the demand for natural rubber rose only from about 0.7 to 0.8 Mt (by about 14 %) (FAOSTAT, 2016). The export value of palm oil in Indonesia was higher than the export value of crumb rubber (= processed rubber) in

2014, at about 17.5 billion USD for palm oil and 4.5 billion USD for crumb rubber (BPS, 2015).

While there are many economic benefits of palm oil production, the downside is the associated environmental change. Lately NGOs and global conservationists have decried the expansion of oil palm plantations as it is rapidly converting natural forests into plantations (EIA 2014; Greenpeace 2016; Koh and Wilcove 2008; Peh et al. 2006; Wilcove et al. 2013). In response to this issue, the Roundtable on Sustainable Palm Oil (RSPO) has established a voluntary certification scheme for sustainable palm oil production with the objective of meeting socio-economic and ecological standards. One principle of this certification is to use cleared or degraded areas instead of forests to grow oil palm (RSPO, 2013). However, there is no clear definition of 'degraded area' found in Indonesian policy or law (WRI, 2010). World Resources Institute (WRI) identified that NGOs, private, government and academics in Indonesia used 'degraded forest'[7], 'waste land'[8], or 'abandoned land'[9] as terms to represent degraded land. Ruysschaert et al. (2011) proposed a severely degraded land as a location to grow palm oil instead of leaving the area abandoned. They defined this severely degraded area as fallow land that is covered only by shrubs and bushes. This was because of the gain of above-ground carbon stock, which can reach on average up to 40 ton/ha during one cycle of oil palm plantations (i.e. 25 years), while the maximum is around 60-80 ton/ha for mature palm oil (Ruysschaert et al., 2011).

However, as mentioned above also, degraded (secondary) forest can be interpreted as degraded land. This interpretation further impacts the exclusion of secondary forest from Indonesia's forest moratorium which aims to suspend new concessions in primary forests and peatlands. At the first period of the forest moratorium, during the years 2011-2013, it was set for primary forests and also peatlands but it excluded secondary forests (Murdiyarso et al., 2011). The ministry's director general of forestry planning and environmental governance from the MoEF, Ruandha Agung Sugariman said that secondary forest was excluded to provide production area (The Jakarta Post, 2015). In fact, a similar condition applies to the second and third extension of the moratorium for the years 2013-2015 and 2015-2017, respectively. For Jambi province, the implementation of this policy had a positive impact, with the loss of primary forests remarkably decreasing in the last

[7] Degraded forest is a secondary forest where a forest provides a reduced capacity of ecosystem services (e.g. carbon storage, timber production) because of the anthropogenic and environmental alteration (BP-REDD+, 2015)

[8] Waste land is also called as marginal land where the land is not profitable or does not have economic potential due to low productivity for agricultural activities (WRI, 2010)

[9] Abandoned land is an empty area where there is no productive utilization. For example, the land where the permit holder has not yet utilized it (WRI, 2010)

period of 2011-2013 as shown in Figure 4.1. However, the loss of secondary forests in this period was considerably higher than that of primary forests. This high loss of secondary forest can be interpreted because there was no suspension of secondary forests' conversion.

In order for the previously-mentioned RSPO certification of sustainable palm oil to succeed, a strong legal regulation and enforcement would be necessary as it is currently still voluntary. For instance, China and India are the major markets for oil palm but have been criticized because of the low concern they have in purchasing certified palm oil (Wilcove & Koh, 2010). In Indonesia, the government has established the MoA Regulation 11 of 2015, which is the so-called Indonesian Sustainable Palm Oil (ISPO) (MoA, 2015). This regulation is mandatory for the big palm oil industries. Such commitment indicates government awareness in producing sustainable palm oil while protecting forest areas. Therefore, it is expected to reduce emissions from deforestation and forest degradation while maintaining the increase of overall welfare. To succeed this program, the regulation needs to be strongly implemented

5.2. Evaluation of tree crops mapping using high spatial resolution images

5.2.1. Object-based mapping

As the expansion of tree crops comes at the expense of forest areas, monitoring these crops becomes a high concern for forest conservation because it provides information on the extent of tree crops and of the remaining forest to respective stakeholders for better land use planning. This information can be spatial information provided by maps that produce the details of tree crops and remaining forests and also portray their spatial distribution. It might serve as baseline information for other research on the ecosystem services, and also for decision makers. By knowing the information on the extent of the remaining forests, further regulation related to forest protection and deforestation reduction can be taken.

Through this study, an operational approach using object-based classification was proposed to fulfill this need. For this approach, RapidEye satellite images with high spatial resolution were used as materials for image segmentation. According to the image segmentation results using different parameter settings, it becomes obvious that lesser number of clusters are produced with larger scale parameter radii (Figure 4.5), which is in line with Bo & Jing (2012). In fact, these authors mentioned that a larger radius might enlarge error probability. Thus, a way to choose the best parameter settings among the different results of segmentations from different parameter settings must be found.

In comparison to other studies that evaluated a selection of different segmentation results as mentioned in subsection 3.2.3, the approach proposed in the present study provides an objective selection to determine the best parameter settings. Another method by Smith (2010) is quite efficient in selecting the best settings based on the high accuracy assessment of land use classification. This high accuracy assessment was presented by low error rate produced by the model-based error provided by the RF classifier. However, this method focused more on the accuracy of the land use classification than on the optimization of image segmentation. Thus, this method ignores the evaluation of image segmentation with the reference objects in the field. Later evaluations were conducted by Carleer et al. (2005) and Marpu et al. (2010). They evaluated the image segmentation with reference objects on the ground. Both of these methods consider high over-segmentation to select the best parameter settings. However, they did not calculate the correct percentage. In fact, the correct percentage is also relevant as guidance to indicate the performance of segmentation algorithms with different parameter settings.

In this study, the selection was evaluated by Hoover metrics, where a comparison among different results of segmentations and reference objects was conducted. According to the proposed method, a selection of optimum segmentation parameters was based on the trade-offs between over-segmentation and correct detection. This method is more advanced than traditional approaches that use trial and error to choose the best image segmentation, as the trial and error approach is not objective in finding the best segmentation parameter settings (Smith, 2010).

5.2.2. Land use classification

In this study, land use classification was conducted using the RF classifier. This classification was produced with high OA according to the model-based cross validation but low OA according to the independent validation data. The lower OA produced by using independent validation data was also found by Magdon et al. (2014). To assess OA, independent data from the ground used to validate the land use classification is however always suggested to have knowledge of the map accuracy according to site-specific information (Foody, 2002).

From the land use systems classification, a remarkable confusion occurred for the jungle rubber and rubber plantation classes. Confusion took place in the mixture of grasses and low woody vegetation that grew among them. This finding is in line with the study conducted by Ekadinata & Vincent (2011) in which they discovered that jungle rubber was

confused with the class of rubber plantation as well as forest because of the similarity in structures and, thus, similar spectral response was expected. For instance, the low management intensity of the rubber plantations has made the rubber trees grow with other vegetation and has also produced confusion with shrub/bush. Apparently, different management intensity has played a role in this class confusion. The confusion can also be in regard to the acquisition time of RapidEye images, which were captured in June during the dry season, when rubber trees' defoliation (leaf-off) takes place. Therefore, spectral response captured by RapidEye images is mostly reflected by the shrubs, grasses, or other kinds of green vegetation. This could have led to the confusion among the classes of jungle rubber, rubber plantations and shrub/bush. Therefore, it was recommended to use high temporal resolution of remote sensing data to produce rubber mapping due to the evidence that rubber trees have such seasonal characteristics (Dong et al., 2013; Li & Fox, 2012; Senf et al., 2013).

For the mapping of oil palm plantations, the information on the spatial distribution produced by this study is reliable with a high UA. Nonetheless, the area could be lesser than the existing area due to the low PA. This confusion took place because of the different ages among the oil palm plantations. Thus, the spectral response coming from the grasses that were grown among the young oil palm plantations produced confusion with the class of shrub/bush (Li et al., 2015). For further work, it should be considered to differentiate the class of oil palm into young, middle, and old.

5.3. Assessment of key variables of secondary rainforest

Predictions of forest variables including above-ground biomass (AGB, ton/ha), basal area (BA, m^2/ha), stand density (N, trees/ha), and quadratic mean diameter (dq, cm) were assessed by combining field inventory and remote sensing data derived from RapidEye images. Field inventory with small sample sizes ($n = 29$) was conducted over a large study area of around 40,000 ha.

According to the field inventory data, only the estimated mean value of AGB could be compared to the previous study conducted by Briggs et al. (2012) in the Harapan rainforest. The result of our study showed that the mean AGB value at 238.82 ton/ha is within the range of their values studied. Briggs et al. (2012) found that the range of AGC is between 85 ton/ha and 141 ton/ha, where AGC is estimated at about half of AGB.

In regard to the model prediction that relates the forest variables and image features derived from RapidEye images, each model that predicted the respective forest variables contained a vegetation index, such as NDVI, NDVI Red-edge, CGM, or CRM (Table 4.13). These vegetation indices are relevant when assessing vegetation conditions (Jackson & Huete, 1991), and, thus, improve the relation between indices derived from satellite images and the forest variables, particularly in the regions that have complex stand structures (Lu et al., 2004).

In combination with vegetation indices, the model predictions of AGB, BA, and dq were mostly built with texture indices (see Table 4.13), indicating the potential role of texture indices. In subtropical and tropical forests with high biomass, where high species diversity and high heterogeneity of canopy layers are present, the canopy shadow effect increases (Nichol & Sarker, 2011). For this case, the texture index reduces the high difference of spectral reflectance due to the shadow effect (Lu & Batistella, 2005). Choosing the appropriate texture indices is challenging. The selection of texture features varies with different characteristics of landscape and satellite images used, including the use of moving window sizes and the image bands (Lu, 2005). In this study, the texture indices were computed using the NIR band for three different moving window sizes of 3x3, 9x9, and 15x15. Different combinations of higher-moving window sizes and spectral bands were not tested. Therefore, it might be worthy for future work to test such different combinations to observe if the model prediction can be improved.

In this study, the model prediction provided models for AGB, BA, and dq with an $R^2/RMSE_r$ of 0.73/26.8 %, 0.62/25.9 %, and 0.55/18.9 %, respectively. RapidEye images used in this study obviously capture the reflectance from vegetation over secondary rainforest and are promising for predicting AGB, BA, and dq. However, the prediction of N was quite low, with an R^2/$RMSE_r$ of 0.29/40 %. The insufficient model prediction of N is interpreted due to the complex layers that are present in the successional forests, which is also a typical forest within the study area (Harrison & Swinfield, 2015). Besides large trees, a large number of young trees are grown in this successional forest where various stages of degraded forest can be found. Optical sensors are more sensitive in capturing the reflectance coming from the top canopy than the low layers. Therefore, optical sensors are expected to be less sensitive when capturing information from low layers where young trees exist. In this case, predictions on stand density in the forest with complex layers face challenges.

Predicted forest variables using image features derived from remote sensing data are challenging when compared across studies. This can be explained due to the differences of the remote sensing data that are used, forest types, data-collection methods in the field, and also statistical modeling (Castillo-Santiago et al., 2010; Ozdemir & Karnieli, 2011). Therefore, R^2 and/or $RMSE_r$ are commonly used as indicators (Castillo-Santiago et al., 2010). For the evaluation of $RMSE_r$, this study did not use independent test data and the error estimation was done by common cross-validation LOOCV that is widely used with small sample sizes (Fuchs et al., 2009; Kayitakire et al., 2006; Ozdemir & Karnieli, 2011). For comparison with other studies, there was no study that predicts a forest variable of dq in the rainforests and, therefore, dq was not able to compare. However, there was one study found which combined field inventory data and RapidEye images to predict some selected forest variables in a Bavarian forest where dq was one of the variables (Wallner et al., 2014). Their model produced R^2 of 0.55 with $RMSE_r$ of 24.9 % for a pure coniferous forest. This result had similar result with present study producing R^2/$RMSE_r$ of 0.55/18.9 %.

The study conducted by Wijaya et al. (2010) did predict forest variables using Landsat images in a concession forest in Borneo, where logging is ongoing. The $RMSE_r$ values based on the model fitting through multiple linear regressions of AGB and BA in their study were 13.2 % and 13.3 %, respectively. These values were better than the ones produced in present study with a $RMSE_r$ of AGB at 26.8 % and BA at 25.9 %. Nonetheless, the model produced by present study had better R^2. Their model prediction was produced with $R^2 < 0.4$, which is much lower than the one produced in this study at around 0.73 for AGB, and 0.62 for BA. It points to the fact that RapidEye images with higher spatial resolution than Landsat images have more ability to predict such forest variables by producing higher R^2.

By using similar satellite image, i.e. RapidEye images, a prediction of AGB was conducted by Englhart et al. (2012) in different types of forest in Borneo, which is a peat swamp forest. Their study found that combining field inventory and image features derived from RapidEye images is promising when predicting AGB, where a high R^2 of 0.92 with $RMSE_r$ of 44% was produced from their model prediction. Compared to their study, the present study produced lower R^2 of 0.73. Their high R^2 with large sample size ($n = 53$) may cover a high variability of the surface reflectance. However, in term of covering different variability of the surface reflectance, the stratification of NDVI that was used in this study as the reference to determine the sample plots already ensured a proper representation of the population.

There was a challenge when implementing the model to produce regionalization maps due to negative values in the maps. Such extreme values occur when the model is applied beyond the observation values and therefore zero was constantly used for negative values (Fuchs et al., 2009). Moreover, high values also occurred even though their frequency was not high, as can be seen in the histogram of the images where AGB was at > 600 ton/ha, BA at > 70 m^2/ha, and dq at > 60 cm^2 (Figure 4.13). The high values of AGB also occurred in another study conducted by Englhart et al. (2012), in which the values of AGB reached more than 600 ton/ha. Therefore, they assumed those values as overestimated values, without doing any change of these high values. In this case, caution should be taken when using the regionalization maps produced in present study. The extrapolation values from the model could produce uncertainty for the area outside observed areas where model was built. In this study, multiple linear regression was used as model prediction and, therefore, different model prediction can be tested for the future work to see whether the model is able to avoid extreme values.

The class categorization provided by the regionalization maps delivers practical information for a better strategy of forest management. Through the maps, areas of high priority can be identified to promptly take measures which strengthen forest conservation and restoration. For instance, an area with low above ground biomass due to high degradation should be prioritized for increasing the biomass through the reforestation. This will be useful for Harapan rainforest where immediate conservation is necessary because of illegal encroachment and the expansion of oil palm plantations (Laumonier et al., 2010).

Chapter 6
Conclusion

Monitoring of forests and land use dynamics is of great interest providing the database required to identify and analyze causes and impacts of land use change. In turn, this valuable information serves to better land use designation and planning by decision makers, particularly in tropical forested landscapes. Furthermore, it might contribute to developing polices to combat the conversion of forests and, thus, mitigating climate change as well as threats to the conservation of biodiversity. This study provides scientific-based knowledge on the monitoring of land use systems being transformed in Jambi province of Sumatra, Indonesia, where economic cash crops have increasingly threatened the existence of forest lands. In order to monitor large areas, remote sensing data combined with sample-based field data are therefore essential sources of information. The use of these data might overcome the limitation of the high-intensity of data collection, which is labor intensive and costly. Additionally, multi-series remote sensing data bring an advantage to understanding the land use change at different points in time.

Through multi-series Landsat images within Jambi province, historical land use maps were available based on the visual interpretation of the images. It is evident that a loss of secondary forests continuously occurred from 1990 to 2013 as rubber and oil palm plantations expanded. The expansion of oil palm plantations, in particular, indicates a pattern of large-scale industrialization. The expansion of those typical tree crop plantations might stimulate the increase of both the crops' productivity within the study area and, thus, was found to be one of the factors related to deforestation. On the other hand, the increase of population density was not related to deforestation. It might be informative for further research to differentiate the population density between urban and rural, and analyze their specific relation to deforestation in Jambi province. As urbanization could impact the high demand of agricultural products from rural areas, the increase of urban population density is expected to threat the surrounding forests (DeFries et al., 2010).

The rate of secondary forest loss has decreased over the last years; however, it was still higher than the loss of primary forests. Such low rates of primary forest loss indicate the success of a forest moratorium policy protecting the primary forests. It is therefore highly recommended to protect secondary forests due to their high value for providing ecosystem services and preserving biodiversity. For instance, to avoid the conversion of forest land, severely degraded land has been introduced as an alternative location for new tree crop plantations; however, the feasibility of land productivity is still questioned.

For the study of the tree crop mapping, high spatial resolution satellite images, i.e. RapidEye images, were used. To distinguish the land use systems, the object-based classification was evaluated. The result of the map-accuracy assessment with ground truthing validation data indicated that the object-based classification produced sufficient accuracy in distinguishing secondary forest with high PA and UA. The classification of the tree crops, rubber land and oil palm plantation, produced a high UA but a low PA. For rubber land that includes jungle rubber and rubber plantations, the use of multi-temporal remote sensing images is suggested due to the seasonality characteristics of rubber trees. Additionally, to increase the classification accuracy of oil palm plantations, it is recommended to differentiate the young and mature oil palms. In this regard, the training area of young oil palm plantations should be cautiously determined, in which the training area should represent the true young oil palms since confusion with the shrub/bush class might arise due to the presence of grasses surrounding young oil palm plantations.

As secondary forests are threatened by the expansion of tree crop plantations, immediate conservation is of high concern. To succeed the conservation, managing the forest is necessary. For this purpose, reliable information on the forest variables such as forest carbon stock is necessary. From this information, knowledge about the forest resources can be identified and is thus useful for taking measures towards better forest management and ultimately forest preservation.

In this study, forest variables (i.e. above ground biomass, basal area, quadratic mean diameter, and stand density) were predicted by combining small sample sizes of forest inventory and remote sensing data from high spatial resolution RapidEye images. The proposed approach produced sufficient R^2 *and* $RMSE_r$ for predicting the forest variables (i.e. above ground biomass, basal area, and quadratic mean diameter). The approach is also operational and can be applied particularly to large forest areas. However, further studies need to be conducted to find better approaches for predicting the stand density as this was

unsuccessful in this study; this can be attributed to the lack of optical sensor to capture information in the forest with its complex layer as discussed in the chapter before. The regionalization maps generated based on the model prediction might further support the delivering of information to forest managers and other decision-makers.

References

Allen, K., Corre, M. D., Tjoa, A., & Veldkamp, E. (2015). Soil Nitrogen-Cycling Responses to Conversion of Lowland Forests to Oil Palm and Rubber Plantations in Sumatra, Indonesia. *PLOS ONE*, *10*(7), e0133325. https://doi.org/10.1371/journal.pone.0133325

Alonso, A., Dallmeier, F., Granek, E., & Raven, P. (2001). Biodiversity: Connecting with the Tapestry of Life. *Smithsonian Institution/Monitoring and Assessment of Biodiversity Program and President's Committee of Advisors on Science and Technology. Washington, D.C., U.S.A.*

Basuki, T. M., Skidmore, A. K., Hussin, Y. A., & Van Duren, I. (2013). Estimating tropical forest biomass more accurately by integrating ALOS PALSAR and Landsat-7 ETM+ data. *International Journal of Remote Sensing*, *34*(13), 4871–4888. https://doi.org/10.1080/01431161.2013.777486

Beckschäfer, P., Fehrmann, L., Harrison, R. D., Xu, J., & Kleinn, C. (2014). Mapping Leaf Area Index in subtropical upland ecosystems using RapidEye imagery and the randomForest algorithm. *IForest - Biogeosciences and Forestry*, *7*(1), 1. https://doi.org/10.3832/ifor0968-006

Beukema, H., & van Noordwijk, M. (2004). Terrestrial pteridophytes as indicators of a forest-like environment in rubber production systems in the lowlands of Jambi, Sumatra. *Agriculture, Ecosystems & Environment*, *104*(1), 63–73. https://doi.org/10.1016/j.agee.2004.01.007

BIG. (2016). Teknis Implementasi Renaksi Kebijakan Satu Peta (Action Plan Implementation of One Map Policy). Presented at the Rakornas IG, Jakarta, 27 April 2016. Retrieved from http://www.bakosurtanal.go.id/assets/download/Rakornas-2016/Paparan-deputi-igt-big.pdf

Blackbridge. (2013). Satellite Imagery Product Specifications. Blackbridge. Retrieved from http://www.blackbridge.com/rapideye/upload/RE_Product_Specifications_ENG.pdf

Blaschke, T., Hay, G. J., Kelly, M., Lang, S., Hofmann, P., Addink, E., … Tiede, D. (2014). Geographic Object-Based Image Analysis – Towards a new paradigm. *ISPRS Journal of Photogrammetry and Remote Sensing*, *87*, 180–191. https://doi.org/10.1016/j.isprsjprs.2013.09.014

Bo, S., Ding, L., Li, H., Di, F., & Zhu, C. (2009). Mean shift-based clustering analysis of multispectral remote sensing imagery. *International Journal of Remote Sensing*, *30*(4), 817–827. https://doi.org/10.1080/01431160802395193

Bo, S., & Jing, Y. (2012). Image Clustering Using Mean Shift Algorithm. In *2012 Fourth International Conference on Computational Intelligence and Communication Networks (CICN)* (pp. 327–330). https://doi.org/10.1109/CICN.2012.128

Bojanowski, J. (2007). The analysis of sensibility to the change of the input parameters in the 6S model.

Box, G. E., & Cox, D. R. (1964). An analysis of transformations. *Journal of the Royal Statistical Society: Series B*, 211–252.

BP-REDD+. (2015). *National Forest Reference Emission Level for Deforestation and Forest Degradation in the Context of the Activities Referred to in Decision 1/CP. 16, Paragraph 70 (REDD+) Under the UNFCCC: A Reference for Decision Makers*. Jakarta, Indonesia.

BPS (Badan Pusat Statistik). (2015). *Statistical Yearbook of Indonesia in 2015*. Jakarta: BPS - Statistics Indonesia.

BPS (Badan Pust Statistik). (2014). Jambi in Figures 2014. BPS - Statistics of Jambi Province.

BPS (Badan Pust Statistik). (2013). Jambi in Figures 2013. BPS - Statistics of Jambi Province.

BPS (Badan Pust Statistik). (2011). Jambi in Figures 2011. BPS - Statistics of Jambi Province.

BPS (Badan Pust Statistik). (2002). Jambi in Figures 2001. BPS - Statistics of Jambi Province.

BPS (Badan Pust Statistik). (2001). Jambi in Figures 2000. BPS - Statistics of Jambi Province.

Breiman, L. (1996). Technical Note: Some Properties of Splitting Criteria. *Machine Learning*, *24*(1), 41–47. https://doi.org/10.1023/A:1018094028462

Breiman, L. (2001). Random forests. *Machine Learning*, *45*(1), 5–32.

Breiman, L., & Cutler, A. (2004). Random Forests. Retrieved July 15, 2015, from http://www.stat.berkeley.edu/~breiman/RandomForests/

Breiman, L., Friedman, J., Stone, C. J., & Olshen, R. A. (1984). *Classification and regression trees*. CRC press.

Briggs, M., de Kok, R., Moat, J., Whaley, O., & Williams, J. (2012). Vegetation Mapping for Reforestation and Carbon Capture in the Harapan Rainforest. *Unpublished Report to DEFRA Grant: DX11-04.* Retrieved from http://www.researchgate.net/publication/265913379_Vegetation_Mapping_for_Reforestation_and_Carbon_Capture_in_the_Harapan_Rainforest

Broich, M., Hansen, M. C., Potapov, P., Adusei, B., Lindquist, E., & Stehman, S. V. (2011a). Time-series analysis of multi-resolution optical imagery for quantifying forest cover loss in Sumatra and Kalimantan, Indonesia. *International Journal of Applied Earth Observation and Geoinformation*, *13*(2), 277–291. https://doi.org/10.1016/j.jag.2010.11.004

Broich, M., Hansen, M., Stolle, F., Potapov, P., Margono, B. A., & Adusei, B. (2011b). Remotely sensed forest cover loss shows high spatial and temporal variation across Sumatera and Kalimantan, Indonesia 2000–2008. *Environmental Research Letters*, *6*(1), 014010. https://doi.org/10.1088/1748-9326/6/1/014010

Brown, S. (1997). *Estimating biomass and biomass change of tropical forests: a primer* (Vol. 134). Food & Agriculture Org.

Büschenfeld, T., & Ostermann, J. (2012). Edge Preserving Land Cover Classification Refinement Using Mean Shift Segmentation. *Proceedings Of The 4th GEOBIA*.

Buschmann, C., & Nagel, E. (1993). In vivo spectroscopy and internal optics of leaves as basis for remote sensing of vegetation. *International Journal of Remote Sensing*, *14*(4), 711–722. https://doi.org/10.1080/01431169308904370

Butt, S., Garcia, B., Parsons, J., & Stephens, T. (2013). Brazil and Indonesia: REaDD+y or not?, 251–274.

Caldas, M. M., Goodin, D., Sherwood, S., Krauer, J. M. C., & Wisely, S. M. (2015). Land-cover change in the Paraguayan Chaco: 2000–2011. *Journal of Land Use Science*, *10*(1), 1–18. https://doi.org/10.1080/1747423X.2013.807314

Carleer, A., Debeir, O., & Wolff, E. (2005). Assessment of very high spatial resolution satellite image segmentations. *Photogrammetric Engineering & Remote Sensing*, *71*(11), 1285–1294.

Casson, A. (2000). The Hesitant boom: Indonesia's oil palm sub-sector in an era of economic crisis and political change. Retrieved from http:/www.cifor.org/online-library/browse/view-publication/publication/625.html

Castillo-Santiago, M. A., Ricker, M., & Jong, B. H. J. de. (2010). Estimation of tropical forest structure from SPOT-5 satellite images. *International Journal of Remote Sensing*, *31*(10), 2767–2782. https://doi.org/10.1080/01431160903095460

CBD. (2010). COP 10 Decision X/2. Strategic Plan for Biodiversity 2011-2020. Retrieved May 9, 2016, from https://www.cbd.int/decision/cop/?id=12268

CBD. (2013). *Quick guides to the Aichi Biodiversity Targets*. Retrieved from https://www.cbd.int/doc/strategic-plan/targets/compilation-quick-guide-en.pdf

Chan, J., Spanhove, T., Ma, J., Vanden Borre, J., Paelinckx, D., & Canters, F. (2010). Natura 2000 habitat identification and conservation status assessment with superresolution enhanced hyperspectral (CHRIS/Proba) imagery. *Proceedings of GEOBIA*.

Chapman, D. S., Bonn, A., Kunin, W. E., & Cornell, S. J. (2010). Random Forest characterization of upland vegetation and management burning from aerial imagery. *Journal of Biogeography*, *37*(1), 37–46. https://doi.org/10.1111/j.1365-2699.2009.02186.x

Chave, J., Andalo, C., Brown, S., Cairns, M. A., Chambers, J. Q., Eamus, D., … Yamakura, T. (2005). Tree allometry and improved estimation of carbon stocks and balance in tropical forests. *Oecologia*, *145*(1), 87–99. https://doi.org/10.1007/s00442-005-0100-x

Comaniciu, D., & Meer, P. (2002). Mean shift: a robust approach toward feature space analysis. *IEEE Transactions on Pattern Analysis and Machine Intelligence*, *24*(5), 603–619. https://doi.org/10.1109/34.1000236

Corlett, R. T., & Primack, R. B. (2011). *Tropical rain forests: an ecological and biogeographical comparison*. John Wiley & Sons.

Curatola Fernández, G. F., Obermeier, W. A., Gerique, A., López Sandoval, M. F., Lehnert, L. W., Thies, B., & Bendix, J. (2015). Land Cover Change in the Andes of Southern Ecuador—Patterns and Drivers. *Remote Sensing*, *7*(3), 2509–2542. https://doi.org/10.3390/rs70302509

Curtis, R. O., & Marshall, D. D. (2000). Technical Note: Why Quadratic Mean Diameter? *Western Journal of Applied Forestry*, *15*(3), 137–139.

De Sousa, C., Souza, C., Zanella, L., & de Carvalho, L. (2012). Analysis of Rapideye's Red Edge Band for Image Segmentation and Classification. *Proceedings of the 4th GEOBIA, Rio de Janeiro, Brazil*, *79*, 518.

DeFries, R. S., Rudel, T., Uriarte, M., & Hansen, M. (2010). Deforestation driven by urban population growth and agricultural trade in the twenty-first century. *Nature Geoscience*, *3*(3), 178–181. https://doi.org/10.1038/ngeo756

Disbun (Dinas Perkebunan). (2002). *Statistik Perkebunan Provinsi Jambi tahun 2001 (Statistical Book of Estate Crops in Jambi Province in 2001)*. Jambi.

Disbun (Dinas Perkebunan). (2012). *Statistik Perkebunan Provinsi Jambi tahun 2012 (Statistical Book of Estate Crops in Jambi Province in 2012)*. Jambi.

Dong, J., Xiao, X., Chen, B., Torbick, N., Jin, C., Zhang, G., & Biradar, C. (2013). Mapping deciduous rubber plantations through integration of PALSAR and multi-temporal Landsat imagery. *Remote Sensing of Environment*, *134*, 392–402. https://doi.org/10.1016/j.rse.2013.03.014

Drescher, J., Rembold, K., Allen, K., Beckschäfer, P., Buchori, D., Clough, Y., … Scheu, S. (2016). Ecological and socio-economic functions across tropical land use systems after rainforest conversion. *Phil. Trans. R. Soc. B*, *371*(1694), 20150275. https://doi.org/10.1098/rstb.2015.0275

Du, X., Jin, X., Yang, X., Yang, X., & Zhou, Y. (2014). Spatial Pattern of Land Use Change and Its Driving Force in Jiangsu Province. *International Journal of Environmental Research and Public Health*, *11*(3), 3215–3232. https://doi.org/10.3390/ijerph110303215

Duro, D. C., Franklin, S. E., & Dubé, M. G. (2012). A comparison of pixel-based and object-based image analysis with selected machine learning algorithms for the classification of agricultural landscapes using SPOT-5 HRG imagery. *Remote Sensing of Environment*, *118*, 259–272. https://doi.org/10.1016/j.rse.2011.11.020

Eckert, S. (2012). Improved Forest Biomass and Carbon Estimations Using Texture Measures from WorldView-2 Satellite Data. *Remote Sensing*, *4*(12), 810–829. https://doi.org/10.3390/rs4040810

Edwards, D. P., Larsen, T. H., Docherty, T. D. S., Ansell, F. A., Hsu, W. W., Derhé, M. A., … Wilcove, D. S. (2011). Degraded lands worth protecting: the biological importance of Southeast Asia's repeatedly logged forests. *Proceedings of the Royal Society of London B: Biological Sciences*, *278*(1702), 82–90. https://doi.org/10.1098/rspb.2010.1062

EIA (Environmental Investigation Agency). (2014). PERMITTING CRIME: How palm oil expansion drives illegal logging in Indonesia. Retrieved from https://eia-international.org/wp-content/uploads/Permitting-Crime.pdf

Ekadinata, A., & Vincent, G. (2011). Rubber Agroforests in a Changing Landscape: Analysis of Land Use/Cover Trajectories in Bungo District, Indonesia. *Forests, Trees and Livelihoods*, *20*(1), 3–14. https://doi.org/10.1080/14728028.2011.9756694

Englhart, S., Keuck, V., & Siegert, F. (2011). Aboveground biomass retrieval in tropical forests — The potential of combined X- and L-band SAR data use. *Remote Sensing of Environment*, *115*(5), 1260–1271. https://doi.org/10.1016/j.rse.2011.01.008

Englhart, S., Keuck, V., & Siegert, F. (2012). Modeling Aboveground Biomass in Tropical Forests Using Multi-Frequency SAR Data #x2014;A Comparison of Methods. *IEEE Journal of Selected Topics in Applied Earth Observations and Remote Sensing*, *5*(1), 298–306. https://doi.org/10.1109/JSTARS.2011.2176720

Englhart, S., Keuck, V., & Siegert, F. (2012). Modeling aboveground biomass in tropical forests using multi-frequency SAR data—A comparison of methods. *IEEE Journal of Selected Topics in Applied Earth Observations and Remote Sensing*, *1*(5), 298–306.

Enrici, A., & Hubacek, K. (2016). Business as usual in Indonesia: governance factors effecting the acceleration of the deforestation rate after the introduction of REDD+. *Energy, Ecology and Environment*, *1*(4), 183–196. https://doi.org/10.1007/s40974-016-0037-4

ESRI, R. (2011). ArcGIS desktop: release 10. *Environmental Systems Research Institute, CA*. Retrieved from http://pro.arcgis.com/en/pro-app/help/mapping/symbols-and-styles/data-classification-methods.htm#ESRI_SECTION1_B47C458CFF6A4EEC933A8C7612DA558B

Euler, M., Krishna, V., Schwarze, S., Siregar, H., & Qaim, M. (2015). *Oil palm adoption, household welfare and nutrition among smallholder farmers in Indonesia*. EFForTS Discussion Paper Series.

Euler, M., Schwarze, S., Siregar, H., & Qaim, M. (2015). *Oil palm expansion among smallholder farmers in Sumatra, Indonesia*. EFForTS Discussion Paper Series.

Fahrig, L. (2003). Effects of Habitat Fragmentation on Biodiversity. *Annual Review of Ecology, Evolution, and Systematics*, *34*(1), 487–515. https://doi.org/10.1146/annurev.ecolsys.34.011802.132419

Fahrmeir, L., Kneib, T., Lang, S., & Marx, B. (2013). *Regression*. Berlin, Heidelberg: Springer Berlin Heidelberg. Retrieved from http://link.springer.com/10.1007/978-3-642-34333-9

Fairhurst, T., & McLaughlin, D. (2009). Sustainable oil palm development on degraded land in Kalimantan. *Washington, DC: World Wildlife Fund*. Retrieved from http://tropcropconsult.com/downloads_files/Fairhurst2009.pdf

FAO. (2015). *Global Forest Resources Assessment 2015: How have the world's forests changing?* Rome, Italy. Retrieved from http://www.fao.org/3/a-i4793e.pdf

FAOSTAT. (2016). FAO Statistics Division. Retrieved April 22, 2016, from http://faostat.fao.org/

Fearnside, P. M. (1997). Transmigration in Indonesia: Lessons from Its Environmental and Social Impacts. *Environmental Management*, *21*(4), 553–570. https://doi.org/10.1007/s002679900049

Feintrenie, L., Chong, W. K., & Levang, P. (2010). Why do farmers prefer oil palm? Lessons learnt from Bungo district, Indonesia. *Small-Scale Forestry*, *9*(3), 379–396.

Feintrenie, L., & Levang, P. (2009). Sumatra's rubber agroforests: advent, rise and fall of a sustainable cropping system. *Small-Scale Forestry*, (3 SP 323-335). Retrieved from http:/www.cifor.org/online-library/browse/view-publication/publication/2847.html

Foley, J. A., DeFries, R., Asner, G. P., Barford, C., Bonan, G., Carpenter, S. R., … Gibbs, H. K. (2005). Global consequences of land use. *Science*, *309*(5734), 570–574.

Foody, G. M. (2002a). Status of land cover classification accuracy assessment. *Remote Sensing of Environment*, *80*(1), 185–201. https://doi.org/10.1016/S0034-4257(01)00295-4

Foody, G. M. (2002b). Status of land cover classification accuracy assessment. *Remote Sensing of Environment*, *80*(1), 185–201. https://doi.org/10.1016/S0034-4257(01)00295-4

Franklin, S. E. (2001). *Remote sensing for sustainable forest management*. CRC Press.

Fuchs, H., Magdon, P., Kleinn, C., & Flessa, H. (2009). Estimating aboveground carbon in a catchment of the Siberian forest tundra: Combining satellite imagery and field inventory. *Remote Sensing of Environment*, *113*(3), 518–531. https://doi.org/10.1016/j.rse.2008.07.017

Gamon, J. A., Field, C. B., Goulden, M. L., Griffin, K. L., Hartley, A. E., Joel, G., … Valentini, R. (1995). Relationships Between NDVI, Canopy Structure, and Photosynthesis in Three Californian Vegetation Types. *Ecological Applications*, *5*(1), 28–41. https://doi.org/10.2307/1942049

Gatto, M., Wollni, M., & Qaim, M. (2015). Oil palm boom and land-use dynamics in Indonesia: The role of policies and socioeconomic factors. *Land Use Policy*, *46*, 292–303. https://doi.org/10.1016/j.landusepol.2015.03.001

Geist, H. J., & Lambin, E. F. (2002). Proximate Causes and Underlying Driving Forces of Tropical Deforestation. *BioScience*, *52*(2), 143–150. https://doi.org/10.1641/0006-3568(2002)052[0143:PCAUDF]2.0.CO;2

Ghazoul, J., & Sheil, D. (2010). *Tropical Rain Forest Ecology, Diversity, and Conservation*. Oxford University Press Oxford.

Gibbs, H. K., Ruesch, A. S., Achard, F., Clayton, M. K., Holmgren, P., Ramankutty, N., & Foley, J. A. (2010). Tropical forests were the primary sources of new agricultural land in the 1980s and 1990s. *Proceedings of the National Academy of Sciences*, *107*(38), 16732–16737. https://doi.org/10.1073/pnas.0910275107

Gitelson, A. A., & Merzlyak, M. N. (1997). Remote estimation of chlorophyll content in higher plant leaves. *International Journal of Remote Sensing*, *18*(12), 2691–2697. https://doi.org/10.1080/014311697217558

Gitelson, A. A., Viña, A., Ciganda, V., Rundquist, D. C., & Arkebauer, T. J. (2005). Remote estimation of canopy chlorophyll content in crops. *Geophysical Research Letters*, *32*(8), L08403. https://doi.org/10.1029/2005GL022688

GOFC-GOLD. (2013). *A sourcebook of methods and procedures for monitoring and reporting anthropogenic greenhouse gas emissions and removals associated with deforestation, gains and losses of carbon stocks in forests remaining forests, and forestation*. GOFC-GOLD Report version COP19-2, (GOFC-GOLD Land Cover Project Office, Wageningen University, The Netherlands).

GoI. (1986). Presidential Instruction 1 of 1986. Estate crop development through Nucleaus Estates and Smallholders scheme related to transmigration (Pengembangan perkebunan dengan pola perusahaan inti rakyat yang dikaitkan dengan program transmigrasi). Retrieved from http://ditjenbun.pertanian.go.id/tinymcpuk/gambar/file/inpres01-1986_Pengembangan_perkebunan.pdf

GoI. (2008). Peraturan Pemerintah No. 3 Tahun 2008 tentang Perubahan atas Peraturan Pemerintah Nomor 6 Tahun 2007 tentang Tata Hutan dan Penyusunan Rencana Pengelolaan Hutan, serta Pemanfaatan Hutan (Forest Management Plan and The Use of Forest).

GoI. (2017). *Menuju Sinkronisasi IGT Antar Sektor dan Partisipasi Mitra Pembangunan-Satu Tahun Implementasi Kebijakan Satu Peta (Synchronization of Thematic Geospatial Information and the Participation of Stakeholders-One Year Implementation of One Map Policy)*. Presented at the National Seminar on One Year Implementation of One Map Policy by the Secretariat Team for the Acceleration of One Map Policy (Unpublished Presentation).

Gouyon, A., Foresta, H. de, & Levang, P. (1993). Does 'jungle rubber' deserve its name? An analysis of rubber agroforestry systems in southeast Sumatra. *Agroforestry Systems*, *22*(3), 181–206. https://doi.org/10.1007/BF00705233

Greenpeace. (2016). Palm oil: who's still trashing forests? Retrieved March 29, 2016, from http://www.greenpeace.org/international/en/news/Blogs/makingwaves/palm-oil-whos-still-trashing-forests/blog/55724/

Griffith, J. A., Martinko, E. A., & Price, K. P. (2000). Landscape structure analysis of Kansas at three scales. *Landscape and Urban Planning*, *52*(1), 45–61. https://doi.org/10.1016/S0169-2046(00)00112-2

Guillaume, T., Damris, M., & Kuzyakov, Y. (2015). Losses of soil carbon by converting tropical forest to plantations: erosion and decomposition estimated by δ(13) C. *Global Change Biology*. https://doi.org/10.1111/gcb.12907

Hair, J. F., Black, W. C., Babin, B. J., & Anderson, R. E. (2010). *Multivariate data analysis: A Global Perspective* (Vol. 7). Pearson Prentice Hall, Upper Saddle River, NJ.

Hall-Beyer, M. (2007). GLCM Texture Tutorial. Retrieved June 23, 2016, from http://www.fp.ucalgary.ca/mhallbey/tutorial.htm

Hannah, L., & Lovejoy, T. (2011). Conservation, climate change, and tropical forests. In M. Bush, J. Flenley, & W. Gosling (Eds.), *Tropical Rainforest Responses to Climatic Change* (pp. 431–443). Springer Berlin Heidelberg. Retrieved from http://link.springer.com/chapter/10.1007/978-3-642-05383-2_16

Hansen, M. C., Potapov, P. V., Moore, R., Hancher, M., Turubanova, S. A., Tyukavina, A., … Townshend, J. R. G. (2013). High-Resolution Global Maps of 21st-Century Forest Cover Change. *Science*, *342*(6160), 850–853. https://doi.org/10.1126/science.1244693

Hansen, M. C., Stehman, S. V., Potapov, P. V., Arunarwati, B., Stolle, F., & Pittman, K. (2009). Quantifying changes in the rates of forest clearing in Indonesia from 1990 to 2005 using remotely sensed data sets. *Environmental Research Letters*, *4*(3), 034001. https://doi.org/10.1088/1748-9326/4/3/034001

Haralick, R. M., Shanmugam, K., & Dinstein, I. H. (1973). Textural features for image classification. *Systems, Man and Cybernetics, IEEE Transactions On*, (6), 610–621.

Hargrave, J., & Kis-Katos, K. (2013). Economic Causes of Deforestation in the Brazilian Amazon: A Panel Data Analysis for the 2000s. *Environmental and Resource Economics*, *54*(4), 471–494. https://doi.org/10.1007/s10640-012-9610-2

Harrison, R. D. (2015). Introduction: Restoring lowland rain forests in Indonesia. *Tropical Conservation Science*, *8*(1), 1–3.

Harrison, R. D., & Swinfield, T. (2015). Restoration of logged humid tropical forests: An experimental programme at Harapan Rainforest, Indonesia. *Tropical Conservation Science*, *8*(1), 4–16.

He, H. S., DeZonia, B. E., & Mladenoff, D. J. (2000). An aggregation index (AI) to quantify spatial patterns of landscapes. *Landscape Ecology*, *15*(7), 591–601. https://doi.org/10.1023/A:1008102521322

Hoover, A., Jean-Baptiste, G., Jiang, X., Flynn, P. J., Bunke, H., Goldgof, D. B., … Fisher, R. B. (1996). An experimental comparison of range image segmentation algorithms. *Pattern Analysis and Machine Intelligence, IEEE Transactions On*, *18*(7), 673–689.

Hoppe, M., & Faust, H. (2004). Transmigration and Integration in Indonesia. *University of Göttingen, Germany*. Retrieved from http://www.uni-gottingen.de/de/document/download/6c9f16f2c51b29135a0a87b1b24b86ca-en.pdf/SDP13.pdf

Horning, N. (2010). Random Forests: An algorithm for image classification and generation of continuous fields data sets. Presented at the Proceeding of International Conference on Geoinformatics for Spatial Infrastructure Development in Earth and Allied Sciences.

Horning, N., Robinson, J. A., Sterling, E. J., Turner, W., & Spector, S. (2010). *Remote Sensing for Ecology and Conservation: A Handbook of Techniques*. OUP Oxford.

Hosonuma, N., Herold, M., Sy, V. D., Fries, R. S. D., Brockhaus, M., Verchot, L., … Romijn, E. (2012). An assessment of deforestation and forest degradation drivers in developing countries. *Environmental Research Letters*, *7*(4), 044009. https://doi.org/10.1088/1748-9326/7/4/044009

Huang, X., & Zhang, L. (2008). An Adaptive Mean-Shift Analysis Approach for Object Extraction and Classification From Urban Hyperspectral Imagery. *IEEE Transactions on Geoscience and Remote Sensing*, *46*(12), 4173–4185. https://doi.org/10.1109/TGRS.2008.2002577

Hutan Harapan. (2016). Sejarah Hutan Harapan (History of Harapan Forest). Retrieved February 20, 2017, from http://harapanrainforest.org/read/sejarah#.WKrN5vJTLWx

Immitzer, M., Atzberger, C., & Koukal, T. (2012). Tree Species Classification with Random Forest Using Very High Spatial Resolution 8-Band WorldView-2 Satellite Data. *Remote Sensing*, *4*(12), 2661–2693. https://doi.org/10.3390/rs4092661

Jackson, R. D., & Huete, A. R. (1991). Interpreting vegetation indices. *Preventive Veterinary Medicine*, *11*(3–4), 185–200. https://doi.org/10.1016/S0167-5877(05)80004-2

James, G., Witten, D., Hastie, T., & Tibshirani, R. (2013). *An Introduction to Statistical Learning* (Vol. 103). New York, NY: Springer New York. Retrieved from http://link.springer.com/10.1007/978-1-4614-7138-7

Jung-Rothenhäusler, F., Weichelt, H., & Pach, M. (2007). RapidEye. A novel approach to space borne geo-information solutions. In *ISPRS Hanover Workshop*. Retrieved from https://t3sec3.rrzn.uni-hannover.de/cmsv021a.rrzn.uni-hannover.de/fileadmin/institut/pdf/Jung-roth_weichelt_pach.pdf

Kartodihardjo, H., & Supriono, A. (2000). *The impact of sectoral development on natural forest conversion and degradation: The case of timber and tree crop plantations in Indonesia*. CIFOR, Bogor, Indonesia. Retrieved from http://www.cifor.org/library/628/the-impact-of-sectoral-development-on-natural-forest-conversion-and-degradation-the-case-of-timber-and-tree-crop-plantations-in-indonesia/

Kayitakire, F., Hamel, C., & Defourny, P. (2006). Retrieving forest structure variables based on image texture analysis and IKONOS-2 imagery. *Remote Sensing of Environment*, *102*(3–4), 390–401. https://doi.org/10.1016/j.rse.2006.02.022

Ketterings, Q. M., Tri Wibowo, T., van Noordwijk, M., & Penot, E. (1999). Farmers' perspectives on slash-and-burn as a land clearing method for small-scale rubber producers in Sepunggur, Jambi Province, Sumatra, Indonesia. *Forest Ecology and Management*, *120*(1–3), 157–169. https://doi.org/10.1016/S0378-1127(98)00532-5

Koh, L. P., & Wilcove, D. S. (2008). Is oil palm agriculture really destroying tropical biodiversity? *Conservation Letters*, *1*(2), 60–64. https://doi.org/10.1111/j.1755-263X.2008.00011.x

Kotowska, M. M., Leuschner, C., Triadiati, T., Meriem, S., & Hertel, D. (2015). Quantifying above- and belowground biomass carbon loss with forest conversion in tropical lowlands of Sumatra (Indonesia). *Global Change Biology*, n/a-n/a. https://doi.org/10.1111/gcb.12979

KPA. (2012). *Laporan Akhir Tahun 2012 Konsorsium Pembaruan Agraria (Annual Report in 2012 of the Consortium of Agraria Reform)*. Jakarta, Indonesia.

Kummer, D. M., & Turner, B. L. (1994). The Human Causes of Deforestation in Southeast Asia. *BioScience*, *44*(5), 323–328. https://doi.org/10.2307/1312382

Kun, L., Ran, Y., & Qianqing, Q. (2010). Object-Oriented Port Detection Based on Mean Shift Segmentation. In *2010 International Conference on Electrical and Control Engineering (ICECE)* (pp. 1399–1402). https://doi.org/10.1109/iCECE.2010.346

Lambin, E. F., & Meyfroidt, P. (2011). Global land use change, economic globalization, and the looming land scarcity. *Proceedings of the National Academy of Sciences*, *108*(9), 3465–3472. https://doi.org/10.1073/pnas.1100480108

Lambin, E. F., Turner, B. L., Geist, H. J., Agbola, S. B., Angelsen, A., Bruce, J. W., … Xu, J. (2001). The causes of land-use and land-cover change: moving beyond the myths. *Global Environmental Change*, *11*(4), 261–269. https://doi.org/10.1016/S0959-3780(01)00007-3

Laumonier, Y. (1997). *The Vegetation and Physiography of Sumatra* (Vol. 22). Dordrecht: Kluwer Academic Publisher.

Laumonier, Y., Edin, A., Kanninen, M., & Munandar, A. W. (2010). Landscape-scale variation in the structure and biomass of the hill dipterocarp forest of Sumatra: Implications for carbon stock assessments. *Forest Ecology and Management*, *259*(3), 505–513. https://doi.org/10.1016/j.foreco.2009.11.007

Laumonier, Y., Uryu, Y., Stüwe, M., Budiman, A., Setiabudi, B., & Hadian, O. (2010). Eco-floristic sectors and deforestation threats in Sumatra: identifying new conservation area network priorities for ecosystem-based land use planning. *Biodiversity and Conservation*, *19*(4), 1153–1174. https://doi.org/10.1007/s10531-010-9784-2

Law 4 of 2011. (2011). Undang-Undang No. 4 Tahun 2011 tentang Informasi Geospasial (Geospatial Information).

Li, L., Dong, J., Njeudeng Tenku, S., & Xiao, X. (2015). Mapping Oil Palm Plantations in Cameroon Using PALSAR 50-m Orthorectified Mosaic Images. *Remote Sensing*, *7*(2), 1206–1224. https://doi.org/10.3390/rs70201206

Li, Z., & Fox, J. M. (2012). Mapping rubber tree growth in mainland Southeast Asia using time-series MODIS 250 m NDVI and statistical data. *Applied Geography*, *32*(2), 420–432. https://doi.org/10.1016/j.apgeog.2011.06.018

Liaw, A., & Wiener, M. (2002). Classification and regression by randomForest. *R News*, *2*(3), 18–22.

Liaw, A., Wiener, M., Breiman, L., & Cutler, A. (2014). Package "randomForest." Retrieved from http://cran.r-project.org/web/packages/randomForest/randomForest.pdf

Lillesand, T. M., Kiefer, R. W., & Chipman, J. W. (2008). *Remote sensing and image interpretation.* John Wiley & Sons Ltd.

Lu, D. (2005). Aboveground biomass estimation using Landsat TM data in the Brazilian Amazon. *International Journal of Remote Sensing*, *26*(12), 2509–2525. https://doi.org/10.1080/01431160500142145

Lu, D., & Batistella, M. (2005). Exploring TM image texture and its relationships with biomass estimation in Rondônia, Brazilian Amazon. *Acta Amazonica*, *35*(2), 249–257. https://doi.org/10.1590/S0044-59672005000200015

Lu, D., Mausel, P., Brondizio, E., & Moran, E. (2002). Assessment of atmospheric correction methods for Landsat TM data applicable to Amazon basin LBA research. *International Journal of Remote Sensing*, *23*(13), 2651–2671. https://doi.org/10.1080/01431160110109642

Lu, D., Mausel, P., Brondı□zio, E., & Moran, E. (2004). Relationships between forest stand parameters and Landsat TM spectral responses in the Brazilian Amazon Basin. *Forest Ecology and Management*, *198*(1–3), 149–167. https://doi.org/10.1016/j.foreco.2004.03.048

Lumley, T., & Miller, A. (2009). Leaps: regression subset selection. R package version 2.9. *See Http://CRAN. R-Project. Org/Package= Leaps*.

Magdon, P., Fischer, C., Fuchs, H., & Kleinn, C. (2014). Translating criteria of international forest definitions into remote sensing image analysis. *Remote Sensing of Environment*, *149*, 252–262. https://doi.org/10.1016/j.rse.2014.03.033

Magdon, P., Fuchs, H., Fischer, C., & Kleinn, C. (2011). Forest cover monitoring using RapidEye: a case study in costa rica. In *RapidEye Science Archive (RESA)-Erste Ergebnisse* (pp. 47–56). GITO mbH Verlag.

Malhi, Y., & Grace, J. (2000). Tropical forests and atmospheric carbon dioxide. *Trends in Ecology & Evolution*, *15*(8), 332–337. https://doi.org/10.1016/S0169-5347(00)01906-6

Malhi, Y., & Marthews, T. R. (2013). Tropical forests: carbon, climate and biodiversity. In R. Lyster, C. MacKenzie, & C. McDermott (Eds.), *Law, Tropical Forests and Carbon: The Case of REDD+* (pp. 26–43). Cambridge University Press.

Marcus, B. A. (2009). *Tropical Forests*. Jones and Bartlett Publishers.

Margono, B. A., Potapov, P. V., Turubanova, S., Stolle, F., & Hansen, M. C. (2014). Primary forest cover loss in Indonesia over 2000-2012. *Nature Climate Change*, *4*(8), 730–735. https://doi.org/10.1038/nclimate2277

Margono, B. A., Turubanova, S., Zhuravleva, I., Potapov, P., Tyukavina, A., Baccini, A., … Hansen, M. C. (2012). Mapping and monitoring deforestation and forest degradation in Sumatra (Indonesia) using Landsat time series data sets from 1990 to 2010. *Environmental Research Letters*, *7*(3), 034010. https://doi.org/10.1088/1748-9326/7/3/034010

Marlier, M. E., DeFries, R., Pennington, D., Nelson, E., Ordway, E. M., Lewis, J., … Mickley, L. J. (2015). Future fire emissions associated with projected land use change in Sumatra. *Global Change Biology*, *21*(1), 345–362. https://doi.org/10.1111/gcb.12691

Marpu, P. R., Neubert, M., Herold, H., & Niemeyer, I. (2010). Enhanced evaluation of image segmentation results. *Journal of Spatial Science*, *55*(1), 55–68. https://doi.org/10.1080/14498596.2010.487850

Marx, A. (2010). Detection and Classification of Bark Beetle Infestation in Pure Norway Spruce Stands with Multi-temporal RapidEye Imagery and Data Mining Techniques. *Photogrammetrie - Fernerkundung - Geoinformation*, *2010*(4), 243–252. https://doi.org/10.1127/1432-8364/2010/0052

Mather, P., & Koch, M. (2011). *Computer processing of remotely-sensed images: an introduction*. John Wiley & Sons. Retrieved from https://books.google.de/books?hl=en&lr=&id=GWhvDMNh1hAC&oi=fnd&pg=PT8&dq=computer+processing+of+remotely-sensed+images+an+introduction&ots=rka80DnPIk&sig=Jl0vHBh0wDAaYh44iJjtqlZ0oZA

McGarigal, K. (2015). Fragstats Help. University of Massachusetts. Retrieved from http://www.umass.edu/landeco/research/fragstats/documents/fragstats.help.4.2.pdf

McGarigal, K., & Marks, B. J. ; (1995). *FRAGSTATS: spatial pattern analysis program for quantifying landscape structure.* U.S. Department of Agriculture, Forest Service, Pacific Northwest Research Station.

McMorrow, J., & Talip, M. A. (2001). Decline of forest area in Sabah, Malaysia: Relationship to state policies, land code and land capability. *Global Environmental Change*, *11*(3), 217–230. https://doi.org/10.1016/S0959-3780(00)00059-5

MoA (Ministry of Agriculture). (2015). Indonesian Sustainable Palm Oil Certification System/ISPO. Retrieved from http://ditjenbun.pertanian.go.id/tinymcpuk/gambar/file/Permentan_ISPO_No11_thn_2015.pdf

MoEF 42 of 2015. (n.d.). Peraturan Menteri Lingkungan Hidup dan Kehutanan No 42 tentang Penatausahaan Hasil Hutan Kayu yang Berasal dari Hutan Tanaman pada Hutan Produksi (Management of Timber Production from Plantation Forest in the Production Forest).

MoF. (2008). *Pemantauan Sumber Daya Hutan (Monitoring of Forest Resource)*. Jakarta, Indonesia: Ministry of Forestry.

MoF. (2014). Forestry Statistcs of Indonesia. Ministry of Forestry Indonesia.

MoF Decree 33 of 2009. (n.d.). Guideline on the Periodical Forest Inventory of the Production Forest (Peraturan Menteri Kehutanan Republik Indonesia Nomor: P. 33/Menhut-II/2009 tentang Pedoman Inventarisasi Hutan Menyeluruh Berkala (IHMB) pada Usaha Pemanfaatan Hasil Hutan Kayu pada Hutan Produksi).

Mohan, S. S., & Leela, S. (2013). Importance of Mean Shift in Remote Sensing Segmentation. *IOSR Journal of Computer Engineering (IOSR - JCE)*, *14*(6), 80–83.

Murdiyarso, D., Dewi, S., Lawrence, D., & Seymour, F. (2011). *Indonesia's forest moratorium: A stepping stone to better forest governance?* Bogor, Indonesia: Center for International Forestry Research (CIFOR). Retrieved from http:/www.cifor.org/online-library/browse/view-publication/publication/3561.html

Myint, S. W., Gober, P., Brazel, A., Grossman-Clarke, S., & Weng, Q. (2011). Per-pixel vs. object-based classification of urban land cover extraction using high spatial resolution imagery. *Remote Sensing of Environment*, *115*(5), 1145–1161. https://doi.org/10.1016/j.rse.2010.12.017

Neubert, M., Herold, H., & Meinel, G. (2008). Assessing image segmentation quality – concepts, methods and application. In T. Blaschke, S. Lang, & G. J. Hay (Eds.), *Object-Based Image Analysis* (pp. 769–784). Springer Berlin Heidelberg. Retrieved from http://link.springer.com/chapter/10.1007/978-3-540-77058-9_42

Nichol, J. E., & Sarker, M. L. R. (2011). Improved Biomass Estimation Using the Texture Parameters of Two High-Resolution Optical Sensors. *IEEE Transactions on Geoscience and Remote Sensing*, *49*(3), 930–948. https://doi.org/10.1109/TGRS.2010.2068574

Oppenheimer, M., & Petsonk, A. (2005). Article 2 of the UNFCCC: Historical Origins, Recent Interpretations. *Climatic Change*, *73*(3), 195–226. https://doi.org/10.1007/s10584-005-0434-8

OTB Development Team. (2015). The Orfeo ToolBox Cookbook, a guide for non-developers Updated for OTB-5.0. Retrieved from http://www.orfeo-toolbox.org

Ozdemir, I., & Karnieli, A. (2011). Predicting forest structural parameters using the image texture derived from WorldView-2 multispectral imagery in a dryland forest, Israel. *International Journal of Applied Earth Observation and Geoinformation*, *13*(5), 701–710. https://doi.org/10.1016/j.jag.2011.05.006

Ozertem, U., Erdogmus, D., & Lan, T. (2006). Mean Shift Spectral Clustering for Perceptual Image Segmentation. In *2006 IEEE International Conference on Acoustics, Speech and Signal Processing, 2006. ICASSP 2006 Proceedings* (Vol. 2, pp. II–II). https://doi.org/10.1109/ICASSP.2006.1660293

PEACE. (2007). *Indonesia and Climate Change: Current Status and Policies*. Retrieved from http://siteresources.worldbank.org/INTINDONESIA/Resources/Environment/ClimateChange_Full_EN.pdf

Pearson, T., Walker, S., & Brown, S. (2005). Sourcebook for land use, land-use change and forestry projects.

Peh, K. S.-H., Sodhi, N. S., De Jong, J., Sekercioglu, C. H., Yap, C. A.-M., & Lim, S. L.-H. (2006). Conservation value of degraded habitats for forest birds in southern Peninsular Malaysia. *Diversity and Distributions*, *12*(5), 572–581. https://doi.org/10.1111/j.1366-9516.2006.00257.x

Peskett, L. (2013). REDD+ and development. In R. Lyster, C. MacKenzie, & C. McDermott (Eds.), *Law, Tropical Forests and Carbon: The Case of REDD+* (pp. 26–43). Cambridge University Press.

Pimm, S. L., & Raven, P. (2000). Biodiversity: Extinction by numbers. *Nature*, *403*(6772), 843–845. https://doi.org/10.1038/35002708

Potter, L., & Lee, J. (1998). CIFOR Bogor (Indonesia).

Presidential Instruction 10 of 2011. (2011). Instruksi Presiden No. 10 Tahun 2011 tentang Penundaan Pemberian Izin Baru dan Penyempurnaan Tata Kelola Hutan Alam Primer dan Lahan Gambut (Postponement of Issuance of New Licenses and Improving Governance of Primary Natural Forests and Peatland).

Presidential Regulation 9 of 2016. (2016). Peraturan Presiden Republik Indonesia No. 9 tahun 2016 tentang Percepatan Pelaksanaan Kebijakan Satu Peta pada Tingkat Ketelitian Peta Skala 1.50,000 (Acceleration of One Map Policy Implementation at the Scale of 1:50,000).

Pu, R., Landry, S., & Yu, Q. (2011). Object-based urban detailed land cover classification with high spatial resolution IKONOS imagery. *International Journal of Remote Sensing*, *32*(12), 3285–3308. https://doi.org/10.1080/01431161003745657

Puissant, A., Rougier, S., & Stumpf, A. (2014). Object-oriented mapping of urban trees using Random Forest classifiers. *International Journal of Applied Earth Observation and Geoinformation*, *26*, 235–245. https://doi.org/10.1016/j.jag.2013.07.002

R Core Team. (2015). R: A language and environment for statistical computing. Retrieved from https://www.r-project.org/

REDD-Monitor. (2012). Interview with Kuntoro Mangkusubroto, head of Indonesia's REDD+ Task Force: "We are starting a new programme, a new paradigm, a new concept, a new way of seeing things." Retrieved February 6, 2017, from http://www.redd-monitor.org/2012/09/20/interview-with-kuntoro-mangkusubroto/

Richardson, A. J., & Everitt, J. H. (1992). Using spectral vegetation indices to estimate rangeland productivity. *Geocarto International*, *7*(1), 63–69. https://doi.org/10.1080/10106049209354353

Rico, E. C., & Maseda, R. C. (2012). An Object-Oriented Approach to Automatic Classification of Panchromatic Aerial Photographs with GRASS GIS and R. In E. Bocher & M. Neteler (Eds.), *Geospatial Free and Open Source Software in the 21st Century* (pp. 123–137). Springer Berlin Heidelberg. Retrieved from http://link.springer.com/chapter/10.1007/978-3-642-10595-1_8

Rodriguez-Galiano, V. F., Chica-Olmo, M., Abarca-Hernandez, F., Atkinson, P. M., & Jeganathan, C. (2012). Random Forest classification of Mediterranean land cover using multi-seasonal imagery and multi-seasonal texture. *Remote Sensing of Environment*, *121*, 93–107. https://doi.org/10.1016/j.rse.2011.12.003

Rosa, I. M. D., Smith, M. J., Wearn, O. R., Purves, D., & Ewers, R. M. (2016). The Environmental Legacy of Modern Tropical Deforestation. *Current Biology*, *26*(16), 2161–2166. https://doi.org/10.1016/j.cub.2016.06.013

RSPO. (2013). Principles and criteria for the production of sustainable palm oil. RSPO, Kuala Lumpur. Retrieved from http://www.rspo.org/file/PnC_RSPO_Rev1.pdf

Rutishauser, E., Noor'an, F., Laumonier, Y., Halperin, J., Rufi'ie, Hergoualc'h, K., & Verchot, L. (2013). Generic allometric models including height best estimate

forest biomass and carbon stocks in Indonesia. *Forest Ecology and Management*, *307*, 219–225. https://doi.org/10.1016/j.foreco.2013.07.013

Ruysschaert, D., Darsoyo, A., Zen, R., Gea, G., & Singleton, I. (2011). Developing palm-oil production on degraded land : Technical, economic, biodiversity, climate, legal and policy implications.

Samadhi, N. (2013). Indonesia One Map: assuring better delivery of national development goals. In *Geospatial World Forum 2013, 12-13 May 2013, Rotterdam*. Retrieved from http://geospatialworldforum.org/2013/presentation/Nirata%20Samdhi.pdf

Sarker, L. R., & Nichol, J. E. (2011). Improved forest biomass estimates using ALOS AVNIR-2 texture indices. *Remote Sensing of Environment*, *115*(4), 968–977.

Schmidt, L., Prasetyonohadi, D., & Swinfield, T. (2015). Restoration of artificial ponds in logging concessions: a case-study from Harapan Rainforest, Sumatra. *Tropical Conservation Science*, *8*(1), 33–44.

Schuster, C., Förster, M., & Kleinschmit, B. (2012). Testing the red edge channel for improving land-use classifications based on high-resolution multi-spectral satellite data. *International Journal of Remote Sensing*, *33*(17), 5583–5599. https://doi.org/10.1080/01431161.2012.666812

Schwarze, S., Euler, M., Gatto, M., Hein, J., Hettig, E., Holtkamp, A. M., … Merten, J. (2015). *Rubber vs. oil palm: an analysis of factors influencing smallholders' crop choice in Jambi, Indonesia*. EFForTS Discussion Paper Series.

Senf, C., Pflugmacher, D., van der Linden, S., & Hostert, P. (2013). Mapping Rubber Plantations and Natural Forests in Xishuangbanna (Southwest China) Using Multi-Spectral Phenological Metrics from MODIS Time Series. *Remote Sensing*, *5*(6), 2795–2812. https://doi.org/10.3390/rs5062795

Smith, A. (2010). Image segmentation scale parameter optimization and land cover classification using the Random Forest algorithm. *Journal of Spatial Science*, *55*(1), 69–79. https://doi.org/10.1080/14498596.2010.487851

SNI (Standar Nasional Indonesia). (2010). *Klasifikasi penutup lahan (Land cover classification)* (No. SNI 7645:2010). Jakarta, Indonesia: Badan Standardisasi Nasional.

Southworth, J., Munroe, D., & Nagendra, H. (2004). Land cover change and landscape fragmentation—comparing the utility of continuous and discrete analyses for a western Honduras region. *Agriculture, Ecosystems & Environment*, *101*(2–3), 185–205. https://doi.org/10.1016/j.agee.2003.09.011

Stas, S. M. (2014). *Above-ground biomass and carbon stocks in a secondary forest in comparison with adjacent primary forest on limestone in Seram, the Moluccas, Indonesia* (Vol. 145). CIFOR. Retrieved from https://books.google.com/books?hl=en&lr=&id=ZMqUCgAAQBAJ&oi=fnd&pg=PP5&dq=%22Comparison+of+results+with+different+allometric%22+%22during+the+destructive%22+%22Data+on+the+structure+of+the+secondary+and+primary%22+%22Allometric+equations+developed+for+the+secondary+forest.+The+logarithmic+above-ground%22+&ots=pgEwMuC3rO&sig=Q7FFrq84O9eeqLa_0bxLdvUt7Vg

Stibig, H.-J., Achard, F., Carboni, S., Raši, R., & Miettinen, J. (2014). Change in tropical forest cover of Southeast Asia from 1990 to 2010. *Biogeosciences*, *11*(2), 247–258. https://doi.org/10.5194/bg-11-247-2014

Stolle, F., Chomitz, K. M., Lambin, E. F., & Tomich, T. P. (2003). Land use and vegetation fires in Jambi Province, Sumatra, Indonesia. *Forest Ecology and Management*, *179*(1–3), 277–292. https://doi.org/10.1016/S0378-1127(02)00547-9

SushmaLeela, T., Chandrakanth, R., Saibaba, J., Varadan, G., & Mohan. (2013). Mean-shift based object detection and clustering from high resolution remote sensing imagery. In *2013 Fourth National Conference on Computer Vision, Pattern Recognition, Image Processing and Graphics (NCVPRIPG)* (pp. 1–4). https://doi.org/10.1109/NCVPRIPG.2013.6776271

Susila, W. R. (1998). Perkembangan dan Prospek Komoditas Utama Perkebunan. *Pusat Studi Ekonomi*, (Lembaga Penelitian dan Pengembangan Pertanian Bogor).

The Jakarta Post. (2015). Forest moratorium fails to meet target - National. Retrieved October 12, 2017, from about:reader?url=http%3A%2F%2Fwww.thejakartapost.com%2Fnews%2F2015%2F06%2F13%2Fforest-moratorium-fails-meet-target.html

The World Bank. (1994). *Indonesia - Environment and development : challenges for the future* (No. 12083) (pp. 1–314). The World Bank. Retrieved from http://documents.worldbank.org/curated/en/1994/03/698503/indonesia-environment-development-challenges-future

Thompson, I., Mackey, B., McNulty, S., & Mosseler, A. (2009). *Forest Resilience, Biodiversity, and Climate Change. A synthesis of the biodiversity/resilience/stability relationship in forest ecosystems*. Secretariat of the Convention on Biological Diversity, Montreal. Retrieved from http://alltitles.ebrary.com/Doc?id=10886304

Tropek, R., Sedláček, O., Beck, J., Keil, P., Musilová, Z., Šímová, I., & Storch, D. (2014). Comment on "High-resolution global maps of 21st-century forest cover change." *Science*, *344*(6187), 981–981. https://doi.org/10.1126/science.1248753

Tso, B., & Mather, P. (2009). *Classification methods for remotely sensed data*. CRC press.

UN. (1998). Kyoto Protocol to the United Nations Framework Convention on Climate Change.

UN. (2015). *Transforming Our World: The 2030 Agenda for Sustainable Development*. Retrieved from https://sustainabledevelopment.un.org/content/documents/21252030%20Agenda%20for%20Sustainable%20Development%20web.pdf

UNEP. (2009). *Vital forest graphics*. UNEP/GRID-Arendal. Retrieved from https://books.google.com/books?hl=en&lr=&id=iXA5nwDNuLYC&oi=fnd&pg=PA4&dq=%22are+pleased+to+present+this+publication,+and+hope+that+you+will+%EF%AC%81nd+it+both+informative+and%22+%22de%EF%AC%81nition+and%22+%22change+and+its+impact+on+forests+-+will+forests+migrate%3F+.....%22+&ots=AJUDdfVDI8&sig=dR0fSqTPPkcDvnh8UpjgtGTAQrw

UNFCCC. (1992). United Nations Framework Convention on Climate Change. Retrieved from http://unfccc.int/resource/docs/convkp/conveng.pdf

UN-REDD. (2015). Forests and REDD+ recognized as key components of landmark climate deal agreed in Paris. Retrieved February 9, 2016, from http://www.unredd.net/index.php?option=com_content&view=article&id=2334:f

orests-included-in-landmark-climate-deal-agreed-in-paris&catid=98:general&Itemid=749

USGS. (2016). Landsat 8 (L8) data Users Handbook. EROS, Sioux Falls, South Dakota. Retrieved from https://landsat.usgs.gov/documents/Landsat8DataUsersHandbook.pdf

Van der Werf, G. R., Morton, D. C., DeFries, R. S., Olivier, J. G., Kasibhatla, P. S., Jackson, R. B., … Randerson, J. T. (2009). CO2 emissions from forest loss. *Nature Geoscience*, *2*(11), 737–738.

Van Laar, A., & Akça, A. (2007). *Forest mensuration* (Vol. 13). Springer Science & Business Media.

VanDerWal, J., Falconi, L., Januchowski, S., & Storlie, L. S. and C. (2014). SDMTools: Species Distribution Modelling Tools: Tools for processing data associated with species distribution modelling exercises (Version 1.1-221). Retrieved from http://cran.r-project.org/web/packages/SDMTools/index.html

Vermote, E., Tanré, D., Deuzé, J., Herman, M., Morcrette, J., & Kotchenova, S. (2006). Second simulation of a satellite signal in the solar spectrum-vector (6SV). *6S User Guide Version*, *3*.

Villamor, G. B., Jr, R. G. P., & Noordwijk, M. van. (2013). Agroforest's growing role in reducing carbon losses from Jambi (Sumatra), Indonesia. *Regional Environmental Change*, 1–10. https://doi.org/10.1007/s10113-013-0525-4

Wallner, A., Elatawneh, A., Schneider, T., & Knoke, T. (2014). Estimation of forest structural information using RapidEye satellite data. *Forestry*. https://doi.org/10.1093/forestry/cpu032

Whitmore, T. C. (1998). *An introduction to tropical rain forests*. Oxford University Press.

Whitten, T., Damanik, S. J., Anwar, J., & Hisyam, N. (2000). *The ecology of Sumatra (The Ecology of Indonesia Series vol I)* (Vol. 1). Periplus Editions.

Wibowo, A., & Giessen, L. (2015). Absolute and relative power gains among state agencies in forest-related land use politics: The Ministry of Forestry and its competitors in the REDD+ Programme and the One Map Policy in Indonesia. *Land Use Policy*, *49*, 131–141. https://doi.org/10.1016/j.landusepol.2015.07.018

Wijaya, A., & Gloaguen, R. (2009). Fusion of ALOS Palsar and Landsat ETM data for land cover classification and biomass modeling using non-linear methods. In *Geoscience and Remote Sensing Symposium,2009 IEEE International,IGARSS 2009* (Vol. 3, p. III-581-III-584). https://doi.org/10.1109/IGARSS.2009.5417824

Wijaya, A., Liesenberg, V., & Gloaguen, R. (2010). Retrieval of forest attributes in complex successional forests of Central Indonesia: Modeling and estimation of bitemporal data. *Forest Ecology and Management*, *259*(12), 2315–2326. https://doi.org/10.1016/j.foreco.2010.03.004

Wilcove, D. S., Giam, X., Edwards, D. P., Fisher, B., & Koh, L. P. (2013). Navjot's nightmare revisited: logging, agriculture, and biodiversity in Southeast Asia. *Trends in Ecology & Evolution*, *28*(9), 531–540. https://doi.org/10.1016/j.tree.2013.04.005

Wilcove, D. S., & Koh, L. P. (2010). Addressing the threats to biodiversity from oil-palm agriculture. *Biodiversity and Conservation*, *19*(4), 999–1007. https://doi.org/10.1007/s10531-009-9760-x

WRI (Ed.). (1994). *World Resources 1994-95: A Guide to the Global Environment*. New York: Oxford Univ. Press.

WRI. (2010). FAQ: Indonesia, Degraded Land and Sustainable Palm Oil | World Resources Institute. Retrieved April 4, 2017, from http://www.wri.org/blog/2010/11/faq-indonesia-degraded-land-and-sustainable-palm-oil

Wyman, M. S., & Stein, T. V. (2010). Modeling social and land-use/land-cover change data to assess drivers of smallholder deforestation in Belize. *Applied Geography*, *30*(3), 329–342. https://doi.org/10.1016/j.apgeog.2009.10.001

Xiao-gu, S., Man-chun, L., Yong-xue, L., Lu, T., & Wei, L. (2009). Accelerated segmentation approach with CUDA for high spatial resolution remotely sensed imagery based on improved Mean Shift. In *Urban Remote Sensing Event, 2009 Joint* (pp. 1–6). https://doi.org/10.1109/URS.2009.5137568

Yang, G., Pu, R., Zhang, J., Zhao, C., Feng, H., & Wang, J. (2013). Remote sensing of seasonal variability of fractional vegetation cover and its object-based spatial pattern analysis over mountain areas. *ISPRS Journal of Photogrammetry and Remote Sensing*, *77*, 79–93. https://doi.org/10.1016/j.isprsjprs.2012.11.008

Appendices

A.1. Land use mapping derived from Landsat images

Time-series data from five tiles of Landsat images were collected to map the land use systems in the Jambi province. Of these images, Landsat TM from 1989-1990, TM/ETM+ from 1999-2001, TM/ETM+ from 2009-2011, and OLI from 2013 were prepared to produce historical land use maps for the years 1990, 2000, 2011, and 2013, respectively.

In the image pre-processing phase, image-to-image registration was conducted as the first step. In this process, the master images were the most recent images (the 2013 images) and the slave images were the other respective images. As the study area was located in the tropics, the Landsat images were highly covered by cloud and cloud-shadow, both of which had to be removed. In addition, the Landsat images with acquisition time after May 31st, 2013 have strips consisting of no data because of the Scan Line Corrector (SLC) failure. Therefore, the procedure of filling the gaps was also carried out. Afterwards, image enhancement using the histogram matching method was implemented before mosaicking the five tiles of Landsat images. Finally, the mosaics of Landsat images were available for each year of 1990, 2000, 2011, and 2013.

For the image classification, techniques of automatic and visual image interpretation to derive the land use classes were implemented. Initially, an automatic technique was implemented to determine vegetation and non-vegetation classes. Secondly, further classification of land use systems was carried out using visual interpretation. The false color composite images of Landsat TM/ETM+ with an RGB combination of red: band 5, green: band 4, blue: band 3, and of Landsat OLI with an RGB combination of red: band 6, green: band 5, blue: band 4 were displayed throughout the visual interpretation. From those composite images, visual interpretation and on-screen digitization were performed for each land use class by competent image interpreters. As a reference for the interpretation, a guideline of the land use classification key for 23 land use classes was used, which was provided by the Indonesian Ministry of Forestry (MoF, 2008). Additional classes like jungle rubber, rubber, and oil palm plantations were also determined. In order to produce maps with high accuracy, visual interpretation was assisted with data from field observations, local knowledge, and RapidEye images. Finally, the minimum mapping unit (MMU) of the resulting land use maps was 6.25 ha (0.25 cm^2 at a scale of 1:50,000).

A.2. Confusion matrix of land use classification derived from Landsat images based on ground truthing data (the numbers are rounded to the nearest tenth).

			Classification																
			1	2	3	4	5	6	7	8	9	10	11	12	13	14	15	16	Total	PA (%)
Reference	1	Secondary dryland forest	19					1	1						1				22	86.4
	2	Secondary mangrove forest		4															4	100.0
	3	Secondary swamp forest			11			2				2							15	73.3
	4	Jungle rubber				13		8	3					1	1			1	27	48.1
	5	Plantation forest					12		1										13	92.3
	6	Rubber plantation				3	1	46	2						1				53	86.8
	7	Oil palm plantation	1					5	45	2			1		4			1	59	76.3
	8	Dryland agriculture								8									8	100.0
	9	Mixed dryland agriculture									7								7	100.0
	10	Water body										3							3	100.0
	11	Settlement						2			1		13	1		1			18	72.2
	12	Shrub/bush							1	1				20	2	1	1		26	76.9
	13	Swamp bush							1		2	1	2		17				23	73.9
	14	Paddy field						1						1		6		1	9	66.7
	15	Mining															3		3	100.0
	16	Bare land	1											1				6	8	75.0
		Total	21	4	11	16	13	65	54	11	10	6	16	24	26	8	4	9	298	
		UA (%)	90.5	100.0	100.0	81.3	92.3	70.8	83.3	72.7	70.0	50.0	81.3	83.3	65.4	75.0	75.0	66.7		
		OAA	78.2																	
		Kappa	0.8																	

A.3. An example of the calculations for each forest variable from the field measurement

This is an example for calculating the target variables (i.e. AGB, BA, N, and dq) of two plots (i.e. Plot 1 and Plot 2). The diameter at breast height (dbh) is measured for different sized subplots (i.e. 25 m^2, 100 m^2, 1000 m^2). For the smallest nested subplot (i.e. 25 m^2), the expansion factor (EF) is 400; for the second nested subplot (i.e. 100 m^2), the EF is 100; and for the largest subplot (i.e. 1000 m^2), the EF is 10. At each nested subplot, AGB and BA were initially calculated per tree. AGB and BA are then calculated per ha by multiplying the value of each tree with the EF as illustrated in Table 1.

Table 1. An illustration of AGB and BA calculation. The measurement of dbh is classified in three different nested subplots of class *i* (*i* = 1, 2, or 3 where each of *i* represents nested subplot of 25 m^2, 100 m^2, 1000 m^2, respectively). In this table, x_i is dbh in class *i*, w_i is the AGB value in class *i*, and g_i is the BA value in class *i*.

PLOT	SUBPLOT	PLOT_ID	dbh (cm)	AGB (kg/tree)	EF	BA (cm^2/tree)	AGB (kg/ha)	BA (m^2/ha)
1	A	1A	x1	w1	400	g1	400w1	$400g1x10^{-4}$
1	A	1A	x2	w2	100	g2	100w2	$100g2x10^{-4}$
1	A	1A	x1	w1	400	g1	400w1	$400g1x10^{-4}$
1	A	1A	x2	w2	100	g2	100w2	$100g2x10^{-4}$
1	A	1A	x3	w3	10	g3	10w3	$10g3x10^{-4}$
1	B	1B	x3	w3	10	g3	10w3	$10g3x10^{-4}$
1	B	1B	x3	w3	10	g3	10w3	$10g3x10^{-4}$
1	B	1B	x1	w1	400	g1	400w1	$400g1x10^{-4}$
1	B	1B	x2	w2	100	g2	100w2	$100g2x10^{-4}$
1	B	1B	x2	w2	100	g2	100w2	$100g2x10^{-4}$
2	A	2A	x1	w1	400	g1	400w1	$400g1x10^{-4}$
2	A	2A	x2	w2	100	g2	100w2	$100g2x10^{-4}$
2	A	2A	x1	w1	400	g1	400w1	$400g1x10^{-4}$
2	A	2A	x2	w2	100	g2	100w2	$100g2x10^{-4}$
2	A	2A	x3	w3	10	g3	10w3	$10g3x10^{-4}$
2	B	2B	x3	w3	10	g3	10w3	$10g3x10^{-4}$
2	B	2B	x3	w3	10	g3	10w3	$10g3x10^{-4}$
2	B	2B	x1	w1	400	g1	400w1	$400g1x10^{-4}$
2	B	2B	x2	w2	100	g2	100w2	$100g2x10^{-4}$
2	B	2B	x2	w2	100	g2	100w2	$100g2x10^{-4}$

Each respective value per ha of AGB, BA, and N for the different nested subplots was then added to obtain the total AGB, BA, and N as illustrated in Table 2. The value of stand density (N) is the total number of trees at each nested subplot.

Table 2. The total values of AGB, BA, N, and dq for each nested subplot.

PLOT_ID	AGB (kg/ha)	BA (m2/ha)	N (trees/ha)
1A	800w1	$800g1x10^{-4}$	800n1
1A	200w2	$200g2x10^{-4}$	200n2
1A	10w3	$10g3x10^{-4}$	10n3
1B	400w1	$400g1x10^{-4}$	400n1
1B	200w2	$200g2x10^{-4}$	200n2
1B	20w3	$20g3x10^{-4}$	20n3
2A	800w1	$800g1x10^{-4}$	800n1
2A	200w2	$200g2x10^{-4}$	200n2
2A	10w3	$10g3x10^{-4}$	10n3
2B	400w1	$400g1x10^{-4}$	400n1
2B	200w2	$200g2x10^{-4}$	200n2
2B	20w3	$20g3x10^{-4}$	20n3

The total value of the three nested subplots is used to obtain the AGB, BA, and N per ha of each subplot (i.e. 1A, 1B, 2A, 2B). For instance, the total AGB of subplot 1A is 800w1+200w2+10w3. From the total of BA and N values at each subplot, dq can be calculated for each subplot using equation (5) as mentioned in subsection 3.3.3.

A.4. The overlap area between forest cover (Hansen et al., 2013) and land use systems (present study) in 2000.

Land use systems in 2000 (present study)	Forest cover in 2000 (Hansen et al., 2013)	
	Area (ha)	%
Agriculture	773,690.8	17.2
Jungle rubber	22,541.0	0.5
Oil palm plantation	480,888.4	10.7
Others	59,157.3	1.3
Plantation forest	171,995.0	3.8
Primary forest	885,018.4	19.6
Rubber plantation	812,638.4	18.0
Secondary forest	860,880.9	19.1
Shrub/bush	441,759.2	9.8
Total	4,508,569.3	100

A.5. The loss and gain of primary forest and secondary forest in the Jambi Province.

	Primary forest		Secondary forest	
	Loss (ha)	Gain (ha)	Loss (ha)	Gain (ha)
1990-2000	452,564.4	4,758.9	383,605.5	346,413.0
2000-2011	61,285.3	322.5	277,263.3	52,550.0
2011-2013	1,070.8	0.0	23,188.4	726.2

A.6. Hoover metrics scoring

For each metric, the descriptions of the scoring are explained below following Hoover et al. (1996). The notations for each equation are explained in the Methods Chapter (see Section 3.2.3.).

1. Correct detection (CD)

   score O_{mn} = T x (min (O_{mn}/ T x P_{n_i}, O_{mn}/ T x P_{m_i}))

   CD_i = score O_{mn} x P_{n_i}

   scoreCD = $\sum_{i=1}^{k} CD_i / \sum_{i=1}^{k} P_{n_i}$

   where k ≥ 1 and k shows the pair number between the segmented and reference object that is being assessed.

2. Over-segmentation (OS)

   score O_{m_in} = O_{m_in} x (O_{m_in}-1)

   sum_score O_{m_in}= $\sum_{i=1}^{x}(O_{m_in}$ x ($O_{m_in} - 1))$
   where 2 ≤ x ≤ M

   $scoreOS_i$ = 1 - sum_score O_{m_in}/ (P_{n_i}x (P_{n_i}-1))
   OS_i = $scoreOS_i$ x P_{n_i}

   scoreOS = $\sum_{i=1}^{k} OS_i / \sum_{i=1}^{k} P_{n_i}$
   where k ≥ 1 and k shows the pair number between the segmented and reference object that is being assessed.

3. Under-segmentation (US)

   score O_{mn_i} = O_{mn_i} x (O_{mn_i}-1)
   sum_score O_{mn_i}= $\sum_{i=1}^{x} O_{mn_i}$ x ($O_{mn_i} - 1$)

   $scoreUS_i$ = 1 - sum_score O_{mn_i}/($\sum_{i=1}^{x} P_{n_i}$x ($\sum_{i=1}^{x} P_{n_i} - 1$))
   US_i = $scoreUS_i$ x $\sum_{i=1}^{x} P_{n_i}$
   where 2 ≤ x ≤ N

   scoreUS = $\sum_{i=1}^{k} US_i / \sum_{i=1}^{k} P_{n_i}$
   where k ≥ 1 and k shows the pair number between the segmented and reference object that is being assessed.

4. Missed detection (M)

   M_i = $\sum_{i=1}^{x} P_{n_i}$

   where 2 ≤ x ≤ N

   scoreM = $\sum_{i=1}^{k} M_i / \sum_{i=1}^{k} P_{n_i}$

where k ≥ 1 and k shows the pair number between the segmented and reference object that is being assessed.

Assuming that there are four pairs reference objects (R_n) and objects from machine segmentation (R_m), each object is labelled, and 0 is the background that has no object. In this case, T = 0.75 is chosen.

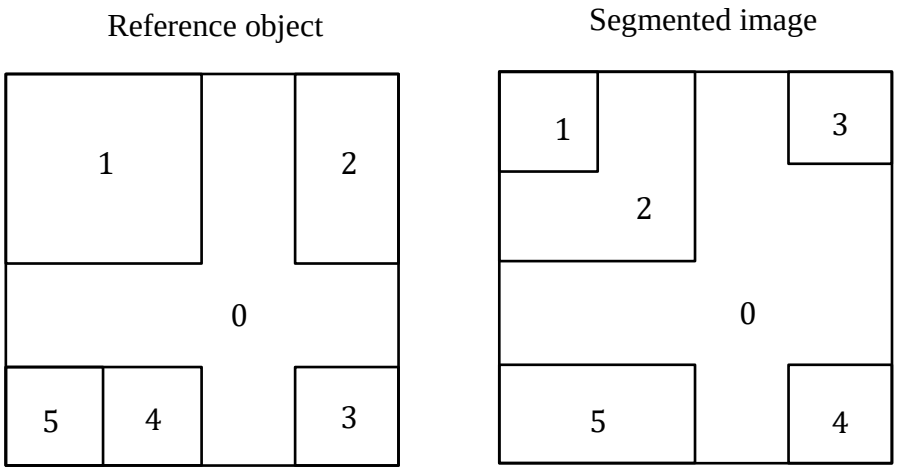

Pair 1

P_{n_1} = 2500 pixels

P_{m_1} = 625 pixels

P_{m_2} = 1875 pixels

Metrics classification:

R_n	R_m	O_{mn}	T x P_{n_i}	T x P_{m_i}	Classification	score O_{m_in}/O_{mn_i}
1	1	625	1875	468.75	OS	390000
1	2	1875	1875	1406.25	CD, OS	3513750
					sum_score O_{m_in}	3903750

Correct detection (CD)

score O_{mn} = 0.75 x (min (1875/1875, 1875/1406.25))

= 0.75

CD_1 = 0.75 x 2500

= 1875

Over-segmentation (OS)

$scoreOS_1$ = 1 - 3903750 / (2500x (2500-1)

= 0.375

OS_1 = 0.375 x 2500

= 937.5

Pair 2
P_{n_2} = 1250 pixels

P_{m_3} = 625 pixels

Metrics classification:

R_n	R_m	O_{mn}	T x P_{n_i}	T x P_{m_i}	Classification	score $O_{m_i n}/O_{mn_i}$
2	3	625	937.5	468.75	M	-
2	-	625	937.5	-	M	-

M_1 = 1250

Pair 3
P_{n_3} = 625 pixels

P_{m_4} = 625 pixels

Metrics classification:

R_n	R_m	O_{mn}	T x P_{n_i}	T x P_{m_i}	Classification	score $O_{m_i n}/O_{mn_i}$
3	4	625	468.75	468.75	CD	-

Correct detection (CD)

score O_{mn} = 0.75 x (min (625/468.75, 625/468.75))

= 1

CD_2 = 1 x 625

= 625

Pair 4
P_{n_4}= 625 pixels

P_{n_5}= 625 pixels

P_{m_5} = 1250 pixels

Metrics classification:

R_n	R_m	O_{mn}	T x P_{n_i}	T x P_{m_i}	Classification	score $O_{m_i n}/O_{mn_i}$
4	5	625	468.75	937.5	US	390000
5	5	625	468.75	937.5	US	390000
					sum_score O_{mn_i}	780000

Under-segmentation (US)

$scoreUS_1$ = 1 - 780000 / (1250x (1250-1)

= 0.5

US_1 = 0.5 x 1250

= 625

scoreCD = (1875 +625)/5625
= 0.4444
scoreOS = 937.5/5625
= 0.1667
scoreUS = 625/5625
= 0.1111
scoreM = 1250/5625
= 0.2222